Rita Valador Fernandes
Licenciada em Biologia Celular e Molecular

Study of the Long Non-Coding RNA *C/EBPβ-AS* in Cutaneous Melanoma

Dissertação para obtenção do Grau de Mestre em
Genética Molecular e Biomedicina

Orientador: Dan Grandér, MD, PhD, Professor, Karolinska Institutet

FACULDADE DE CIÊNCIAS E TECNOLOGIA
UNIVERSIDADE NOVA DE LISBOA
Setembro de 2017

Rita Valador Fernandes
Licenciada em Biologia Celular e Molecular

Study of the Long Non-Coding RNA *C/EBPβ-AS* in Cutaneous Melanoma

Dissertação para obtenção do Grau de Mestre em
Genética Molecular e Biomedicina

Orientador: Dan Grandér, MD, PhD, Professor, Karolinska Institutet

FACULDADE DE CIÊNCIAS E TECNOLOGIA
UNIVERSIDADE NOVA DE LISBOA

Setembro de 2017

Study of the Long Non-Coding RNA *C/EBPβ-AS* in Cutaneous Melanoma

Aknowledgments (Agradecimentos)

I wish to thank Dan Grandér and Katja Pokrovskaja Tamm for accepting me to their lab and experience what was one of the most important and enriching years in all of my academic education, so far. Also, for their kind and amusing personalities.

I would like to express my sincere gratitude to Linda Vidarsdóttir, who very patiently taught me almost everything I learnt throughout this year. From very basic to more excitingly complex scientific contents, and a great deal of laboratorial techniques with all the tips that come along. All the honest conversations on how the scientific world spins around and the sincere advice (that I very much cherished) for my future career and life. Thank you for your great humour, time, patience and care.

I would also like to leave my appreciation words to all the (current and previous) members of Grandér's group Elin, Matheus, Sander, Nathan, Vasilios, Martin, Nicolò, Kristina and Henri, for making life around the lab so amusing and fun. With them, monotony and boredom were never around.

I am very grateful for having Lotte's calmness and experience nearby, crucial in overcoming some initial laboratorial anxiety.

I want to thank Christos and Matheus for all the precious help and patience with confocal microscopy.

Also, Alireza, Rainer and Ishani shared a great deal of melanoma-related knowledge, and revealed to be very kind and nice people. I want to specially thank Ishani for the enriching collaboration.

Life outside the lab wouldn't be the same without Nathan, Bruce, Nicolò and Ernesto. Thank you for all the field trips around Stockholm and the funny greasy-pizza gatherings.

Muitos foram os que contribuíram, directa ou indirectamente, para que há um ano uma grande etapa estivesse a começar e para que aqui tenha chegado, desde amigos a professores que me inspiraram pelo percurso. O meu agradecimento a todos, especialmente:

Obrigada Pedro Fonseca, pela disponibilidade e partilha de experiências, essenciais à candidatura ao mestrado e à posição no Instituto Karolinska.

Obrigada Martocas, não teria superado este louco, mas divertido ano sem a tua companhia, a quase 3000 km de casa. Todas a conversas ao pequeno-almoço e jantares tardios e todas as visitas a Estocolmo e arredores (incluindo obviamente as frequentes viagens ao *Gröna Lund*) ajudaram a aproveitar e apreciar estes meses. *Péliculi*, *Péliculá*.

Obrigada Fernanda e Andreia, pela vossa amizade. As viagens casa-laboratório pelas geladas manhãs de Estocolmo não seriam a mesma coisa sem as divertidas mensagens da Fernanda, certamente.

Obrigada aos meus tios Tópê e Ana pelas palavras de ânimo a longa-distância. Obrigada aos meus primos Simão e Vasco – essas carinhas larocas sempre me encherão o coração de boa disposição.

Obrigada ao meu irmão Guilherme, pelo seu carinho e amizade revelados através das formas mais estrambólicas.

Um profundo obrigada aos meus avós que sempre me irão tratar com todo o afeto e preocupação, onde quer que estejam e para onde quer que eu vá. Obrigada por sempre me transmitirem valores de humildade e gratidão.

Quero ainda agradecer ao meu melhor amigo e namorado – obrigada Pedro, nada seria possível sem o teu infinito e encorajador apoio e amor, permitindo superar toda e qualquer crise-existencial.

Tudo seria impossível sem a ajuda, carinho, amor e apoio incondicional dos meus pais, que sempre me ensinaram a não desistir. Obrigada Mamã. Obrigada Papá.

Resumo

Melanoma Maligno Cutâneo (CMM) é o nono tipo de cancro mais frequentemente diagnosticado em regiões de maior desenvolvimento humano. Apesar de representar menos de 5% de todos os casos de cancro de pele, CMM é a neoplasia de pele com maior taxa de mortalidade, tendo-se detetado um aumento de incidência nas últimas décadas. *Vemurafenib* é um inibidor de *B-Rapidly Accelerated Fibrosarcoma* (BRAF) com eficácia demonstrada em cerca de 80% dos doentes com CMM portadores da mutação $BRAF^{V600E}$. No entanto, a maioria destes doentes tende a desenvolver resistência ao tratamento, o que torna imperativo investigar novas estratégias terapêuticas.

Os *RNAs* longos não-codificantes (*lncRNAs*) representam uma classe diversificada de transcritos funcionais que geralmente não codificam proteínas e possuem mais de 200 nucleótidos de extensão. O progressivo aumento de sensibilidade de métodos de sequenciação de *RNA*, bem como de técnicas computacionais preditivas, permite a identificação de um crescente número de *lncRNAs*. Entre os poucos *lncRNAs* já caracterizados funcionalmente, vários foram relacionados com diversos aspetos da carcinogénese, tendo um papel evidente na regulação da expressão génica.

CCAAT/Enhancer-Binding Protein β (C/EBPβ) é um fator de transcrição envolvido em diversos processos celulares, designadamente senescência e proliferação celular. *CCAAT/Enhancer-Binding Protein β Antisense* (*C/EBPβ-AS*) é um *lncRNA antisense*, transcrito da cadeia complementar à de *C/EBPβ*, com uma sobreposição genómica na região 5' com o gene *C/EBPβ*. Este *lncRNA* não foi, até ao momento, caracterizado.

Neste estudo identificamos características biologicamente relevantes de *C/EBPβ-AS* e propomos um papel para este *lncRNA* na regulação epigenética da expressão de *C/EBPβ* em linhas celulares de melanoma. Demonstramos ainda que a modulação da expressão de *C/EBPβ-AS* ressensibiliza células de melanoma resistentes a *vemurafenib*. Finalmente, investigamos o impacto da modulação da expressão de *C/EBPβ-AS* nas vias de sinalização MAPK/ERK e PI3K/AKT, ambas frequentemente desreguladas em CMM.

Desta forma, este trabalho revela um novo mecanismo de regulação génica mediado por um *lncRNA* com implicações na resistência à terapia direcionada em CMM.

Palavras-chave

Melanoma Maligno Cutâneo
RNA Longo Não-Codificante *Antisense*
C/EBPβ-AS
C/EBPβ
Resistência à Terapia Direcionada

Abstract

Cutaneous malignant melanoma (CMM) is the ninth most common cancer type in more developed regions. Despite comprehending less than 5% of all skin cancer cases, CMM stands as the most lethal skin neoplasm, with a detectable increase in incidence throughout recent decades. While the B-rapidly accelerated fibrosarcoma (BRAF) inhibitor vemurafenib appears to be effective in ~80% of CMM patients carrying the $BRAF^{V600E}$ mutation, the vast majority of patients becomes resistant to treatment. Given that, it is imperative to seek new therapeutic strategies.

Long non-coding RNAs (lncRNAs) are a functionally diverse class of transcripts that lack an evident protein-coding function and have over 200 nucleotides of length. The advent of growing sensitivity of RNA sequencing methods, as well as computational prediction techniques is enabling the increasing identification of such RNA transcripts. Among the few that have been functionally characterized, several have been linked to numerous aspects of carcinogenesis, with an evident role in gene expression regulation.

CCAAT/Enhancer-Binding Protein β (C/EBPβ) is a transcription factor implicated in many fundamental cellular processes, including cellular senescence and proliferation. CCAAT/Enhancer-Binding Protein β Antisense (*C/EBPβ-AS*) is an antisense lncRNA transcribed from the reverse strand of *C/EBPβ*, with a genomic 5' overlap with *C/EBPβ* gene, which has not previously been studied.

Here we characterize biologically relevant features of *C/EBPβ-AS* and propose a role for *C/EBPβ-AS* in epigenetic regulation of *C/EBPβ* expression in melanoma cell lines. Moreover, we show that modulation of *C/EBPβ-AS* expression resensitizes vemurafenib-resistant melanoma cells to vemurafenib. Finally, we investigate the impact of modulation of *C/EBPβ-AS* expression in MAPK/ERK and PI3K/AKT pathways, both commonly found to be dysregulated in CMM.

Taken together, our research provides new insights on an antisense lncRNA-mediated mechanism of gene regulation, with implications on CMM targeted-therapy resistance.

Keywords

Cutaneous Malignant Melanoma
Antisense Long Non-Coding RNA
C/EBPβ-AS
C/EBPβ
Targeted-Therapy Resistance

Contents

List of Figures

List of Tables

List of Abreviations

AIRN	Antisense Of IGF2R Non-Protein Coding RNA
AJCC	American Joint Committee on Cancer
AKT	Protein Kinase B
ANRIL	CDKN2B Antisense RNA 1
ARAF	A Rapidly Accelerated Fibrosarcoma
asRNAs	antisense RNAs
ATCC	American Type Culture Collection
BANCR	BRAF-Regulated lncRNA 1
BRAF	B-Rapidly Accelerated Fibrosarcoma
$BRAF^{V600E}$	BRAF muteted form (substitution of valine to glutamic acid at amino acid 600)
bZIP domain	basic leucine zipper domain
C/EBPβ	CCAAT/Enhancer-Binding Protein β
C/EBPβ-AS	CCAAT/Enhancer-Binding Protein β Antisense
CCAT1-L	Colon Cancer Associated Transcript 1
CDKN2A	Cyclin-Dependent Kinase Inhibitor 2A
cDNA	complementary DNA
ChIP	chromatin immunoprecipitation
ChIP-seq	chromatin immunoprecipitation-sequencing
CMM	Cutaneous Malignant Melanoma
CRAF	C Rapidly Accelerated Fibrosarcoma
CRE	cAMP Response Element
CTLA-4	Cytotoxic T Lymphocyte Antigen-4
DMSO	dimethyl sulfoxide
DNA	deoxyribonucleic acid
DNMT3A	DNA Methyltransferase 3A
dNTPS	nucleotides for DNA synthesis
dsRNA	double-stranded RNA
DTT	dithiothreitol
ENCODE	ENCyclopedia Of DNA Elements
ERK	Extracellular Signal-Regulated Kinase
FACS	Fluorescence Activated Cell Sorting
GAS5	Growth Arrest-Specific Transcript 5
GDP	guanosine diphosphate
Grb2	Growth Factor Receptor-Bound Protein 2
GRCh37/hg17	Genome Reference Consortium Human Build 37
GRCh38/hg38	Genome Reference Consortium Human Build 38
GTP	guanosine triphosphate
GTPase	Guanosine Triphosphatase

H3K27me3	Histone H3 Lysine 27 Trimethylation
H3K9	Histone H3 Lysine 9
HOTAIR	HOX Antisense Intergenic RNA
HOX	Homeobox
HOXC	Homeobox Protein C
HOXD	Homeobox Protein D
IFNα	Interferon Alpha
lincRNAs	large intergenic ncRNAs
lncRNAs	long ncRNAs
MALAT1	Metastasis Associated Lung Adenocarcinoma Transcript 1
MAP2K1	Mitogen-Activated Protein Kinase Kinase 1
MAP2K2	Mitogen-Activated Protein Kinase Kinase 2
MAPK	Mitogen-Activated Protein Kinase
MEFs	Mouse Embryo Fibroblasts
MEK	MAPK/ERK Kinase
MITF	Melanogenesis-Associated Transcription Factor
MMP	Matrix Mettaloproteinase 2 Protein
mTORC2	Mechanistic Target of Rapamycin Complex 2
NCI	National Cancer Institute
ncRNAs	non-coding RNAS
NHGRI	National Human Genome Research Institute
NORAD	Non-Coding RNA Activated By DNA Damage
NRAS	Neuroblastoma RAS Viral Oncogene Homolog
Oct4	Octamer-Binding Transcription Factor 4
ORF	open reading frame
PD-1	Programmed Cell Death-1
PDK1	Kinase-3′-Phosphoinositide-Dependent Kinase 1
PI3K	Phosphatidylinositol 3-Kinase
PIP_3	Phosphatidylinositol-3,4,5-Triphosphate
piRNAs	Piwi-Interacting RNAs
PRC1	Polycomb Repressive Complex 1
PTEN	Phosphatase and Tensin Homologue
PTENpg1 asRNA α	PTEN Pseudogene-Encoded Antisense RNA α
PTENpg1 asRNA β	PTEN Pseudogene-Encoded Antisense RNA β
PTENpg1 sense	PTEN Pseudogene Sense
RT-qPCR	real-time quantitative polymerase chain reaction
RAF	Rapidly Accelerated Fibrosarcoma
RAS	Rat Sarcoma Proteins
RIPA buffer	Radioimmunoprecipitation Assay buffer

RNA	ribonucleic acid
RNA Pol II	RNA Polymerase II
RNAi	RNA interference
RTK	Receptor Tyrosine Kinase
SAMMSON	Survival-Associated Mitochondrial Melanoma-Specific Oncogenic Non-Coding RNA
SEM	standard error of the mean
siRNAs	small interfering RNAs
smFISH	single-molecule RNA Fluorescence *In Situ* Hybridization
sncRNAs	short ncRNAs
snoRNAs	small nucleolar RNAs
snRNAs	small nuclear RNAs
Sos	Son of Sevenless
STAU1	Staufen 1
TAE buffer	Tris-Acetate-EDTA buffer
TBS-T buffer	Tris-buffered saline-Tween 20
TCGA	The Cancer Genome Atlas
tiRNAs	transcription initiation RNAs
Tsix	Reverse of *Xist*
UCSC	University of California Santa Cruz
UVR	Ultra-Violet Radiation
Xist	X-Inactive Specifc Transcript

1. Introduction

1.1. Cutaneous Malignant Melanoma

1.1.1. Epidemiologic Scenario of Cutaneous Malignant Melanoma: Incidence, Geographical Distribution and Mortality

According to GLOBOCAN estimates, cutaneous malignant melanoma (CMM) was accounted for over 1,5% of all new diagnosed cancer cases, worldwide, in 2012, with 191 thousand new cases in more developed regions, both sexes combined, in 2012 (Figure 1.1.), being the ninth most common cancer type in more developed regions (Ferlay *et al*., 2015).

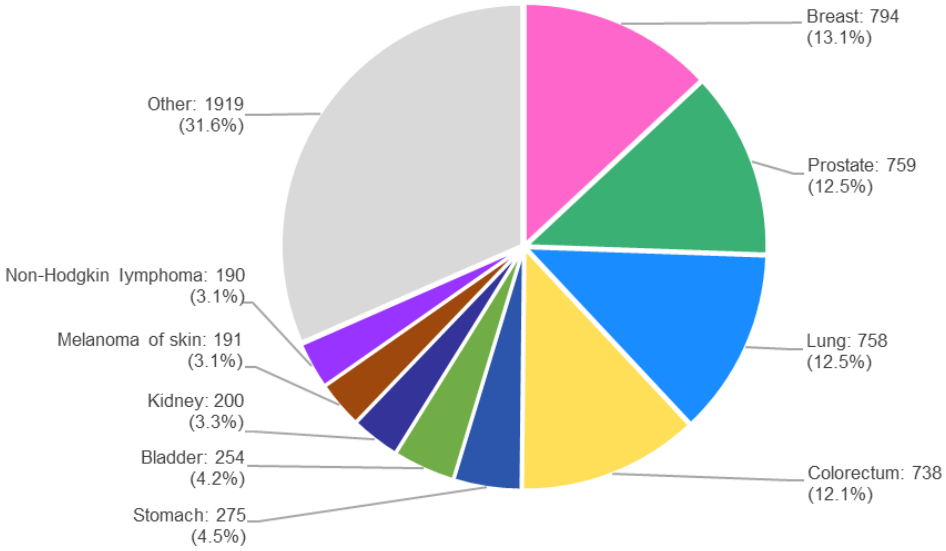

Figure 1.1. Incidence of Melanoma in more developed regions.
Estimated global numbers of new cancer cases (in thousands) with proportions for more developed regions, both sexes combined, in 2012. The area of the pie is proportional to the number of new cases. Melanoma of skin appears as the ninth most common cancer type, with 191 thousand cases (3.1%) out of 6076 thousand total new cancer cases. Adapted from (Ferlay *et al*., 2015).

Throughout recent decades the incidence of CMM has been increasing, with highest reported incidence areas worldwide being Northern Europe, Australia and North America (Erdmann *et al*., 2013). In these regions, Caucasians represent the sub-population that is more prone to develop such cancer type.

Although CMM comprehends less than 5% of all skin cancer cases, it stands as the most lethal skin neoplasm, because of its high mortality when identified at advanced stages, being responsible for about 80% of dermatological cancer related deaths (Miller and Mihm, 2006).

1.1.2. Cutaneous Malignant Melanoma: Development, Staging and Risk Factors

CMM is a type of skin cancer that arises from malignant transformation of melanin-producing cells of the skin found in the basal layer of the epidermis, designated melanocytes. According to the Clark model of development and progression of CMM (Figure 1.2.), the first step is the development of benign melanocytic nevi (commonly designated by moles), resulting from controlled melanocyte proliferation and its transformation into atypical/dysplasic nevi (pre-malignant nevi with aberrant proliferation). Next,

is the Radial Growth Phase, in which transformed cells acquire the ability to intraepidermally proliferate, followed by the Vertical Growth Phase. In this phase, transformed cells acquire the ability to invade the dermis (inner layer of the skin) through the basement membrane. Ultimately, the last step is the metastatic phase, in which malignant melanocytes successfully proliferate and spread to lymph nodes and other tissues (Clark *et al*., 1984).

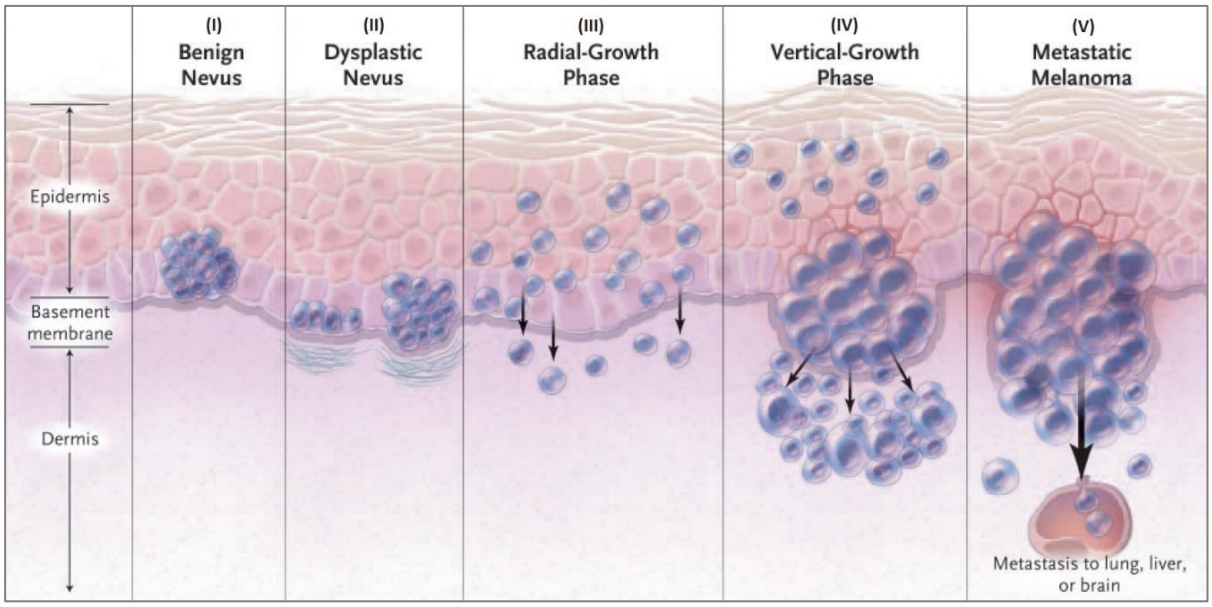

Figure 1.2. The Clark Model of development and progression of melanoma.

The Clark model describes the histological changes that accompany the progression from normal melanocytes to malignant melanoma. The model depicts the proliferation of melanocytes in the process of (**I**) forming benign nevi (resulting from controlled melanocyte proliferation in normal melanocytes), (**II**) the subsequent transformation into atypical/dysplasic nevi (pre-malignant nevi with aberrant proliferation), (**III**) the Radial Growth Phase, in which transformed cells acquire the ability to intraepidermally proliferate, followed by (**IV**) the Vertical Growth Phase, during which transformed cells acquire the ability to invade the dermis (inner layer of the skin) through the basement membrane and ultimately and (**V**) the metastatic phase, in which malignant melanocytes successfully proliferate and spread to lymph nodes and other tissues. Adapted from (Miller and Mihm, 2006).

CMM staging is determined by the American Joint Committee on Cancer (AJCC) system, that incorporates tumour thickness, ulceration (defined as the interruption of the surface epithelium by tumour cells), mitotic index, the lymph node status and distant metastases (Balch *et al*., 2009). This staging system categorizes melanoma patients into three main groups: localized disease with no evidence of metastases (stage I–II), regional disease (stage III) and distant metastatic disease (stage IV).

The etiology of CMM is multifactorial, with the most relevant risk factors being Ultra-Violet Radiation (UVR) exposure, genetic predisposition, light sensitivity – including low skin-phototype (fair skin), multiple benign or atypical nevi –, and immunosuppression of the host (Lo and Fisher, 2014). Intermittent UVR exposure as well as history of severe sunburns in childhood or adolescence have been implicated in epidemiologic studies as conferring the highest risk (Whiteman, *et al*., 2001).

UVR promotes malignant transformation of melanocytes by UVR-induced DNA damage, which is a known fundamental event in photocarcinogenesis, highly connected to CMM development (Sarasin, 1999), by having a systemic as well as local (cutaneous) immunosuppressive effect (Schwarz, 2005) and by promoting reactive oxygen species of melanin that cause DNA damage and suppress apoptosis (Meyskens, *et al*., 2004).

Prolonged UVR exposure is a known fundamental event in photocarcinogenesis and gives rise to characteristic UVR signature-mutations: mainly C-to-T substitutions (Cytosines to Thymines pyrimidine bases). Such signature-mutation is described to be extensively accountable for the high mutation rate in melanoma (Pleasance *et al*., 2010; Lawrence et al., 2013).

1.1.3. Dysregulation of Signalling Pathways in Cutaneous Malignant Melanoma

Melanoma development results from accumulated genetic alterations and activation of main signalling pathways in melanocytes (Thompson *et al*., 2005), including the mitogen-activated protein kinase (MAPK)/extracellular signal-regulated kinase (ERK) pathway and the phosphatidylinositol 3-kinase (PI3K)/ protein kinase B (AKT) pathway, summarized below.

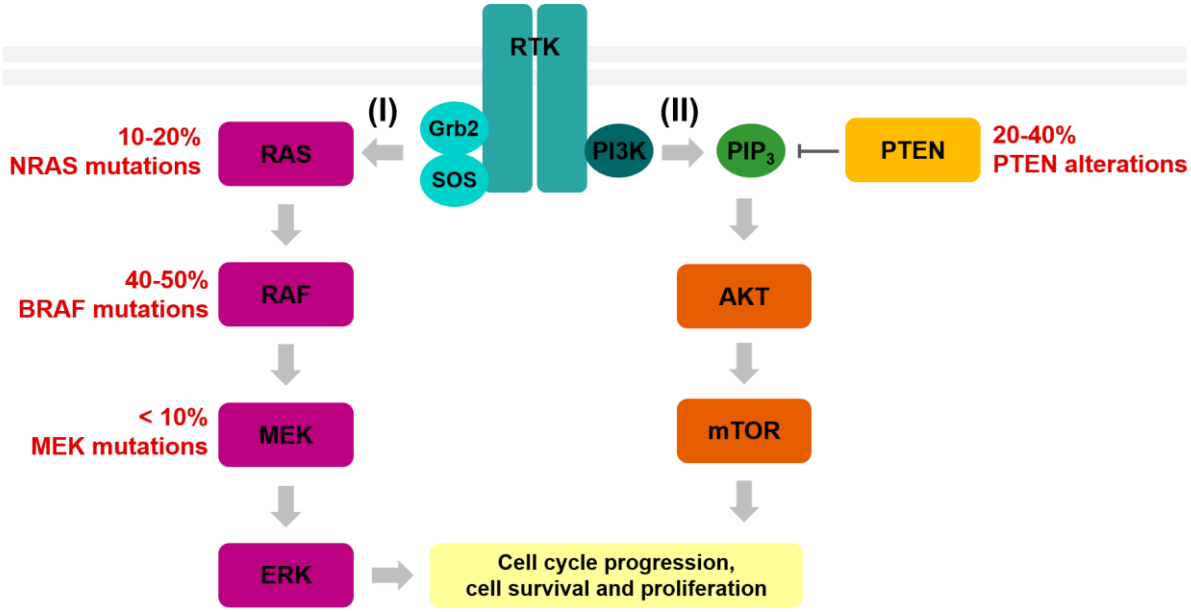

Figure 1.3. Diagram of the MAPK/ERK and PI3K/AKT pathways and common genetic alterations in cutaneous melanoma.

(**I**) Upon Receptor Tyrosine Kinase (RTK) activation, association of the adaptors Grb2 and SOS leads to RAS activation, which in turn results in subsequent activation of a downstream cascade core module. This core modules consists of three kinases: RAF (which exists in 3 isoforms: ARAF, BRAF and CRAF) that phosphorylates and activates MEK, which in turn activates ERK. This leads to transcription factor activation, which can ultimately lead to cell proliferation and survival. (**II**) RTK activation also leads to recruitment of PI3K to the cellular membrane, resulting in the production of PIP_3, which in turn drives the recruitment of a subset of signalling proteins, including AKT. Activation of AKT and mTOR leads to activation of downstream targets, which can ultimately result in cell cycle progression and cell survival. The tumour suppressor PTEN counteracts the PI3K/AKT pathway through PIP_3 dephosphorylation, thus inhibiting recruitment and activation of AKT, inactivating the pathway. The most common alterations in components of MAPK/ERK and PI3K/AKT pathways in cutaneous melanoma are shown in red. Adapted from (Solus and Kraft, 2013).

1.1.3.1. Dysregulation of the MAPK/ERK Pathway in Cutaneous Malignant Melanoma

The MAPK/ERK pathway is one of the primordial signalling systems present in all eukaryotes, controlling such fundamental cellular processes as cell proliferation, differentiation, senescence, survival and apoptosis (Kolch, 2000). The basic arrangement initiates with the interaction of an extracellular ligand with a receptor tyrosine kinase (RTK) and association of the adaptors growth factor receptor-bound protein 2 (Grb2) and son of sevenless (Sos), which activates rat sarcoma proteins (RAS) – members of the small GTPase family of proteins, whose activation depends on guanosine diphosphate (GDP) switch to guanosine triphosphate (GTP) –, that activate a downstream cascade core module. The core module consists of three kinases: rapidly accelerated fibrosarcoma (RAF) (which exists in 3 isoforms: ARAF, BRAF and CRAF), that phosphorylates and activates MAPK/ERK kinase (MEK), which in turn activates ERK (Kolch, 2000). Upon activation, ERK translocates to the nucleus, phosphorylating and activating downstream targets, such as transcription factors (Smalley, 2003). This signalling cascade can ultimately induce cell cycle progression (Katz *et al*., 2007) (Figure 1.3.).

The molecular pathogenesis of CMM is strongly correlated with a constitutive activation of the MAPK/ERK pathway, that appears early in tumorigenesis and is preserved through progression (Omholt *et al*., 2003). Such phenomenon is probably a consequence of mutations in upstream components of this pathway.

An evaluation of mutations in components of the MAPK/ERK pathway in a large panel of common cancers showed that 40 to 50% of melanomas, and 7 to 8% of all cancers, carry an activating mutation in the gene encoding the protein kinase BRAF (a protein that shows higher kinase activity compared to the other RAFs – ARAF and CRAF). Additionally, 90% of reported *BRAF* mutations result in a substitution of valine to glutamic acid at amino acid 600 (the V600E mutation, giving rise to the designated $BRAF^{V600E}$ protein). This mutation increases catalytic activity of BRAF, constitutively activating it, leading to downstream propagation of the MAPK/ERK pathway signalling (Flaherty *et al*., 2010). Mutations in ARAF and CRAF are uncommon.

In CMM, Neuroblastoma RAS Viral Oncogene Homolog (*NRAS*) mutations stand as the most common in RAS-family members – with mutations in other RAS-family members, *KRAS* and *HRAS*, being relatively rare (Smalley, 2003). Additionally, melanomas with wild-type BRAF often display activating mutations in *NRAS* gene (Solus and Kraft, 2013). The prevalence of activating mutations in the gene coding for NRAS protein, predominantly at codon 61, is close to 30% in CMM (Omholt *et al*., 2002). Such mutation constitutively activates NRAS, leading to downstream signal transduction in the MAPK/ERK pathway.

Mutations in other components of the MAPK/ERK pathway were also identified, including MEK1 and MEK2 coding genes – Dual Specificity Mitogen-Activated Protein Kinase Kinase 1 (*MAP2K1*) and Dual Specificity Mitogen-Activated Protein Kinase Kinase 2 (*MAP2K2*), although found to be less frequent in CMM cases (Nikolaev *et al*., 2011). These mutations also result in constitutive downstream signalling.

In melanocytes presence of mutations in components of MAPK/ERK pathway, such as in *BRAF* or *NRAS* genes, appears to induce oncogene-induced senescence (an irreversible form of cell cycle arrest). Generally, to induce malignant transformation of melanocytes to melanoma, additional gene alterations are required, such as in Cyclin-Dependent Kinase Inhibitor 2A (*CDKN2A*) (leading to

inactivation of the *CDKN2A*-encoded protein p16INK4A), *p53* and/or Phosphatase and Tensin Homologue (*PTEN*) gene, affecting the tumour suppressor activity of respectively encoded proteins (Ko *et al*., 2010).

1.1.3.2. Dysregulation of the PI3K/AKT Pathway in Cutaneous Malignant Melanoma

Similarly to the MAPK/ERK pathway, the PI3K/AKT pathway is initiated by activation of a receptor tyrosine kinase through its interaction with an extracellular ligand. Activation of receptor tyrosine kinases leads to recruitment of PI3K to the cellular membrane, which results in the production of the second messenger phosphatidylinositol-3,4,5-triphosphate (PIP_3). In turn, PIP_3 drives the recruitment of a subset of signalling proteins, including kinase-3′-phosphoinositide-dependent kinase 1 (PDK1) and AKT. AKT can then be phosphorylated and activated by PDK1 and mechanistic target of rapamycin complex 2 (mTORC2) and thereafter activate downstream targets, ultimately regulating several cell processes involved in cell cycle progression and cell survival (Chang *et al*., 2003) (Figure 1.3.).

The PI3K/AKT pathway is counteracted by the tumour suppressor PTEN. PTEN regulates PI3K signalling by dephosphorylating the lipid signalling intermediate PIP_3, thus inhibiting recruitment and activation of AKT, inactivating the pathway (Simpson and Parsons, 2001). *PTEN* mutations, deletions or methylation of its promoter result in PTEN loss, ultimately leading to PI3K/AKT signalling activation and cell survival. The rate of such alterations in metastatic CMM is over 20% (Aguissa-Touré and Li, 2012) and is correlated with increased melanoma invasive capacity and decreased overall survival of CMM patients carrying the $BRAF^{V600E}$ mutation (Bucheit *et al*., 2014).

1.1.4. Therapeutic Options for Cutaneous Malignant Melanoma Patients

A brief overview of the main current therapeutic options for cutaneous melanoma patients is presented below, focusing on surgery, chemotherapy, targeted-therapy, immunotherapy and immunostimulants.

The gold standard treatment option for patients with local CMM consists of surgical excision of the primary tumour, with safety margins. Treatment with this method leads to a very good prognosis. Surgery may also be performed in advanced metastatic disease, for complete lymph node dissection – in cases where the sentinel lymph node (first lymph node to which transformed cells are most likely to spread from a primary tumour) is found positive for metastases. However, after this treatment patients will still have a poor prognosis (Schadendorf *et al*., 2015). In some more advanced stages surgery can also be performed, solely as a palliative measure (e.g. to remove obstruction in the bowel), but systemic drug treatment is often used (Schadendorf *et al*., 2015).

Chemotherapy has been, for several decades, used as palliative treatment of patients with metastatic melanoma, either as a systemic mono-therapy – commonly single agent dacarbazine, temozolomide and fotemustine – or combination therapy of chemotherapeutic agents (Thompson *et al*., 2005). However, such regimens result in low therapy response rates (5-12%), with a median overall survival inferior to one year (Garbe *et al*., 2011).

The molecular pathways identified as being central to melanoma development and progression are subject of intense investigation for their potential in “targeted-therapy”. This is approached by design of small molecules, aiming to inhibit specific molecules present in cells driving aberrant proliferation and

growth. High specificity is often pursued, since it may represent elevated efficiency, with fewer side effects than those reported for cytotoxic chemotherapies.

The first targeted-therapies to demonstrate substantial efficacy against advanced CMM with the mutated form of BRAF protein $BRAF^{V600E}$ were two adenosine triphosphate-competitive inhibitors of $BRAF^{V600E}$ – vemurafenib and dabrafenib –, both approved by drug regulatory authorities (Lo *et al*., 2014). These compounds bind to $BRAF^{V600E}$ monomers, inhibiting their activity. Studies comparing the two BRAF inhibitors with the chemotherapy agent dacarbazine showed improved response rates and improved progression-free and overall survival, with the targeted-therapies (Chapman *et al*., 2011; Hauschild *et al*., 2012).

Two inhibitors (cobimetinib and trametinib) targeting the wild type MEK protein (downstream of BRAF/CRAF in the MAPK/ERK pathway) have also been developed and approved, showing an overall survival benefit compared to dacarbazine, in the treatment of metastatic BRAF-mutant CMM (Carlino *et al*., 2015).

Interestingly, BRAF inhibitors possess the remarkable and paradoxical feature of triggering MAPK/ERK pathway reactivation (Heidorn *et al*., 2010) – briefly discussed below. Considering this paradoxical event, the two MEK inhibitors have also been approved for use in patients with mutated BRAF, in combination with vemurafenib or dabrafenib (Lo *et al*., 2014). Although BRAF inhibitors, as well as MEK inhibitors, can be used alone or in combination as described, studies point out that combination therapy is more advantageous than targeted-monotherapy in terms of toxicity and efficacy (Long *et al*., 2014a; Larkin *et al*., 2015).

Attempts to target the major defences that melanoma cells display against an effective immune response have been pursued, counteracting the development of host tolerance to melanoma antigens, mainly due to the production of immunosuppressive factors by melanoma cells. Given that, immunotherapy options continue to be investigated intensively, regarding both adjuvant and advanced CMM settings.

In short, parallel to antigen presentation, activation of T cells (one of the main classes of players in the anti-cancer immune response) requires a costimulatory interaction between T cells and antigen-presenting cells, which can be mediated by either stimulatory or inhibitory receptor-ligand pairs known as “immune-checkpoints” (Sharpe, 2009). Two of the best studied checkpoints involve cytotoxic T lymphocyte antigen-4 (CTLA-4), programmed cell death-1 (PD-1) and its ligand (PDL-1). The most successful immunotherapy approaches to date have been immune checkpoint inhibition, through the administration of antibodies blocking CTLA-4 in advanced CMM – with improved overall survival (Hodi *et al*., 2010) –, as well as antibodies blocking PD-1 and its interaction with PDL-1 – with increased response rate and overall survival in wild type BRAF CMM patients, compared to the chemotherapy agent dacarbazine (Robert *et al*., 2014; Weber *et al*., 2015).

Approaches designed to modulate the immune system to induce an anti-cancer response in CMM patients also include non-specific immunostimulants such as interleukin 2 (IL-2) and interferon alpha (IFNα). Compilation of studies comparing combination therapy of chemotherapy agents, IL-2 and low dose IFNα with the use of chemotherapy agents in monotherapy regimens shows that, despite

moderately improved response rates, increased toxicity and absence of increased overall survival are evident with combination therapy (Bhatia *et al*., 2009).

1.1.5. Therapy Resistance in Cutaneous Malignant Melanoma

Resistance to therapies consists a major problem for CMM treatment. Chemotherapy with dacarbazine and temozolomide has been unsuccessful mainly due to unclear innate and/or acquired resistance of melanoma cells to treatment. Suggested mechanisms that contribute to chemoresistant phenotypes include changes in drug transport and metabolism. This may occur through elevated expression and activity of cell membrane efflux pumps, enzymatic detoxification – e.g. with the involvement of enzyme glutathione-S-transferase, by conjugation of certain chemotherapeutic agents to glutathione –, or through disruption of drug-target interactions possibly due to alterations in the targets which results in reduced binding affinity (Helmbach *et al*., 2003). Anti-apoptotic pathways and enhanced DNA repair in cancer cells also play roles in unresponsiveness to chemotherapy in CMM (Grossman and Altieri, 2001).

Despite the encouraging response rate and improvement in progression-free survival in ~80% of patients carrying the $BRAF^{V600E}$ mutation treated with BRAF inhibitors vemurafenib and dabrafenib, the majority of such patients exhibits disease progression following tumour regression, within 6-8 months (Chapman *et al*., 2011; Hauschild *et al*., 2012). Similarly, one-third of BRAF-mutant metastatic melanoma patients treated with combined BRAF and MEK inhibitors shows disease progression within 6 months (Long *et al*., 2014b). Treatment options for these patients remain limited, motivating the elucidation of underlying intrinsic and acquired resistance mechanisms.

Tumours with mutant BRAF are dependent on the MAPK/ERK signalling pathway for their growth. However, even though BRAF inhibitors prevent ERK signalling in cells with mutant BRAF, an unexpected enhancement effect of ERK signalling has been shown (Poulikakos *et al*., 2010). Given that, among the resistance mechanisms under investigation, reactivation of MAPK/ERK pathway in resistant tumours stands as one of the major phenomenon taking place. Gatekeeper mutations in BRAF, which would prevent vemurafenib from binding to BRAF, have not been observed as a causal event of this phenomenon (Nazarian *et al*., 2010). Instead, currently available data suggests other events namely, genetic alterations such as gene amplification (e.g. amplification of BRAF) (Shi *et al*., 2012), CRAF overexpression (leading to BRAF signalling bypass) (Poulikakos *et al*., 2011) mainly in the co-existence of RAS mutations (Dumaz *et al*., 2006) , secondary mutations in NRAS (Nazarian *et al*., 2010) or novel mutations in MEK (Wagle *et al*., 2011), as well as emergence of novel abnormal hyperactive forms of BRAF that dimerize in a RAS-independent manner (e.g. truncated BRAF) (Poulikakos *et al*., 2011).

Aside from reactivation of MAPK/ERK pathway, other targeted-therapy resistance mechanisms have been proposed, such as the activation of alternative survival pathways (e.g. PI3K/AKT pathway activation), induced by increased expression of receptor tyrosine kinases (Villanueva *et al*., 2010; Nazarian *et al*., 2010) and PTEN alterations – given the lost PTEN counteractive role of PI3K/AKT pathway (Paraiso *et al*., 2011).

Tumour microenvironment-derived acquired resistance appears as another resistance mechanism (Straussman *et al*., 2012).

1.2. Non-Coding RNAs

1.2.1. A Class of Functional RNAs: Non-Coding RNAs

RNA molecules were originally considered to mainly function as intermediates between genes and respectively encoded proteins. However, since the discovery of ribosomal RNA (Palade, 1955) and transfer RNA (Hoagland *et al.*, 1958) in the 1950s, a functional role related to the regulation of genome organization and gene expression has been attributed to RNA molecules that do not encode proteins – designated non-coding RNAS (ncRNAs). Nevertheless, the diversity, biological relevance and myriad of functional roles currently attributed to ncRNAs were only started to be uncovered in recent years. It was only after the publication of genome-wide sequencing data, that it came to the scientific community's awareness that organism complexity and number of protein-coding genes are not necessarily directly proportional. This became evident after the release of the Human genome sequencing data (Venter *et al*., 2001; Lander *et al*., 2001), facing that the number of protein-coding genes in the Human genome – approximately 20.000 – is very close to that found in less complex organisms (Goodstadt *et al*., 2006). Given that, the observed developmental complexity of an organism and the relative amount of non-protein coding DNA (performing its functional role mainly through transcription into ncRNAs) were then proposed to be correlated (Taft *et al*., 2007).

Improvements in RNA sequencing technology enabled the application of high-throughput methods in the generation and analysis of data by international research collaborations, such as ENCyclopedia Of DNA Elements (ENCODE). This lead to findings such as that the majority of bases in the Human genome is associated with at least one primary transcript, assessing that circa three-quarters of the genome is transcribed into ncRNAs (ENCODE Project Consortium, 2007).

ncRNAs are originally described as transcripts lacking an evident protein-coding function, i.e. lacking a long open reading frame (ORF) (traditionally >100 codons) and/or not displaying codon conservation (Morris and Mattick, 2014). While recent studies provide evidence that most ncRNAs do not encode proteins, a few functional peptides have been shown to arise from translation of transcripts identified as ncRNAs (Banfai *et al*., 2012).

Non-coding RNAs regard to two major classes: short ncRNAs (sncRNAs) and long ncRNAs (lncRNAs), broadly and almost arbitrarily defined according to the transcript's length, having <200 and >200 nucleotides long, respectively (Morris and Mattick, 2014). This feature is not regarded to as being entirely arbitrary, since it serves as a threshold, allowing empirical separation of RNAs in common experimental methodologies. The short ncRNAs class comprises the relatively well studied subclass of microRNAs (miRNAs), as well as small nucleolar RNAs (snoRNAs), small nuclear RNAs (snRNAs), piwi-interacting RNAs (piRNAs), small interfering RNAs (siRNAs) and transcription initiation RNAs (tiRNAs). The lncRNAs class comprehends two broad subclasses: large intergenic ncRNAs (lincRNAs) and ncRNAs that overlap with other transcripts, in either a sense or antisense orientation (in focus in this thesis) and transcribed pseudogenes.

1.2.2. Long Non-Coding RNAs

The advent of growing sensitivity of RNA sequencing methods, as well as computational prediction techniques (Clark *et al*., 2015) is enabling the increasing identification of such a diverse class of RNA transcripts as lncRNAs, including the detection of transcripts arising from lowly expressed genes.

This has stimulated interest and focus in further characterizing and understanding biology roles played by lncRNAs.

1.2.2.1. Subclasses of Long Non-Coding RNAs

lncRNAs can be divided into subclasses, mainly regarding its genomic origin and orientation, often with respect to that of protein-coding transcripts, with the commonly established subclasses being: large intergenic ncRNAs (lincRNAs) – whose genomic origin does not overlap with that of any known coding or non-coding transcripts –, and lncRNAs that overlap with other transcripts, including antisense (asRNAs), sense overlapping and sense intronic lncRNAs. It should be noted that, according to current knowledge, there is no evidence indicating that this classification respects to functional role differences (Morris and Mattick, 2014).

1.2.2.2. Features of Long Non-Coding RNAs

Many lncRNAs are usually transcribed by RNA Polymerase II (RNA Pol II), are often 5'-capped, 3'-polyadenylated and spliced. These features recapitulate know mRNA characteristics, however, some unique general trends of lncRNAs (comparing to mRNAs) can be listed, such as the absence of a translated ORF, the tendency of being shorter in length – usually with fewer but longer exons – and the lower overall expression levels (Derrien *et al*., 2012; Washietl *et al*., 2014).

While the level of expression of many lncRNAs appears to be lower than mRNAs in whole tissues, lncRNAs are highly expressed and easily detectable in particular cells, with Human and Mouse genome studies showing that lncRNAs have a higher specificity, regarding tissue, cell type and cellular compartment expression, comparing to expression of protein-coding transcripts (Ravasi *et al*., 2006; Mercer *et al*., 2008; Djebali *et al*., 2012).

It is clear that lncRNAs display a wide range of evolutionary conservation – from those categorized as ultraconserved (Calin *et al*., 2007) to those that are primate-specific (Tay *et al*., 2009). Although, the majority of lncRNAs exhibit relatively low evolutionary conservation (Johnsson *et al*., 2014). However, studies provide evidence that a lack of conservation does not imply a lack of function (Pang *et al*., 2006).

1.2.2.3. Mechanisms of Regulation Mediated by Antisense Non-Coding RNAs: an Overview

Multiple studies have shown evidence that more than 63% of transcripts have antisense partners, many of which do not encode proteins (Katayama *et al*., 2005; Carninci *et al*., 2005; Li and Ramchandran, 2010; Nishizawa *et al*., 2012). The magnitude of identified arising antisense transcripts has stimulated attention to such class of RNA molecules, namely to non-protein coding antisense RNAs.

asRNAs are transcribed from the opposite DNA strand of that of a sense transcript (which can either be a protein-coding or non-protein-coding RNA) (Katayama *et al*., 2005).

Antisense RNAs can exert their function in a cis- or in a trans-acting manner, whether the interacting sense transcript is transcribed from the same genomic region, or from a distant locus, respectively. Despite low global expression levels of asRNA, a plausible biological role played by cis-acting transcripts can be hypothesized: given that there are two copies of DNA for a given gene in a cell, two antisense lncRNA molecules are theoretically sufficient to interact with the two gene copies and elicit a regulatory effect (Faghihi and Wahlestedt, 2009). Cis-acting antisense transcripts can be further categorized according to their genomic origin, regarding proximity between sense and antisense partners in the

genome (Figure 1.4.): nearby to head, when the 5' end of the sense gene is in proximity to the 5' end of the antisense gene (commonly with bidirectional promoters); nearby to tail, when the 3' end of the sense gene is in proximity to the 3' end of the antisense gene; head-to-head, when the 5' ends of both sense and antisense genes overlap (divergent); tail-to-tail, when the 3' ends of both sense and antisense genes overlap (convergent); and fully overlapping, when the sense gene completely overlaps with the antisense one (Villegas and Zaphiropoulos, 2015). Partially or fully overlapping asRNAs share complementarity to the sense expressed transcript and are found to overlap promoters, exons, 5'- and 3'-UTRs, as well as introns.

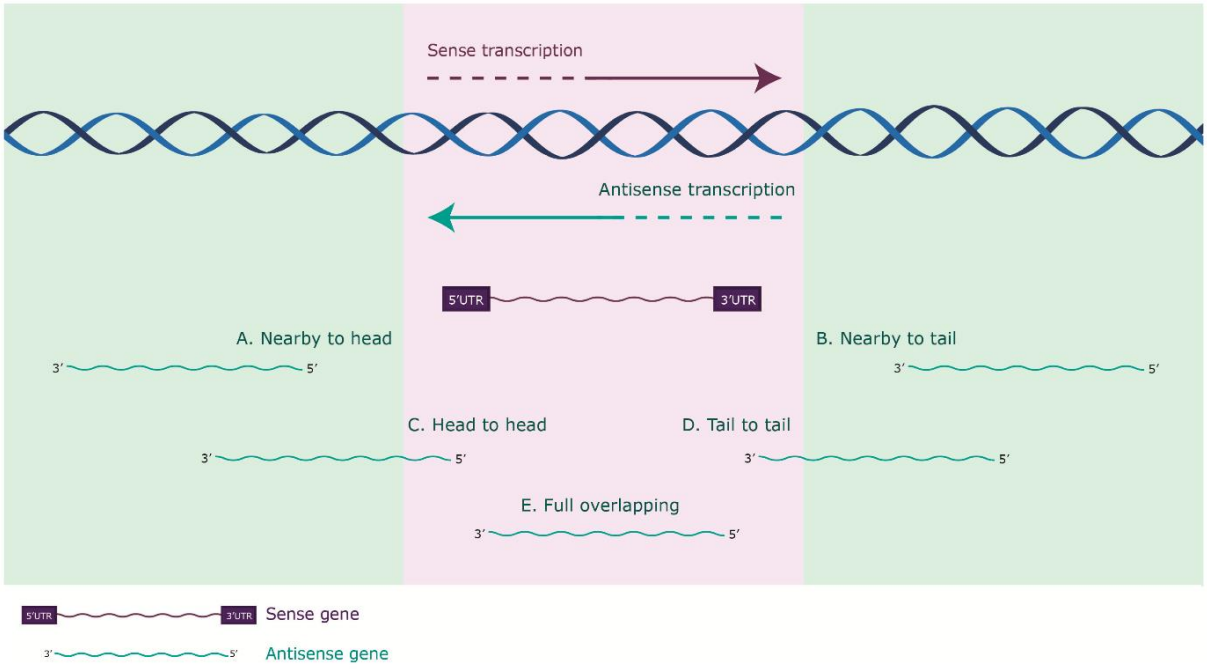

Figure 1.4. Categorization of antisense transcripts according to genomic origin.
Categorization of antisense transcripts according to their genomic origin, regarding proximity between sense (depicted in purple) and antisense non-coding (depicted in green) genes in the genome. **(A)** Nearby to head, the 5' end of the sense gene is in proximity to the 5' end of the antisense gene; **(B)** Nearby to tail, the 3' end of the sense gene is in proximity to the 3' end of the antisense gene; **(C)** Head-to-head, the 5' ends of both sense and antisense genes overlap (divergent); **(D)** Tail-to-tail, the 3' ends of both sense and antisense genes overlap (convergent); **(E)** Full overlapping where the sense gene completely overlaps with the antisense gene. Adapted from (Villegas and Zaphiropoulos, 2015).

Basal expression levels of sense transcripts and respective antisense non-coding transcripts may be positively or negatively correlated in different tissues and cell lines (Katayama *et al*., 2005). Moreover, antisense lncRNAs are functionally very diverse, as they can act as positive or negative modulators of expression of their counterpart sense transcripts (Numata and Kiyosawa, 2012).

A myriad of mechanisms has been proposed for asRNA-mediated regulatory mechanisms, acting at nearly every level of gene regulation. As such, asRNA-mediated regulatory mechanisms can be divided in three main categories, briefly approached below: pretranscriptional asRNA-mediated regulation, transcriptional asRNA-mediated regulation and posttranscriptional asRNA-mediated regulation (Villegas and Zaphiropoulos, 2015) (Figure 1.5.).

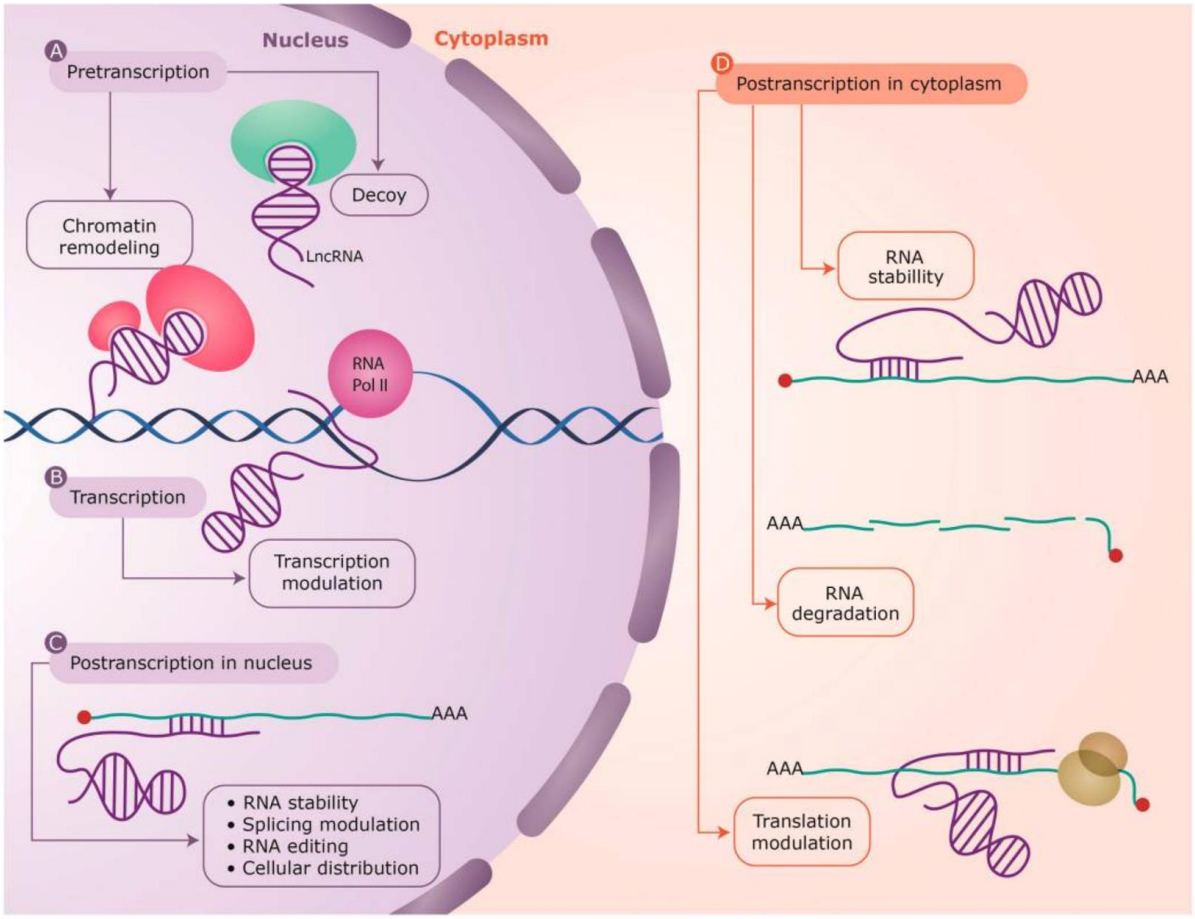

Figure 1.5. Antisense lncRNA-mediated regulatory mechanisms found at every level of gene regulation. Representation of antisense lncRNA-mediated regulatory mechanisms. **(A)** Pretranscriptionally, antisense lncRNAs can act as protein guides, scaffolds or decoys (as depicted), recruiting proteins into specific parts of the genome or holding proteins away from chromatin; **(B)** Antisense lncRNAs may also be involved in the modulation of an ongoing-transcriptional process, affecting gene expression; **(C, D)** Posttrancriptionally, antisense lncRNA can affect sense RNA structure (interfering with RNA stability, splicing or RNA editing), or cellular compartmental distribution, either in the nucleus or in the cytoplasm. LncRNAs are depicted in purple, and the interacting protein factors in green and red. Sense RNAs are shown as green lines and the base pair interactions highlighted by short purple lines. RNA polymerase II (RNA pol II) is depicted in pink, genomic DNA is depicted as a blue helix and a translating ribosome on the mRNA is depicted in yellow. Adapted from (Villegas and Zaphiropoulos, 2015).

Pretranscriptionally, antisense lncRNAs can act as guides or scaffolds of proteins into specific parts of the genome, or as decoys keeping proteins away from chromatin. Such regulatory mechanisms rest upon the formation of RNA:protein complexes, as lncRNAs – namely antisense lncRNAs – comprise distinct protein-binding domains (Mercer and Mattick, 2013). Specific RNA:DNA interactions can efficiently and selectively recruit proteins to genomic loci. As RNA-interacting proteins are often found to be key regulators of gene transcription – namely epigenetic factors (Mercer and Mattick, 2013) – antisense lnRNAs in the nucleus can act as regulators of their counterpart expression by modulating chromatin structure and bridging epigenetic effectors and regulatory complexes at specific loci (Magistri *et al.*, 2012). Proteins found among such key epigenetic factors are the following: DNA methyltransferases, such as DNA methyltransferase 3A (DNMT3A); members of the Polycomb Repressive Complex PRC2, such as the histone methyltransferase enhancer of zeste homolog 2

(EZH2), which elicits histone H3 lysine 27 trimethylation (H3K27me3); or G9a/GLP methyltransferases, targeting histone H3 lysine 9 (H3K9).

The X-inactivation centre illustrates how an intricate network of lncRNAs regulates gene expression pretranscriptionally, being pivotal in such a fundamental process as the inactivation of one X-chromosome in an early development stage. Such process involves asymmetric expression of the lncRNAs X-inactive specifc transcript (*Xist*) and reverse of *Xist* (*Tsix*) in a pair of X-chromosomes. At the onset of X-inactivation, *Xist* accumulates on one of two Xs, working as a functional lncRNA molecule that recruits the PRC2 towards one of the female X-chromosomes, in cis, establishing and spreading the H3K27me3 repressive chromatin mark, leading to heterochromatinization and inactivation of the chromosome. In the other X-chromosome, the antisense lncRNA *Tsix* is transcribed, negatively regulates *Xist* by recruiting the DNA methyltransferase DNMT3A in cis. This induces DNA methylation at the *Xist* promoter and protects heterochromatinization of the X-chromosome by *Xist*, allowing such chromosome to remain active (Sun *et al*., 2006).

Even though the genomic arrangement of sense:asRNA transcription suggests a more plausible regulatory role in a cis-acting manner, trans-regulatory mechanisms have also been identified and described for antisense lncRNAs. The functional mechanism of the lncRNA HOX Antisense Intergenic RNA (*HOTAIR*) exemplifies a trans-acting asRNA-mediated pretranscriptional regulatory role played by an antisense ncRNA. *HOTAIR* is transcribed from the Homeobox Protein C (*HOXC)* locus, one of the identified human Homeobox (*HOX*) loci, crucial in the morphogenesis process of development. *HOTAIR* represses transcription in trans across 40 kilobases of the Homeobox Protein D (*HOXD)* locus, by interacting with PRC2 and establishing the H3K27me3 chromatin mark at *HOXD* locus. Thus, this antisense lncRNA demarcates chromosomal domains of gene silencing at a distance (Rinn *et al*., 2007).

Antisense lncRNAs may also be involved in the modulation of an ongoing-transcriptional process, affecting gene expression. According to this mechanism, the act of transcription in the antisense direction, but not the antisense RNA molecule *per se*, modulates transcription of the sense gene. Transcription in the antisense direction is suggested to exert alterations in gene expression in the event of transcriptional collision (Faghihi and Wahlestedt, 2009). An *in silico* study showed that, in humans and in mice, the expression levels of cis-acting asRNAs decreases as the length of the overlapping region increases (Osato *et al*., 2007). Such observation may suggest a putative clash of RNA polymerases, to the point that the probability of collision increases as the length of the overlapping region increases.

Posttranscriptionally, functions of antisense lncRNAs can be exerted through RNA:RNA interactions, affecting sense RNA structure or cellular compartmentalization, either in the nucleus or the cytoplasm. Given the sequence complementarity found among antisense and sense partner transcripts, RNA duplexes tend to be formed. This can have different posttranscriptional outcomes, all of which modulate sense RNA expression: interfering with splicing, RNA editing, stability, subcellular distribution, transport, nuclear retention or even modulating translation of the sense RNA transcripts (Faghihi and Wahlestedt, 2009).

An example of antisense lncRNA-mediated posttrancriptional modulation of sense RNA, namely through regulation of RNA stability, is the PTEN pseudogene-encoded antisense RNA β (*PTENpg1*

asRNA β). This antisense lncRNA is transcribed from the reverse strand of the locus from which the lncRNA PTEN pseudogene sense (*PTENpg1 sense*) is transcribed. These transcripts interact through an RNA:RNA pairing interaction, maintaining stable levels of *PTENpg1 sense* in the cytoplasm. Ultimately, such interaction affects the stability of Phosphatase and Tensin Homolog (*PTEN*) mRNA through microRNA (miRNA) sponge activity, by sequestering *PTEN*-targeting miRNAs away from *PTEN* protein-coding transcript. This results in an increased amount of PTEN protein (Johnsson *et al*., 2013).

1.2.3. Biological Settings of Long Non-Coding RNAs

As the extensive diversity found at the level of cell phenotypes lays upon intricate and complex networks of regulation of gene expression, most of the mammalian genome and indeed that of all eukaryotes is expressed in a cell- and tissue-specific manner. While non-protein-coding sequences increasingly dominate the genomes of multicellular organisms as their complexity increases, the number of protein-coding genes remains relatively static. (Amaral and Mattick, 2008). Given that, there is growing evidence that the observed transcription of non-coding sequences, namely of lncRNAs, is involved in the regulation of fundamental cell biological processes associated with differentiation and development. Such processes include maintenance of telomeric structure (Silanes *et al*., 2010), alternative splicing (Tripathi *et al*., 2010), retinal, erythroid and breast development (Young *et al*., 2005; Hu *et al*., 2011; Askarian-Amiri *et al*., 2011), epidermal differentiation (Kretz *et al*., 2013), among many others.

Besides the described involvement of lncRNAs in a multitude of physiological mechanisms, these RNA molecules are also found in association with dysregulation of cellular events tied to pathological conditions, namely to disorders that stand amongst leading causes of death in western societies, including cancer (further discussed below), cardiovascular diseases, such as coronary artery disease, and diabetes (Broadbent *et al*., 2008).

It is increasingly evident that many of the genomic mutations in cancer reside inside regions that do not encode proteins, namely regions that are transcribed into, or directly regulate the expression of, ncRNAs. The recent application of next-generation sequencing to a growing number of cancer transcriptomes has revealed many lncRNAs whose aberrant expression is associated with specific cancer types (Yan *et al*., 2015). Among the few that have been functionally characterized, several have been linked to malignant transformation (Huarte, 2015). Given that, participation of lncRNAs in the regulation of cellular pathways whose disruption is associated with cancer ensures a link between lncRNAs and tumorigenesis. Such pathways relate to chromosome maintenance, transcriptional regulation, mRNA and protein control, apoptosis and senescence (Khorkova *et al*., 2015).

An example of a lncRNA with a vastly characterized oncogenic function is the well-studied Metastasis Associated Lung Adenocarcinoma Transcript 1 (*MALAT1*). This lncRNA has been found to promote cell proliferation and metastasis, and its overexpression has been linked to lung adenocarcinoma, breast, pancreatic, colon, prostate and hepatocellular carcinomas. A single-nucleotide polymorphism in *MALAT1* gene has been associated with hepatocellular carcinoma (Huarte, 2015).

1.2.3.1. Long Non-Coding RNAs in Melanoma

Despite the limited amount of studies focused on the characterization of functional roles of lncRNAs, there is increasing evidence for the involvement of lncRNAs in cancer progression and a role for several lncRNAs in development and progression of melanoma has been suggested.

Examples of melanoma-related lncRNAs associated with cellular proliferation, migration and apoptosis are presented below, focusing on the lncRNAs *BANCR*, *GAS5* and *SAMMSON*.

Activating mutations in the *BRAF* gene, namely mutations that give rise to expression of active mutant $BRAF^{V600E}$ protein, have previously been implicated in development of CMM – as discussed in subsection 1.1.3.1. Transcriptome analysis of $BRAF^{V600E}$-mutant human melanomas revealed that induced expression of $BRAF^{V600E}$ regulates expression of ~100 lncRNAs. One of the transcripts most highly induced by oncogenic BRAF, which is recurrently overexpressed in melanoma, is BRAF-regulated lncRNA 1 (*BANCR*). This lncRNA is known to regulate a set of genes involved in cell migration and is required for full migratory capacity of melanoma cells (Flockhart *et al*., 2012). Additionally, *BANCR* was demonstrated to activate ERK1/2 and CRAF *in vitro* and *in vivo*, thus being implicated in regulation of MAPK/ERK pathway, which led to proliferation of melanoma cells. Its expression was also directly correlated with tumour stage (Li *et al*., 2014). Altogether, a novel lncRNA-mediated regulatory mechanism of melanoma proliferation has been proposed.

The Growth Arrest-Specific Transcript 5 (*GAS5*) is a lncRNA whose expression has been shown to be downregulated in melanoma cell lines. It has been demonstrated that suppression of *GAS5* leads to higher ability of melanoma cells to migrate. Additionally, induced overexpression in such cells reduced migratory ability, partially as a consequence of decreased expression and activity of matrix mettaloproteinase 2 protein (MMP) – a protein required for breakdown of extracellular matrix and cell migration (Chen *et al*., 2016). Ultimately, *GAS5* may function as a tumour suppressor associated with melanoma.

Survival-Associated Mitochondrial Melanoma-Specific Oncogenic Non-Coding RNA (*SAMMSON*) is located downstream of the melanoma-specific oncogene Melanogenesis-Associated Transcription Factor (*MITF*) and is co-amplified in around 10% of all melanoma cases. Mechanistically, the lncRNA *SAMMSON* acts in trans as a decoy, by targeting p32 – a master regulator of mitochondrial homeostasis and metabolism associated with cell apoptosis. This increases mitochondrial targeting and pro-oncogenic function of p32. While expression of *SAMMSON* was detectable in over 90% of human primary melanoma and metastasis, no expression is observed in normal healthy tissue. Knockdown experiments established a role for this lncRNA in melanoma cell viability and growth, irrespective of mutational status of melanoma cells. Additionally, suppression of *SAMMSON* transcript led to enhanced cell sensitivity towards MAPK-targeting therapeutics (Leucci *et al*., 2016; Richtig *et al*., 2017).

1.2.4. Therapeutic Aspects of Long Non-Coding RNAs

The study of ncRNAs, namely lncRNAs, has become increasingly attractive as a starting point for identification of new therapeutic targets and development of new pharmacological compounds, as further efforts are concentrated in the characterization of such RNA molecules. This rests upon observed biological features of lncRNAs, such as the identified functional roles related to the regulation of

expression of a myriad of protein-coding and other non-protein coding genes, in a multitude of biological settings, including many pathological contexts.

Regarding the effects of lncRNAs in gene expression regulation, namely in gene repression, one of the main advantages of lncRNAs as therapeutic targets is that these molecules may allow the indirect manipulation of proteins previously considerable as "undruggable". Such proteins are commonly required to be specifically manipulated and/or activated/upregulated in order to achieve beneficial outcomes in disease management/treatment. Resorting to novel strategies to specifically suppress expression of lncRNAs – easily achieved through oligonucleotide-based drugs –, consequent activation/upregulation of desired genes may be attained. Additionally, blockage of interacting motifs in the structure of lncRNA molecules, as protein-interacting sites, may also be employed to achieve an identical outcome. Moreover, the elevated target-specificity of lncRNAs makes these molecules highly suitable for modulating the expression of one gene or a small group of related genes (Khorkova *et al*., 2015).

Furthermore, the detection of lncRNAs in biological fluids and their vast involvement in pathological settings makes such molecules as ideal candidates for the development of diagnostic assays, namely as prognosis and/or predictive biomarkers (Khorkova *et al*., 2015). Additionally, expression profiling of human tumours based on the expression of ncRNAs, namely lncRNAs, has identified signatures associated with diagnosis, staging, progression, prognosis, and response to treatment (Kim and Reitmair, 2013). As an example, the ncRNA *HOTAIR* (whose functional molecular mechanism was briefly described in subsection 1.2.2.3 of this thesis) was shown to be involved in cancer metastasis, with an up to 2000-fold increased transcription being observed in breast cancer cells over normal breast tissue. As such, the detection of this lncRNA may present a potential application as a marker of prognosis in patients with primary breast cancer (Gupta *et al*., 2010; Kim and Reitmair, 2013).

1.3. C/EBPβ and *C/EBPβ-AS*

1.3.1. C/EBPβ

The CCAAT/enhancer-binding proteins (C/EBPs) are a family of exclusively eukaryotic transcription factors, that bind as dimers to sequence-specific, double-stranded DNA. Such proteins contain a highly conserved C-terminal basic leucine zipper domain (bZIP domain) – involved in dimerization and sequence-specific DNA binding – and a less conserved N-terminal domain – comprising three short motifs, referred to as activation domains, which interact with transcriptional coactivators and components of the basal transcription machinery (Ramji and Foka, 2002). Dimerization is a prerequisite for DNA binding of C/EBPs and because the bZIP domain is conserved, all the C/EBPs are capable of forming intrafamilial homodimers or heterodimers with each other (Vinson *et al*., 1989). Additionally, heterodimerization among C/EBP family members can result in a myriad of regulatory effects on gene expression (Zahnow, 2009). All C/EBP dimers bind to the same DNA consensus sequence: RTTGCGYAAY, where A, T, G and C stand for the nucleotides adenine, thymine, guanine and cytosine, respectively, R stands for nucleotides adenine or guanine, and Y for nucleotides cytosine or thymine (Osada *et al*., 1996).

CCAAT/enhancer-binding protein β (C/EBPβ) is a member of the C/EBP family of proteins and is encoded by an intronless gene – *C/EBPβ* – located in human chromosome 20 at position q13.13,

according to the Genome Reference Consortium Human Build 38 (Human GRCh38/hg38) – University of California Santa Cruz (UCSC) Genome Browser. C/EBPβ is expressed as multiple protein isoforms, including LAP1, LAP2 and LIP (Descombes and Schibler, 1991), either by alternative use of multiple translation initiation codons in the same mRNA (Xiong *et al*., 2011) or via regulated proteolysis (Welm *et al*., 1999). Generally, LAP isoforms are associated with transcriptional activation, whereas LIP isoform is associated with transcriptional repression, counteracting LAP activity (since it lacks the activation domain, acting as a dominant-negative inhibitor of C/EBP function by forming non-functional heterodimers with the other members). The ratio of the activator LAP form to the repressor LIP polypeptide has been shown to increase under a number of conditions, and such changes are likely to be functionally important, resulting in a significantly higher transcriptional activation of downstream target genes (Descombes and Schibler, 1991). Post-translational modifications such as, phosphorylation, acetylation, methylation and sumoylation, play crucial roles in the regulation of C/EBPβ binding, its transcriptional activity, protein-protein interactions and subcellular localization (Zahnow, 2009). C/EBPβ has been implicated in a numerous processes, including cellular differentiation of adipocytes, macrophages and mammary epithelial cells, metabolism regulation and inflammation, and has been attributed a central role in cellular proliferation (Ramji and Foka, 2002).

Oncogene-induced senescence is an irreversible form of cell cycle arrest that can be elicited by overexpression of oncogenes. Increasing evidence implicates senescence as a central tumour suppression mechanism. C/EBPβ was found to be post-translationally activated by oncogenic signals that dysregulate Ras signalling or its effector pathways (e.g., expression of constitutively active forms of Ras or Raf proteins). Moreover, C/EBPβ was identified as an essential component of cellular senescence mediated by Ras^{V12} – an oncogenic mutant form of Ras – in mouse embryo fibroblasts (MEFs) (Sebastian *et al*., 2005). On the other hand, despite tumour suppressor-like activity of C/EBPβ in MEFs, other studies point towards a critical pro-oncogenic function of C/EBPβ in certain cancers. Altogether, there is evidence for positive and negative cell cycle regulation by C/EBPβ, participating in both cellular senescence and oncogenic transformation (Sebastian and Johnson, 2006).

1.3.2. The Long Non-Coding RNA *C/EBPβ-AS*

CCAAT/Enhancer-Binding Protein β Antisense (*C/EBPβ-AS*) is an antisense long non-coding RNA transcribed from the reverse strand of *C/EBPβ* locus (Figure 1.6.). *C/EBPβ-AS* gene overlaps *C/EBPβ* gene head-to-head (5' overlap), extending over 700 bp, according to Human GRCh38/hg38 – UCSC Genome Browser annotations. Currently, there are no publications regarding this antisense lncRNA.

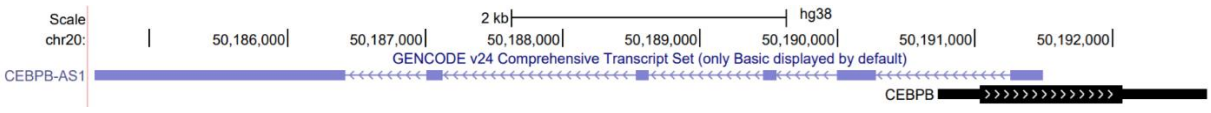

Figure 1.6. Representation of the genomic arrangement of *C/EBPβ* and *C/EBPβ-AS* locus.
Overview of *C/EBPβ* and *C/EBPβ*-AS locus, at chromosome 20, according to Genome Reference Consortium Human Build 38 – UCSC Genome Browser). *C/EBPβ* is depicted in black: thicker line represents the translated region, while thinner lines represent 3' and 5' untranslated regions. *C/EBPβ-AS* is depicted in purple, thicker lines represent the exons (1 to 6), while thinner lines represent the introns (1 to 5). Arrows indicate the strands from which transcripts arise, in a 5' to 3' orientation. The representation displays *C/EBPβ* and *C/EBPβ-AS* 5' end overlap of over 700 bp. Scale bar 2kb.

1.3.3. *C/EBPβ* and *C/EBPβ-AS* in Cutaneous Malignant Melanoma

Regarding C/EBPβ identification as a downstream target of Ras signalling, as well as its association with both cellular senescence and oncogenic transformation, further investigation of this transcription factor in cancer stands as an interesting and probably valuable research subject.

A previous study demonstrates the role of the transcription factor C/EBPβ in the positive regulation of PTEN pseudogene-encoded antisense RNA α (*PTENpg1 asRNA α*) (unpublished data produced by Dan Grandér's group), which in turn plays a part in the repression of *PTEN* expression (Johnsson et al., 2013). Additionally, loss of PTEN is an intensively studied molecular event directly associated with reactivation of the PI3K/AKT signalling pathway (Simpson and Parsons, 2001), ultimately contributing to melanoma development and progression (Aguissa-Touré and Li, 2012). Such observations suggest an association between the transcription factor C/EBPβ and melanoma. However, there are no research publications specifically regarding the study of C/EBPβ regulation in such cancer type.

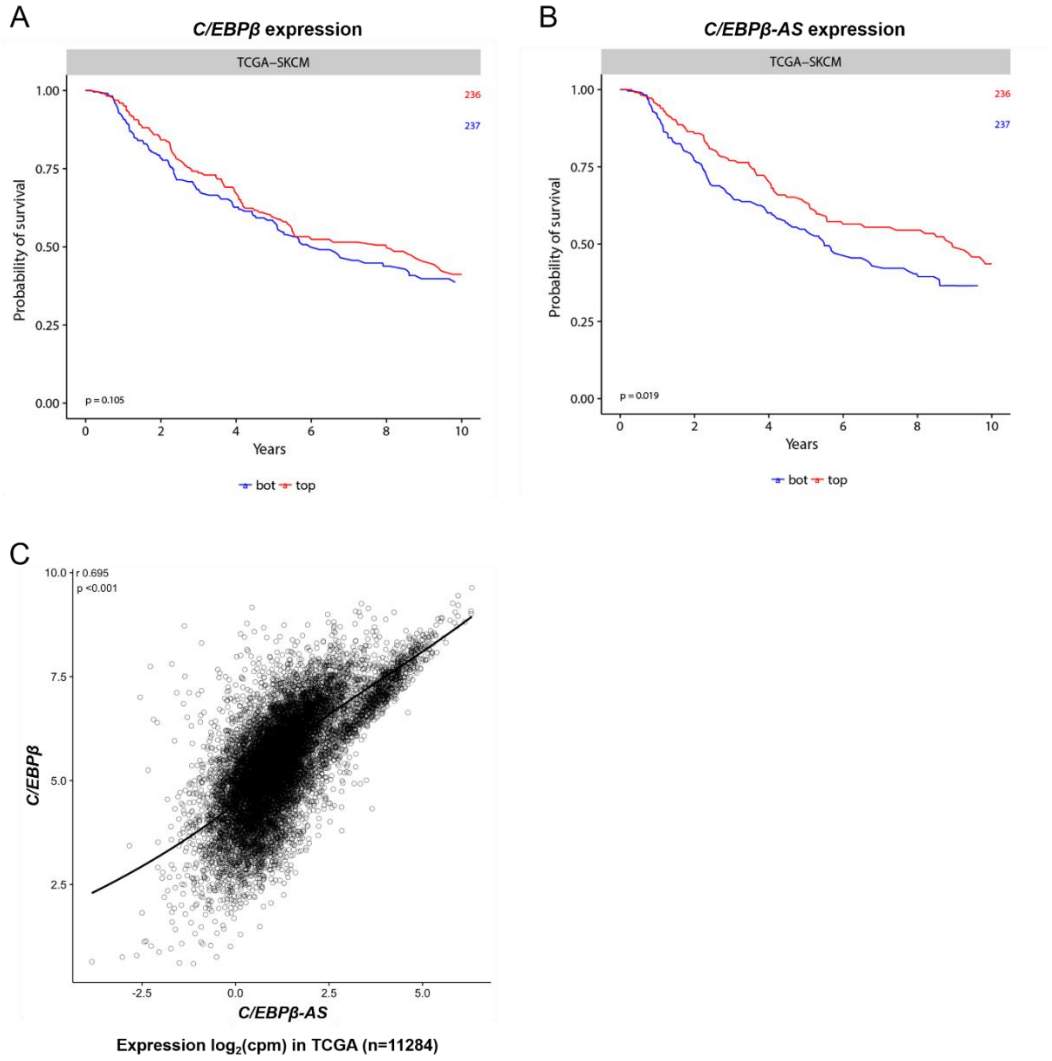

Figure 1.7. *C/EBPβ* and *C/EBPβ-AS* in melanoma.

Bioinformatical analysis of *C/EBPβ* and *C/EBPβ-AS* expression in melanoma (unpublished data analysis by Dan Grandér's group), regarding genomic data published by The Cancer Genome Atlas (TCGA) – a collaboration between the National Cancer Institute (NCI) and the National Human Genome Research Institute (NHGRI), obtained by RNA-sequencing and generated by the University of California Santa Cruz (UCSC). …/…

…/… The expression of *C/EBPβ* or *C/EBPβ-AS* was determined in melanoma patients. The patients were divided according to high (red line) or low (blue line) expression of **(A)** *C/EBPβ* or **(B)** *C/EBPβ-AS* and probability of survival was analysed in Kaplan-Meier plots. Data shows an elevated expression of either gene being correlated with increased patient survival. **(C)** The basal expression of *C/EBPβ* and *C/EBPβ-AS* in TCGA Skin Cutaneous Melanoma cohort (n=11284) was correlated. Expression values are presented as $\log_2$(counts per million). A positive correlation was established between *C/EBPβ* and *C/EBPβ-AS* expression, in TCGA Skin Cutaneous Melanoma cohort.

Bioinformatical analysis of *C/EBPβ* and *C/EBPβ-AS* expression in melanoma was previously performed (unpublished data analysis by Dan Grandér's group). This analysis was performed regarding genomic data published by The Cancer Genome Atlas (TCGA) – a collaboration between the National Cancer Institute (NCI) and the National Human Genome Research Institute (NHGRI), obtained by RNA-sequencing and generated by UCSC. Melanoma patients were divided according to high or low expression (regarding median expression) of *C/EBPβ* or *C/EBPβ-AS* and overall survival was analysed in Kaplan-Meier plots (Figure 1.7. A-B).

Data shows an elevated expression of either gene being correlated with increased patient survival. Additionally, a positive correlation was established between *C/EBPβ* and *C/EBPβ-AS* expression, in TCGA Skin Cutaneous Melanoma cohort (Figure 1.7. C).

1.4. Aims

Considering the diverse reported functions of antisense lncRNAs in gene regulation, great relevance is found in the study of such RNA molecules. Bearing in mind the therapeutic drawbacks of currently implemented main therapeutic approaches available for CMM patients, the identification of novel therapeutic targets and strategies is of great clinical value. Therefore, the characterization of the lncRNA *C/EBPβ-AS* in a cutaneous melanoma context is a promising research quest, not previously regarded.

In this thesis, we aim to study *C/EBPβ-AS*, focusing on three main aspects: to characterize biologically relevant features of *C/EBPβ-AS* transcript, such as subcellular localization, stability and polyadenylation status, to characterize the functional role of *C/EBPβ-AS* in gene regulation, and finally, to investigate *C/EBPβ-AS* therapeutic value in cutaneous melanoma.

2. Materials and Methods

2.1. Cell Culture

2.1.1. Cell Lines

The following cell lines, were used: A-375 (CRL-1619, ATCC) – referred to as A375 – derived from human malignant melanoma harbouring the $BRAF^{V600E}$ mutation and obtained from a 54-year-old female; SK-MEL-24 (HTB-71, ATCC) – referred to as SKMEL24 – derived from human malignant melanoma metastatic to the lymph node and expressing the wildtype form of the protein B-Raf; SK-MEL-28 (HTB-72, ATCC) – referred to as SKMEL28 – derived from human malignant melanoma harbouring the $BRAF^{V600E}$ mutation, obtained from a 51-year-old male; ESTDAB-049 (obtained from the Center for Medical Research, University of Tübingen) derived from human malignant melanoma; MNT1 (generated and provided by Sapienza University) derived from human malignant melanoma metastatic to the lymph node, harbouring the $BRAF^{V600E}$ mutation; HEK293T (CRL-3216, ATCC) – derived from human embryonic kidney, originally generated by transformation of HEK293, a human embryonic kidney cell line – merely used as a cell biology model.

A375 PR1 is a vemurafenib resistant cell line, derived from the parental cell line A375, previously generated by repeated exposure to increasing concentrations of the vemurafenib analogue PLX4720 (a selective inhibitor of $BRAF^{V600E}$). MNT1DR100 – referred to as MNT1R – is a vemurafenib and dabrafenib resistant cell line, derived from the parental cell line MNT1, previously generated by repeated exposure to increasing concentrations of dabrafenib (a selective inhibitor of $BRAF^{V600E}$).

2.1.2. Cell Culture Conditions

All cell lines were cultured in Minimum Essential Media supplemented with 10% (v/v) heat-inactivated fetal bovine serum, 2 mM L-glutamine, 100 µg/ml of streptomycin, 100 U/ml of penicillin, 1 mM Sodium Pyruvate and 1% MEM Non-Essential Amino Acids. Cells were maintained in a controlled humidified atmosphere with 5% (v/v) CO_2, at 37ºC.

All media components were purchased from Thermo Fisher Scientific.

2.2. Transfection of Melanoma Cell Lines; siRNAs

Cells were plated 24 hours prior transfection, at a density of 40,000 cells/ml, in an antibiotic-free medium. Cationic lipid-mediated transfection of cells was performed using Lipofectamine 2000 (Life Technologies) diluted 1:25 in OptiMEM reduced serum medium (Life Technologies) and incubated at room temperature for 5 minutes. Small interfering RNA (siRNA) of interest (final concentration of 10-20 nM) was diluted in OptiMEM medium and added to the Lipofectamine mixture, followed by incubation at room temperature for 15 minutes, prior to addition to each well, dropwise. Cell were harvested 48 hours after transfection.

Customized siRNAs were designed and purchased from Integrated DNA Technologies, using Custom Dicer-Substrate siRNA tool, and pre-designed siRNAs were purchased from Eurofins and Qiagen (summarized in Table 2.1.; Supplementary Table S.1. is an extended version of Table 2.1, with targets sequences of designed siRNAs). A pool of two siRNAs was used for DNMT3A knockdown, aiming to increase knockdown efficiency (according to optimization experiments previously performed by Dan Grandér's group). The siRNA referred to as siCont was used as a non-targeting negative control.

Table 2.1. siRNAs used in cationic lipid-mediated transfection of cells.

Designation of used siRNAs, respective RNA targets and suppliers.

siRNA designation	Target	Supplier
siC/EBPβ-AS	*C/EBPβ-AS*	IDT
siC/EBPβ	*C/EBPβ*	IDT
siEZH2	*EZH2*	Eurofins
siDNMT3a (a pool of two siRNAs was used)	*DNMT3A*	Eurofins
		Qiagen
siG9a	*G9a*	Qiagen
siCont	(non-targeting negative control)	IDT

2.3. RNA Extraction, DNase Treatment and cDNA Synthesis

2.3.1. RNA Extraction

RNA was extracted according to manufacturer's instructions using the NucleoSpin RNA Kit (Macherey-Nagel). This method relies on cell lysis by incubation in a solution containing an elevated concentration of chaotropic guanidine salts, also allowing inactivation of RNases. Subsequent addition of ethanol creates appropriate binding conditions which favour adsorption of RNA to a silica-based membrane, washing away contaminating salts, metabolites and macromolecular cellular components. Pure RNA is finally eluted under low ionic strength conditions (Macherey-Nagel, 2015).

2.3.2. DNase Treatment

RNA extraction was followed by DNase treatment (Ambion Turbo DNA-free, Life Technologies). RNA concentration was determined by ultraviolet spectrophotometry at 260 nm, using NanoDrop 1000 Spectrophotometer (Thermo Fisher Scientific).

2.3.3. cDNA Synthesis

DNase treated RNA (400 ng) was used as template for generating complementary DNA (cDNA), using the reverse transcriptase enzyme M-MLV (Life Technologies), a mixture of oligo(dT)18 and nonamers (in order to amplify total RNA, including non-polyadenylated RNAs), and nucleotides for DNA synthesis (dNTPS). The reaction was performed on a Veriti Thermal Cycler (Thermo Fisher Scientific), with the following cycling conditions: 25ºC for 10 minutes, followed by 37ºC for 30 minutes and 95ºC for 5 minutes.

2.4. Assessment of Gene Expression at RNA Level

2.4.1. Semi-Quantitative Polymerase Chain Reaction and Agarose Gel Electrophoresis

Semi-quantitative polymerase chain reaction was carried out on cDNA samples, using the KAPA2G FAST mix (Kapa Biosystems) with the appropriate primer set (see subsection 2.4.3 for used primer sets). The reaction was performed on a Veriti Thermal Cycler (Thermo Fisher Scientific), with the following cycling conditions: 95ºC for 2 minutes, followed by appropriate number of cycles at 95ºC for 10 seconds, 60ºC for 10 seconds and 72ºC for 1 second, and finally 72ºC for 1 minute.

Following semi-quantitative PCR, product samples were mixed with Orange DNA Loading Dye 6x (New England Bio Labs) to a final concentration of 1x, and loaded onto a 2% (w/v) agarose gel in Tris-

Acetate-EDTA Buffer (TAE Buffer), stained with SYBR Safe (Invitrogen), and resolved at 120 V, for 25 minutes. The molecular weight (Mw) marker 1 Kb Plus DNA Ladder (Invitrogen) was used to verify the size of obtained fragments, according to predictions. Gel images were acquired using the Gel Doc EZ System (Bio-Rad).

2.4.2. Real-Time Quantitative Polymerase Chain Reaction

Real-time quantitative polymerase chain reaction (RT-qPCR) was carried out on cDNA samples, using the KAPA SYBR FAST RT-qPCR Master Mix (Kapa Biosystems), and appropriate primers (see subsection 2.4.3 for used primer sets), on a CFX96 Touch Real-Time PCR Detection System (Bio-Rad), with the following cycling conditions: 95°C for 3 minutes, followed by 95°C for 3 seconds and 60°C for 30 seconds, for 40 cycles, finishing at 65ºC for 5 seconds.

The real-time quantitative PCR method is enabled by the inclusion of a DNA-binding dye for each reaction, i.e. a fluorescent reporter molecule, that allows the fluorescence detection module of the thermal cycler to monitor the fluorescence signal, as amplification occurs, yielding increased fluorescence with an increasing amount of product DNA. The fluorescence measurement is performed above a given threshold (that excludes the background signal) and the number of cycles required for each sample to reach the threshold fluorescence is designated as the Ct (threshold cycle) value; all samples analysed by RT-qPCR were processed as technical duplicates, allowing the calculation of an average Ct value. Overall, this enables the calculation of the relative expression of a specific target gene in a study sample, compared to a control sample. The comparative Ct Method ($2^{-\Delta\Delta Ct}$) was applied in such calculation. The relative expression was quantified as $2^{-\Delta\Delta Ct}$, as outlined in the following equations (1) and (2):

(1) $2^{-\Delta\Delta Ct} = 2^{-[(\Delta Ct \text{ of treated sample} - \Delta Ct \text{ of control sample})]}$

wherein:

(2) $\Delta Ct = Ct_{\text{target gene}} - Ct_{\text{housekeeping gene}}$

The expression of each target gene in each transfection with siRNA, was normalized to the corresponding housekeeping gene levels, to determine the overall variation in gene expression. *Beta-actin* was used as a housekeeping gene, assuming its expression remains unchanged upon treatment with each siRNA.

2.4.3. Primers

All primers were purchased from Integrated DNA Technologies, and designed using the PrimerQuest tool (Integrated DNA Technologies). Supplementary Table S.2. discriminates the primer sets used in RT-qPCR or semi-quantitative PCR reactions, respective primer sequences and designation of respective experiments in which primers were used in.

2.5. Protein Analysis

2.5.1. Protein Extraction and Quantification

After transfection according to described method, cells were harvested and lysed in 50 mM Tris-HCl, pH 7.4, 1% NP40, 150 mM NaCl, 1 mM EDTA, 1% glycerol (RIPA buffer), supplemented with dithiothreitol (DTT), Complete Protease Inhibitor Cocktail (Merck) and phosphatase inhibitor PhosSTOP (Merck). Samples were incubated on ice for 20 minutes during lysis.

Total protein quantification was determined by a colorimetric Bradford assay (Bio-Rad), using a Spark 10M Multimode Microplate Reader (Tecan), measuring absorbance at 595 nm.

75 µg of protein were mixed with NuPAGE LDS Sample Buffer (Thermo Fisher Scientific) and heat denaturated at 95ºC, for 5 minutes.

2.5.2. Western Blot

Samples, containing equal amounts of protein, were loaded on an NuPAGE 4-12% Bis-Tris Gel (Invitrogen) and transferred onto PVDF Membranes (Invitrogen), with an iBlot Gel Transfer Device (Invitrogen). Membranes were blocked in 5% non-fat dry milk, diluted in Tris-Buffered Saline with 0.1% Tween 20 (TBS-T Buffer) for 1 hour, and proteins were immunoblotted with the appropriate primary antibodies (listed in Table 2.2.) overnight, at 4ºC. Beta-actin antibody was used as a protein loading control. After membrane wash with TBS-T Buffer, membranes were incubated with respective secondary antibody, for 1 hour. After membrane wash with TBS-T Buffer, proteins were detected using the enhanced chemiluminescence system Western Lightning–ECL (PerkinElmer) and developed in an ImageQuant LAS 4000 Biomolecular Imager (GE Healthcare Life Sciences).

Table 2.2. Primary antibodies used for protein immunoblotting.

Primary antibodies used for protein immunoblotting, respective sources and suppliers.

Antibody	Source	Supplier
C/EBPβ	Mouse, monoclonal	Santa Cruz Biotechnology
MEK1/2	Mouse, monoclonal	Cell signalling
Phospho-MEK1/2 Ser221	Rabbit, monoclonal	Cell signalling
ERK1/2	Rabbit, polyclonal	Cell signalling
Phospho-ERK1/2 T202/Y204	Mouse, monoclonal	Cell signalling
AKT	Rabbit, polyclonal	Cell signalling
Phospho-AKT T308	Rabbit, monoclonal	Cell signalling
Phospho-AKT S473	Rabbit, monoclonal	Cell signalling
Beta-actin	Mouse, monoclonal	Merck

2.6. Assessment of RNA Cellular Localization

2.6.1. Subcellular Fractionation

A375 PR1 cells were plated at a density of 40,000 cells/ml, 24 hours prior RNA isolation. Subcellular fractionation of dividing A375 PR1 cells followed by RNA extraction of nuclear and cytoplasmic fractions was performed using the PARIS kit (Life Technologies) according to the manufacturer's instructions. Total RNA was also extracted, as previously described. Extracted RNA fractions, as well as total RNA, were DNase treated and used in cDNA synthesis as described. Specific primers were used in a semi-quantitative PCR, in order to amplify *C/EBPβ-AS* and *C/EBPβ*. 7SK was also amplified by semi-quantitative PCR with specific primers, as a control, since this small nuclear RNA is mainly found in the nucleus (see subsection 2.4.3 for used primer sets). Obtained PCR products were resolved in an agarose gel, according to described method.

2.6.2. Single-Molecule RNA Fluorescence *in Situ* Hybridization

A375 and A375 PR1 were grown on sterilized cover slips and fixed with 4% paraformaldehyde at room temperature for 10 minutes, and stored in 70% ethanol, at 4ºC.

Next, fixed cells were treated with a hybridization buffer containing a mix of eleven different oligonucleotides (Integrated DNA Technologies) (Supplementary Table S.3.), complementary to different regions of the *C/EBPβ-AS* transcript. The cover slides were then incubated in a humidity chamber, at 30ºC overnight. After being washed in RNA Wash Buffer (containing 25% Formamide and 2x SSC), cells were incubated in a hybridization buffer containing a fluorophore-labelled probe – with Alexa Fluor 594 (Integrated DNA Technologies) –, complementary to the overhangs comprised in primarily used oligonucleotides, at 30ºC, for 3 hours. After being washed in RNA Wash Buffer and 2x SSC, cell coated cover slips were mounted in Vectashield Hardset Antifade Mounting Medium with DAPI (Vector Laboratories), and incubated at 4ºC overnight.

Following Single-Molecule RNA Fluorescence *In Situ* Hybridization (smFISH), images were acquired on a Zeiss LSM 880 Confocal Microscope, using a 63x oil immersion objective. Acquisition was performed with Zen 2.1 SP3 Software and Fuji 1.0/ImageJ was used as montage software.

2.7. Actinomycin D Treatment: Assessment of RNA Stability

A375 PR1 cells were seeded at a density of 40,000 cells/ml. After 24 hours, dividing cells were treated with a final concentration of 10 μM/ml actinomycin D (Merck) and incubated at standard culturing conditions. RNA was harvested at four different time points (0, 2, 6 and 10 hours) after addition of actinomycin D. Generation of cDNA was performed as previously described. Appropriate primer sets to evaluate relative abundance of *C/EBPβ* and *C/EBPβ-AS* transcripts were used in RT-qPCR, according to mentioned procedure.

2.8. Polyadenylated RNA Depletion from Total Extracted RNA

5'-biotinylated oligo$(dT)_{18}$ or control biotin-362as oligonucleotides were purchased from Integrated DNA Technologies. Dynabeads MyOne Streptavidin beads (Life Technologies) were blocked in BSA and yeast tRNA in order to minimize nonspecific binding, and were pre-loaded with 5'-biotinylated oligonucleotides. After being washed, the beads were resuspended in 400 ng of DNase treated RNA extracted from HEK293T cells according to aforementioned procedure and incubated at room temperature for 2 hours (RNA isolated from HEK293T was previously used in the optimization of the polyadenylated RNA depletion protocol by Dan Grandér's group, therefore HEK293T cell line was selected). After incubation, beads were pelleted by centrifugation (using a Hettich Mikro 200R Centrifuge) and supernatant was collected (containing polyadenylated (poly(A))-depleted RNA fraction). Poly(A)-depleted RNA was used to generate cDNA, as previously described, and accessed by semi-quantitative PCR, using specific primers sets for: *C/EBPβ-AS*, *Beta-actin* (as a negative control for the poly(A) depletion, since it is known to be a polyadenylated transcript) and *U48* (as a positive control for the poly(A) depletion, since it is known to be a non-polyadenylated transcript) (see subsection 2.4.3 for used primer sets).

2.9. Chromatin Immunoprecipitation

A375 PR1 cells were seeded onto 100 mm culture dishes, at a density of 40,000 cells/ml and transfected with siRNAs, as described. Cells were crosslinked for 10 minutes in 0.75% formaldehyde 48 hours post transfection and subsequently quenched in glycine for 5 minutes. Next, cells were lysed with cell lysis buffer and a nuclei lysis buffer. Lysates were sonicated using a Bioruptor Sonicator (Diagenode) and incubated overnight at 4ºC with appropriate antibodies (Table 2.4.). Salmon Sperm DNA/Protein A Agarose (Millipore) was used to pulldown the antibody. DNA was eluted in elution buffer (containing 1% SDS and 100 mM $NaHCO_3$), followed by reversion of the crosslink with NaCl and treatment with RNaseA (Thermo Fisher Scientific) and proteinase K (Finnzymes Diagnostics). DNA was isolated using the QIAquick PCR purification kit (Qiagen), following the manufacturer's instructions. Following Chromatin Immunoprecipitation (ChIP), enrichment of each target protein at the *C/EBPβ* or *C/EBPβ-AS* promoters was determined by RT-qPCR with appropriate primers (see subsection 2.4.3 for used primer sets).

Table 2.3. Antibodies used for ChIP.

ChIP-grade antibodies used for ChIP, respective sources and suppliers.

Antibody	Source	Supplier
RNA Polymerase II	Rabbit, polyclonal	Santa Cruz Biotechnology
EZH2	Mouse, monoclonal	EMD Millipore
H3K27me3	Rabbit, polyclonal	EMD Millipore
C/EBPβ	Rabbit, polyclonal	Santa Cruz Biotechnology
IgG	Mouse	Santa Cruz Biotechnology
IgG	Rabbit	Santa Cruz Biotechnology

2.10. MrcBC Treatment: Evaluation of Promoter Methylation Status

A375 and A375 PR1 cells were seeded at a density of 40,000 cells/ml and transfected with siRNAs siC/EBPβ-AS or siCont, as previously described. Cells were harvested 48 hours after transfection and DNA was extracted using the QIAamp DNA Mini Kit (Qiagen), according to manufacturer's instructions. NEBuffer (New England BioLabs), supplemented with GTP and BSA, was added to 200 ng of each sample of isolated DNA. Samples were treated with MrcBC enzyme (New England BioLabs), or mock treated, and incubated at 37ºC, overnight. Heat-inactivation of the enzyme was then performed at 65ºC, for 1 hour.

MrcBC is a methylation-dependent endonuclease that cleaves methylated DNA at Pu^{m}CG sequence elements (where Pu stands for Purine, regarding Adenine or Guanine nucleotides, and ^{m}C regards to Methylcytosine), thus methylation status of DNA can be correlated with the amount of digested DNA in MrcBC treated samples and compared to untreated. RT-qPCR was used to assess the methylation status of the *C/EBPβ* promoter upon knockdown of C/EBPβ-AS, and compared to control.

2.11. Cell Viability Assessment

2.11.1. Vemurafenib Treatment

A375 and A375 PR1 were cultured at a density of 40,000 cells/ml and transfected with siRNAs siC/EBPβ-AS or siCont, as described. Cells were treated with the selective inhibitor of $BRAF^{V600E}$ PLX4720 (Selleckchem), a vemurafenib analogue, herein referred to as vemurafenib, 24 hours post transfection. Final concentrations of 1 or 10 μM were used. Dimethyl sulfoxide (DMSO) – vehicle of vemurafenib – was used as a control treatment.

Assessment of the impact of single or combined treatment with siRNAs and vemurafenib in cell viability was performed by Fluorescence Activated Cell Sorting, as described below.

2.11.2. Fluorescence Activated Cell Sorting

A375 and A375 PR1 cells were harvested after 48 hours of vemurafenib treatment and 72 hours after cell transfection. Cells were washed twice in PBS, and suspended in 100 μL Fluorescence Activated Cell Sorting (FACS) incubation buffer, containing 1% Annexin V (Roche Molecular Biochemicals) and 1% Propidium Iodide (PI) (Merck). The samples were incubated for 15 minutes at room temperature, followed by the addition of 200 μL of Annexin V incubation buffer. Assessment of the proportion of early apoptotic and late apoptotic/necrotic cells is made possible by the relative quantification of annexin V and/or PI stained cells in that population. Unstained gated cells are categorized as viable cells. Such assessment was performed in an ACEA Biosciences NovoCyte Flow Cytometer and FSC/SSC gating was used, aiming to exclude cell debris. A minimum of 10,000 cells was gated for each sample.

2.12. Statistical Analysis

Data were presented as mean of values obtained in independent experiments, unless stated otherwise. Error bars represent the standard error of the mean (SEM). Statistical analysis was performed using a Student's t-Test. The (*) indicates significance $p<0.05$, (**) $p<0.01$ and (***) $p<0.005$, whereas (NS) indicates non-significance.

Statistical significance calculation and presentation of data were performed using Microsoft Office Excel (2016) and Adobe Illustrator CS5.

3. RESULTS

The aim of each implemented experimental approach is described in each subsection below, along with acquired results within the course of the project.

3.1. Characterization of the Long Non-Coding RNA *C/EBPβ-AS*

3.1.1. Assessment of the Subcellular Localization of *C/EBPβ-AS*

Aiming to gain some insight on the subcellular localization of the lncRNA *C/EBPβ-AS*, RNA was extracted and isolated from two major cellular compartments – cytoplasm and nucleus – upon subcellular fractionation of A375 PR1 (Figure 3.1. A). Total RNA was also extracted and isolated from the same cell line. The presence of *C/EBPβ-AS* and *C/EBPβ* RNAs in all three samples was assessed, as well as the small nuclear RNA *7SK*, used as fractionation control.

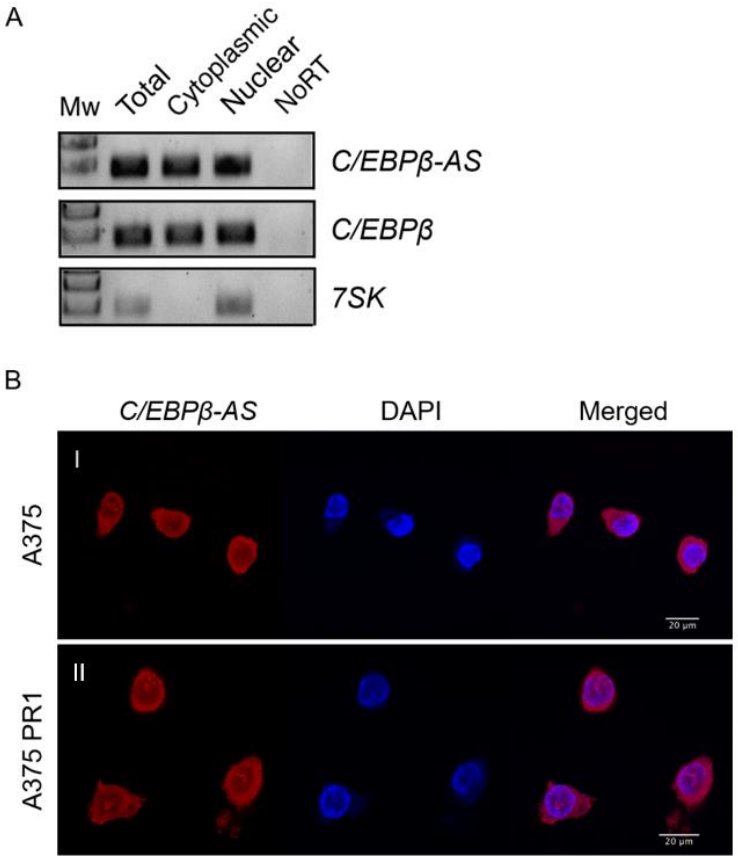

Figure 3.1. Subcellular localization of *C/EBPβ-AS* and *C/EBPβ* transcripts in cutaneous melanoma cell lines. **(A)** Semi-quantitative PCR analysis of *C/EBPβ-AS* (81 bp) and *C/EBPβ* (76 bp) in cytoplasmic and nuclear fractions of A375 PR1 cells. Fractions were obtained by subcellular fractionation followed by RNA extraction of each fraction and cDNA synthesis. *7SK* (96 bp), a nuclear-restricted transcript, was used for fractionation control. Results show presence of transcripts in both assessed cellular compartments. **(B)** Widespread subcellular distribution of *C/EBPβ-AS* (shown in red), detected by single-molecule RNA FISH, in A375 (**I**) and A375 PR1 (**II**) cells. DAPI-stained nuclei are shown in blue. Images were acquired by fluorescence confocal microscopy. Scale bar 20 µm.

As expected, *7SK* RNA was not detected in the cytoplasmic fraction, indicative of a successful isolation of RNA from each of the two cellular compartments and free of visible RNA cross-contamination. Results indicate that *C/EBPβ-AS* RNA is present in both the nuclear and the cytoplasmic fraction and in similar relative amounts.

Pursuing the same goal, smFISH was also used (Figure 3.1. B). This technique allows the detection of *C/EBPβ-AS* with a pool of oligonucleotides complementary to such transcript. In addition, DAPI staining of DNA was used to allow identification of the nuclear compartment.

Merged images confirmed the fractionation results, showing an identical distribution of *C/EBPβ-AS* in the nuclear and the cytoplasmic compartments, in A375 and A375 PR1 cells.

3.1.2. Assessment of the Stability of *C/EBPβ-AS* and *C/EBPβ* Transcripts

Actinomycin D inhibits transcription by preferentially intercalating GC rich sequences and stabilizing type I topoisomerase-DNA covalent complexes. This prevents the RNA polymerase to progress, leading to inhibition of elongation of the nascent RNA chain, thus inhibiting transcription (Trask and Muller, 1988).

In order to examine *C/EBPβ-AS* stability, A375 PR1 cells were treated with actinomycin D for a maximum of 10 hours of treatment (at 14 hours cell viability decreases considerably, hence RNA cannot be properly evaluated by RT-qPCR). The decay of *C/EBPβ-AS* and *C/EBPβ* transcripts was assessed by RT-qPCR and data was normalized to 0 hour time-point (Figure 3.2.).

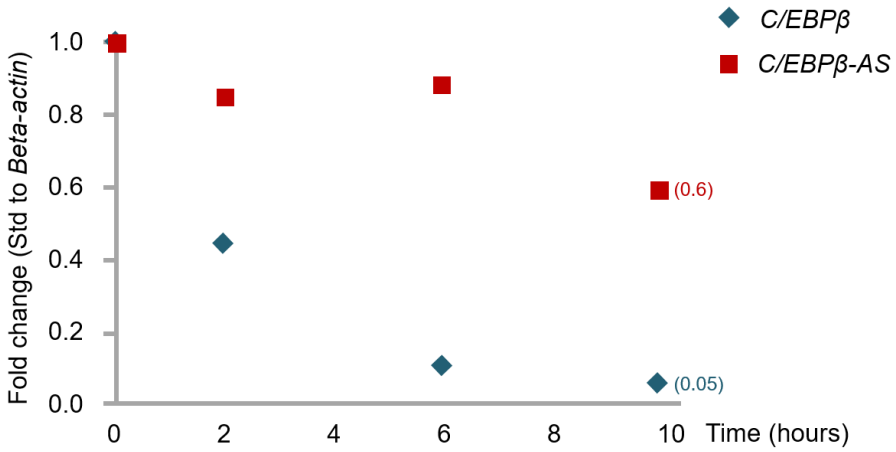

Figure 3.2. Stability analysis of *C/EBPβ-AS* and *C/EBPβ* transcripts.
qRTPCR analysis of stability of *C/EBPβ-AS* and *C/EBPβ* transcripts, after blocking transcription in A375 PR1 cells with 10 μM/ml actinomycin D for 0, 2, 6 and 10 hours. Obtained values were standardized to *Beta-Actin* Data were normalized to the 0 hour time-point and show an elevated stability of the lncRNA *C/EBPβ-AS* compared to *C/EBPβ* mRNA.

Results show that while *C/EBPβ* mRNA is decreased by more than 50% after 2 hours of blocking transcription, 85% of *C/EBPβ-AS* transcript remains in the cell after 2 hours of treatment compared to 0 hours of treatment. Moreover, only 10% of the initial amount of *C/EBPβ* mRNA is detected after 6 hours of actinomycin D treatment, whereas no significant difference is perceived in the levels of the lncRNA *C/EBPβ-AS* after 6 hours of treatment, in comparison with 2 hours of actinomycin exposure. After 10 hours of actinomycin D treatment, solely 5% of *C/EBPβ* mRNA is detected, while 60% of *C/EBPβ-AS* RNA is still measured, compared to 0 hours of treatment.

This shows a considerably higher stability of *C/EBPβ-AS* transcript, comparing to *C/EBPβ* – with half-lives of >10 hours and <2 hours, respectively.

3.1.3. Assessment of the Polyadenylation Status of *C/EBPβ-AS* Transcript

In order to assess the polyadenylation status of the *C/EBPβ-AS* transcript, depletion of polyadenylated (poly(A)) RNA from HEK293T total RNA was performed. Primers sets for *C/EBPβ-AS* were used in a semi-quantitative PCR reaction, as well as primer sets for the poly(A)-depletion negative (*Beta-Actin*) and positive (*U48*) controls (Figure 3.3.).

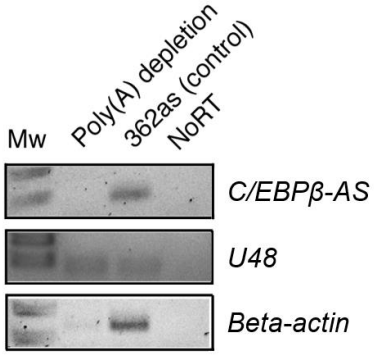

Figure 3.3. Polyadenylation status of *C/EBPβ-AS* transcript.
Poly(A)-depleted RNA from HEK293T cells by RNA pulldown was assessed for *C/EBPβ-AS* transcript (81 bp) by semi-quantitative PCR. 362as-coated beads were used as a pulldown control. *U48* (63 bp) was used as a control for poly(A) negative transcripts and *Beta-actin* (233 bp) as a control for poly(A) positive transcripts. Data demonstrates the lncRNA *C/EBPβ-AS* as a polyadenylated transcript.

The obtained results are indicative of a successful poly(A)-depletion from total RNA, according to negative and positive controls. Given that, experimental results suggest that *C/EBPβ-AS* transcription gives rise to a poly(A) positive lncRNA.

3.1.4. Assessment of the Extent of *C/EBPβ-AS* and *C/EBPβ* 5' End Overlap

Characterization of the overlapping genomic region from which sense and antisense transcripts arise is of relevance as it contributes to the validation of the annotated information about a specific locus, as well as to a potentially improved siRNA and primer design.

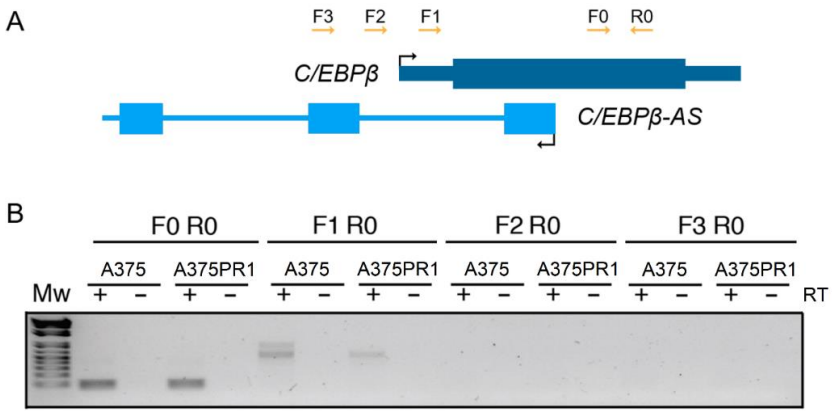

Figure 3.4. Characterization of *C/EBPβ-AS* and *C/EBPβ* overlap.
(A) Schematic representation of *C/EBPβ-AS* and *C/EBPβ* locus. Yellow arrows indicate the primer binding sites used for primer walk in Fig. 3.4.B. **(B)** Primer walk generated by semi-quantitative PCR for the assessment of the extent of *C/EBPβ-AS* and *C/EBPβ* 5' end overlap. Results show that C/EBPβ 5' region does not overlap with the annotated *C/EBPβ-AS* exon 2.

As such, a primer walk was performed by semi-quantitative PCR (Figure 3.4.). Regarding the used primer binding sites, primer walk results show that *C/EBPβ* 5' region (comprising *C/EBPβ* transcription start site) does not overlap with the annotated *C/EBPβ-AS* exon 2.

3.2. Study of the Regulation of *C/EBPβ-AS* and *C/EBPβ* Expression

3.2.1. Evaluation of *C/EBPβ-AS* Role on *C/EBPβ* Expression

Antisense RNAs are known to affect expression of sense counterpart, therefore we set out to investigate a putative impact of the *C/EBPβ-AS* transcript on *C/EBPβ* expression, taking advantage of RNA interference (RNAi). RNAi is defined as the process of sequence-specific, post-transcriptional gene silencing, initiated by double-stranded RNA (dsRNA), comprising a homologous sequence of the gene to be silenced (Fire *et al.*, 1998; Elbashir *et al.*, 2001). This process of sequence-specific RNA degradation is mediated by double-stranded small interfering RNAs (siRNAs).

As such, knockdown with siRNA siC/EBPβ-AS was performed in A375 and A375 PR1 cell lines (Figure 3.5. A-B), targeting exon 2 of the annotated *C/EBPβ-AS* transcript (regarding Human GRCh38/hg38 – UCSC Genome Browser). Real-time quantitative PCR was employed to assess the intended knockdown, as well as its impact on *C/EBPβ* mRNA levels.

Transfection with siC/EBPβ-AS resulted in an average knockdown of *C/EBPβ-AS* in 30% (± SEM of 0.060) and 53% (± SEM of 0.052), in A375 and A375 PR1, respectively. Such knockdowns resulted in 41% (± SEM of 0.097) and a substantial 154% (± SEM of 0.506) average upregulation of *C/EBPβ*, in each cell line, respectively.

The effect of transfection with siRNA siC/EBPβ-AS on *C/EBPβ* mRNA levels was further analysed in a panel of other melanoma cell lines, including SKMEL24, MNT1, MNT1R, SKMEL28 and ESTDAB049 (Figure 3.5 C-G). *C/EBPβ-AS* knockdown consistently induced an upregulation of *C/EBPβ* mRNA levels, in variable extents, with lowest statistically significant average upregulation of 41% (in ESTDAB049 cells) and most prominent statistically significant average upregulation of 429% (in SKMEL24 cells). No significant effect was perceived on *C/EBPβ* mRNA levels, upon *C/EBPβ-AS* knockdown in MNT1R cells.

RNA Polymerase II (RNA Pol II) is required for gene transcription and is known to assemble within the initiation complex at the promoters of most eukaryotic protein-coding genes. Therefore, detection of interaction between RNA Pol II and the promoter region of a gene is suggestive of active transcription.

Given that, to identify a putative role of *C/EBPβ-AS* in the transcriptional regulation of *C/EBPβ,* chromatin immunoprecipitation of RNA Pol II was performed in A375 PR1 cells. Interaction between RNA Pol II and the *C/EBPβ* promoter upon *C/EBPβ-AS* knockdown was assessed by RT-qPCR and compared with mock transfected samples (Figure 3.6.).

Results indicate a close to 3-fold enrichment (± SEM of 1.78) of RNA Pol II at the *C/EBPβ* promoter, when *C/EBPβ-AS* is suppressed, suggesting that *C/EBPβ-AS* contributes to *C/EBPβ* transcription impairment in A375 PR1.

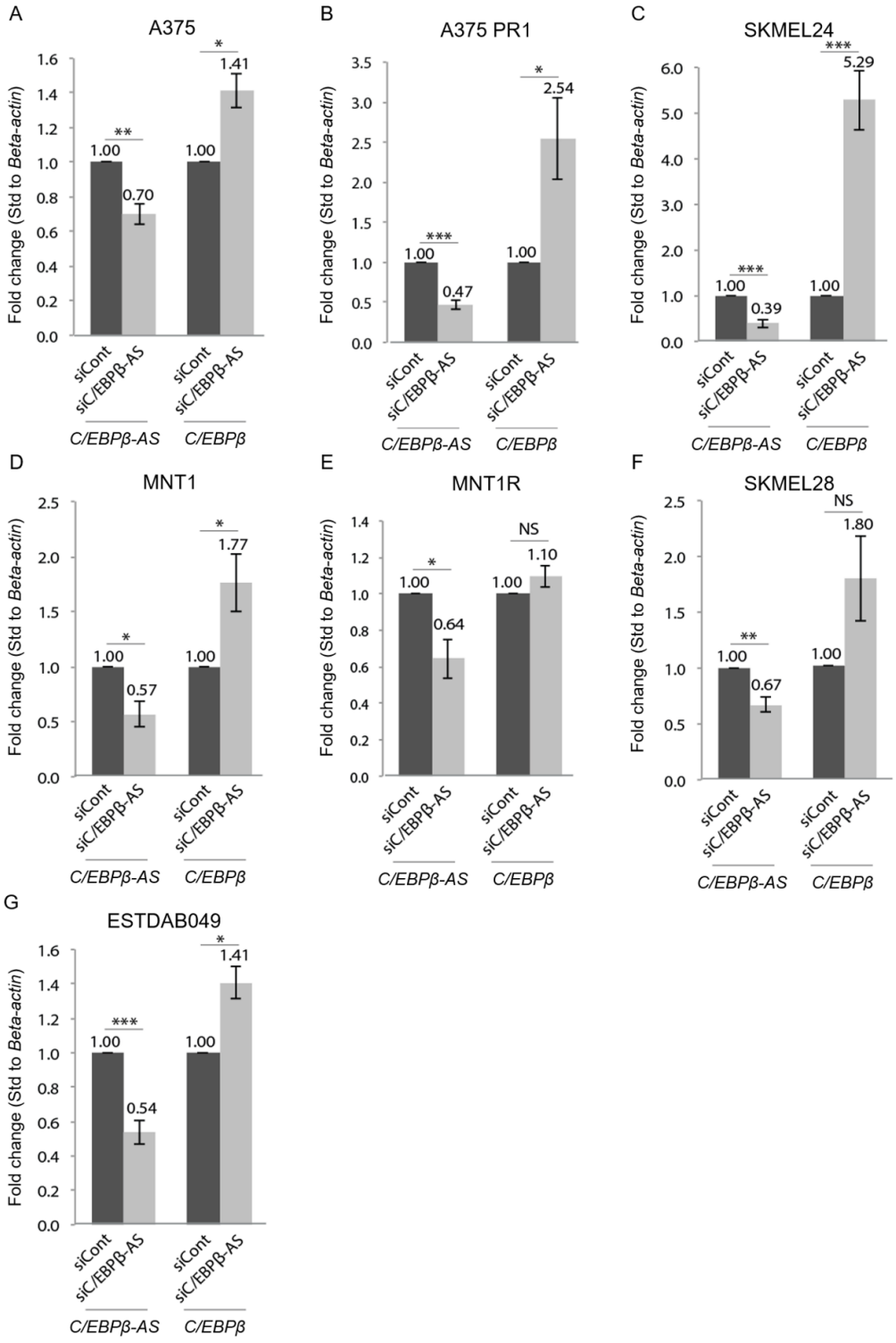

Figure 3.5. *C/EBPβ-AS* knockdown impacts *C/EBPβ* mRNA levels.

qRTPCR analysis of *C/EBPβ* RNA levels after 48h siRNA-induced *C/EBPβ-AS* knockdown, in a panel of cutaneous melanoma cell lines, comprising **(A)** A375, **(B)** A375 PR1, **(C)** SKMEL24, **(D)** MNT1, **(E)** MNT1R, **(F)** SKMEL28 and **(G)** ESTDAB049 cells. Obtained values were standardized to *Beta-Actin*. Results represent the mean of three independent experiments (n=3). The (*) indicates the significance p<0.05, (**) p<0.01, (***) p<0.005, whereas (NS) indicates non-significant, using a Student's T-test. Error bars represent the standard errors of the mean. Efficiency of *C/EBPβ-AS* knockdown varied among different cell lines. *C/EBPβ* mRNA upregulation can be perceived in all cell lines, to variable extents, upon *C/EBPβ-AS* knockdown.

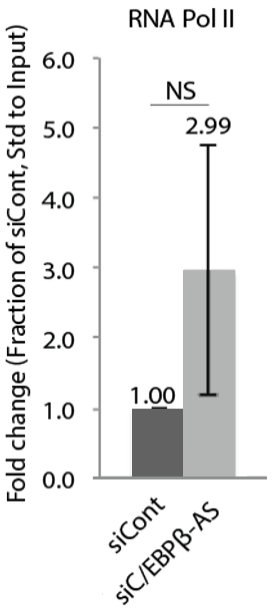

Figure 3.6. *C/EBPβ-AS* knockdown impacts RNA Polymerase II recruitment to the *C/EBPβ* promoter.
qRTPCR analysis of RNA Polymerase II (RNA Pol II) enrichment assessed by ChIP at the *C/EBPβ* promoter, after 48h siRNA-induced *C/EBPβ-AS* knockdown, in A375 PR1 cells. Obtained values were standardized to input. Results represent the mean of four independent experiments (n=4). The (*) indicates the significance $p<0.05$, (**) $p<0.01$, (***) $p<0.005$, whereas (NS) indicates non-significant, using a Student's T-test. Error bars represent the standard errors of the mean. Data suggest an enrichment of RNA Pol II at the *C/EBPβ* promoter upon suppression of *C/EBPβ-AS*.

Protein levels of C/EBPβ were also assessed by Western Blot, after transfection of siRNA siC/EBPβ-AS in A375 and A375 PR1 (Figure 3.7.).

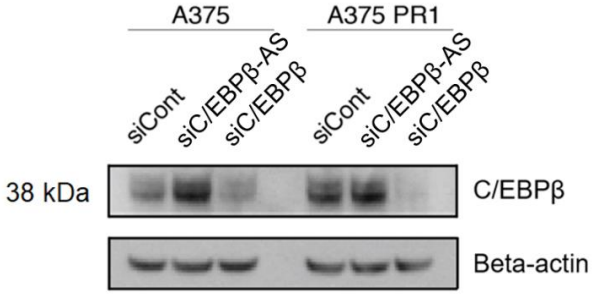

Figure 3.7. *C/EBPβ-AS* knockdown impacts C/EBPβ protein levels.
Western blot analysis of C/EBPβ after 48h siRNA-induced *C/EBPβ-AS* knockdown, in A375 and A375 PR1 cells. The protein input was standardized to Beta-actin. C/EBPβ protein (38kDa) upregulation can be seen in both cell lines, upon *C/EBPβ-AS* knockdown. Downregulation of C/EBPβ protein levels is apparent, upon *C/EBPβ* knockdown.

Results show an increase in C/EBPβ protein levels, compared with control, pointing to an identical trend at the protein level, as that observed at the mRNA level. According to the molecular weight of the obtained band – 38 kDa –, the C/EBPβ predominant isoform detected in the assessed cell lines is LAP isoform, identified as a transcription factor associated with transcription activation. Downregulation of C/EBPβ protein levels is apparent, upon C/EBPβ knockdown.

3.2.2. Evaluation of the Role of Epigenetic Modulators on *C/EBPβ* Expression

Previously described mechanisms observed in gene repression by antisense RNAs include the recruitment of repressive chromatin remodelers to the promoter of the gene susceptible to asRNA-mediated transcriptional regulation.

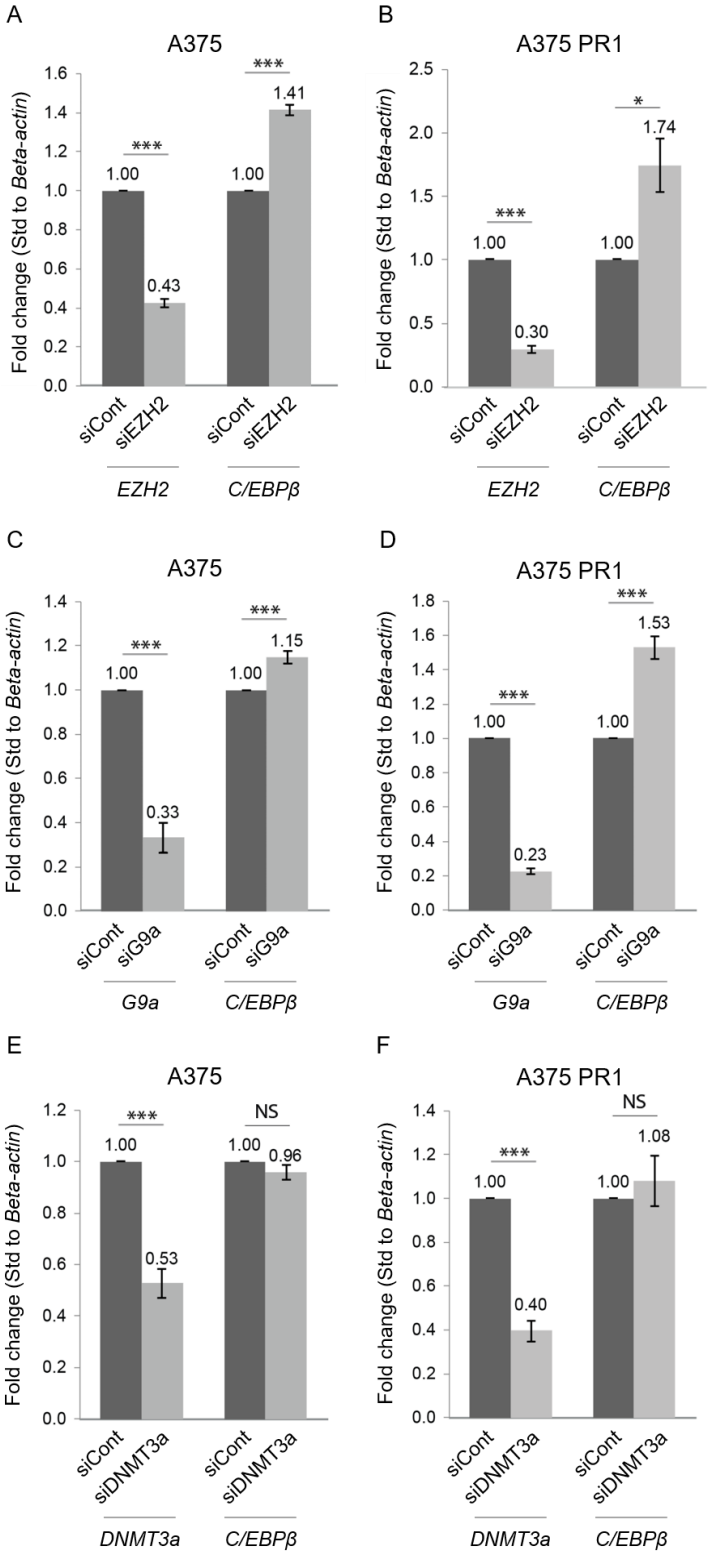

Figure 3.8. Impact of *EZH2, G9a or DNMT3A* knockdown on *C/EBPβ* mRNA levels.

qRTPCR analysis of *C/EBPβ* mRNA levels after 48h siRNA-induced *EZH2* knockdown, in **(A)** A375 and **(B)** A375 PR1 cells. qRTPCR analysis of *C/EBPβ* mRNA levels after 48h siRNA-induced *G9a* knockdown, …/…

…/… in **(C)** A375 and **(D)** A375 PR1 cells. qRTPCR analysis of *C/EBPβ* mRNA levels after 48h siRNA-induced *DNMT3A* knockdown, in **(E)** A375 and **(F)** A375 PR1 cells. Results represent the mean of three independent experiments (n=3). All obtained values were standardized to *Beta-Actin*. The (*) indicates the significance $p<0.05$, (**) $p<0.01$, (***) $p<0.005$, whereas (NS) indicates non-significant, using a Student's T-test. Error bars represent the standard errors of the mean. Data indicate that knockdown of *EZH2* and *G9a* leads to an increase in *C/EBPβ* mRNA levels, while knockdown of *DNMT3A* has no significant effect on *C/EBPβ* expression.

Given that, we set out to investigate the process behind a putative transcriptional regulation of *C/EBPβ* orchestrated by *C/EBPβ-AS*, through recruitment of chromatin remodelers, namely, the well described histone methyltransferase EZH2, the histone methyltransferase G9a and the DNA methyltransferase DNMT3A.

With such aim, siRNA-induced depletion of *EZH2, G9a* and *DNMT3A* was performed in A375 and A375 PR1 cells and *C/EBPβ* RNA levels were assessed by RT-qPCR (Figure 3.8.).

Transfection of A375 and A375 PR1 with siRNA siEZH2 lead to respective average knockdown efficiencies of 57% and 70% (± SEM of 0.023 and 0.028, respectively). This resulted in corresponding average upregulation of *C/EBPβ* in 41% and 74% (± SEM of 0.026 and 0.211, respectively).

An average knockdown of *G9a* of 67% and 77% was achieved in A375 and A375 PR1 (± SEM of 0.068 and 0.017, respectively), resulting in a respective average increase of *C/EBPβ* expression by 15% and 53% (± SEM of 0.029 and 0.064, respectively).

Finally, knockdown of *DNMT3A* was achieved with an efficiency of 47% and 60% (± SEM of 0.055 and 0.048, respectively), in A375 and A375 PR1, respectively, which lead to no significant changes in expression of *C/EBPβ*.

3.2.3. Evaluation of *C/EBPβ-AS* Role on Epigenetic Regulation of the *C/EBPβ* Promoter

Since *C/EBPβ* mRNA levels were significantly elevated when either *C/EBPβ-AS* or *EZH2* were suppressed, a regulatory mechanism involving *C/EBPβ-AS* and EZH2 acting in concert was further evaluated.

Given that, in order to understand if the chromatin remodeler EZH2 is recruited to the *C/EBPβ* promoter in the presence of *C/EBPβ-AS*, we performed ChIP of EZH2 after *C/EBPβ-AS* knockdown. The interaction between EZH2 and the C/EBPβ promoter was assessed by RT-qPCR and compared with mock transfected samples (Figure 3.9. A). The methyltransferase EZH2 is described to play an essential role in catalysing the addition of methyl groups to histone H3 at lysine 27, epigenetically maintaining the H3K27me3 chromatin mark, frequently inducing transcriptional repression. Therefore, putative changes in the levels of H3K27me3 repressive chromatin mark at the C/EBPβ promoter, after *C/EBPβ-AS* knockdown, were also assessed by ChIP, followed by RT-qPCR analysis, compared with mock transfected samples (Figure 3.9. B).

Interestingly, results suggest a 2.6-fold enrichment of EZH2 and H3K27me3 (± SEM of 0.838 and 0.026, respectively), at the *C/EBPβ* promoter, upon *C/EBPβ-AS* suppression.

Finally, the impact of *C/EBPβ-AS* on the *C/EBPβ* promoter methylation was assessed by treating A375 and A375 PR1 DNA extracts with MrcBC, a methylation-dependent endonuclease.

DNA was assessed by RT-qPCR, and MrcBC treated samples were compared with mock treated samples (Figure 3.10.).

Despite non-statistically significant results, data points towards increased DNA cleavage at the *C/EBPβ* promoter upon *C/EBPβ-AS* knockdown, indicating increased DNA methylation.

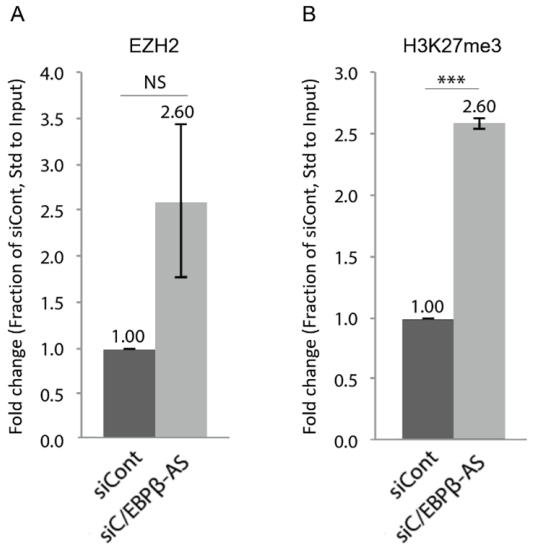

Figure 3.9. *C/EBPβ-AS* knockdown impacts enrichment of EZH2 and H3K27me3 at the *C/EBPβ* promoter.
qRTPCR analysis of **(A)** EZH2 and **(B)** H3K27me3 enrichment assessed by ChIP at the *C/EBPβ* promoter, after 48h siRNA-induced *C/EBPβ-AS* knockdown, in A375 PR1 cells. Obtained values were standardized to input. Results represent the mean of three independent experiments (n=3). The (*) indicates the significance p<0.05, (**) p<0.01, (***) p<0.005, whereas (NS) indicates non-significant, using a Student's T-test. Error bars represent the standard errors of the mean. Data suggest an enrichment of EZH2 and H3K27me3 at the *C/EBPβ* promoter after suppression of *C/EBPβ-AS*.

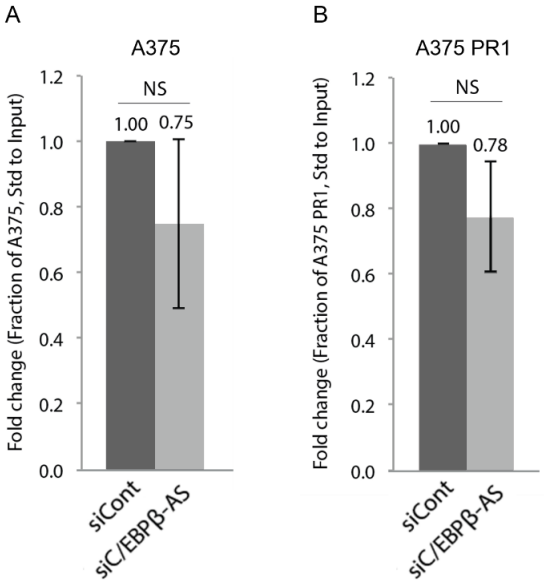

Figure 3.10. *C/EBPβ-AS* knockdown impacts methylation of the *C/EBPβ* promoter.
qRTPCR analysis of DNA extracts treated with the methylation-dependent endonuclease MrcBC, from A375 and A375 PR1 cells. Obtained values were standardized to mock treated samples. Results represent the mean of three independent experiments (n=3). The (*) indicates the significance p<0.05, (**) p<0.01, (***) p<0.005, whereas (NS) indicates non-significant, using a Student's T-test. Error bars represent the standard errors of the mean. Data show a non-statistically significant increase of DNA cleavage at the *C/EBPβ* promoter upon *C/EBPβ-AS* knockdown.

3.2.4. Evaluation of *C/EBPβ-AS* Impact on *C/EBPβ* Recruitment to the *C/EBPβ* Promoter

According to chromatin immunoprecipitation-sequencing (ChIP-seq) data from Genome Reference Consortium Human Build 37 (Human GRCh37/hg19) – UCSC Genome Browser, an enrichment of the transcription factor C/EBPβ at the predicted *C/EBPβ* promoter (estimated as an extension of circa 1000 bp upstream of *C/EBPβ-AS* annotated transcriptional start site) was identified (Figure 3.11. A).

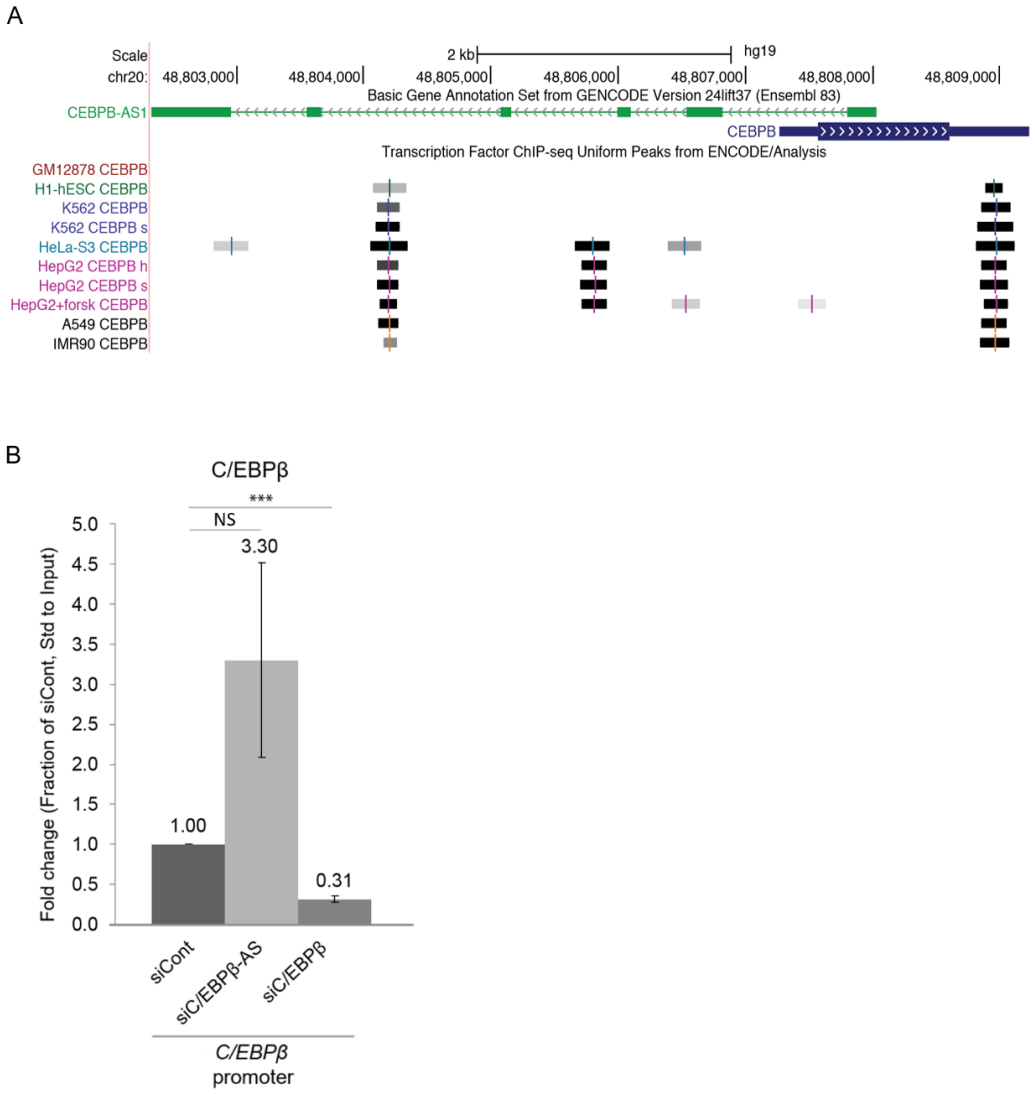

Figure 3.11. *C/EBPβ-AS* knockdown impacts enrichment of C/EBPβ at the *C/EBPβ* promoter.
(A) Overview of *C/EBPβ* and *C/EBPβ-AS* locus, displaying enrichment of C/EBPβ at *C/EBPβ* and *C/EBPβ*-AS predicted proximal promoter regions in different cell lines (ChIP-seq data retrieved from Genome Reference Consortium Human Build 37 – UCSC Genome Browser, scale bar 2kb). **(B)** qRTPCR analysis of C/EBPβ enrichment assessed by ChIP at the *C/EBPβ* promoter, after 48h siRNA-induced *C/EBPβ*-AS *or C/EBPβ* knockdown (pulldown control), in A375 PR1 cells. Obtained values were standardized to input. Results represent the mean of three independent experiments (n=3). The (*) indicates the significance $p<0.05$, (**) $p<0.01$, (***) $p<0.005$, whereas (NS) indicates non-significant, using a Student's T-test. Error bars represent the standard errors of the mean. Data suggest an enrichment of C/EBPβ at the *C/EBPβ* promoter upon *C/EBPβ-AS* suppression. A less amount of C/EBPβ is detected at the *C/EBPβ* promoter upon *C/EBPβ* suppression at the RNA level.

Given that, we set out to investigate if the transcription factor C/EBPβ takes part of *C/EBPβ* gene regulation, in a *C/EBPβ-AS*-dependent manner. C/EBPβ interaction with the *C/EBPβ* promoter was evaluated by chromatin immunoprecipitation (ChIP) of C/EBPβ in A375 PR1 cells, upon *C/EBPβ-AS* knockdown or *C/EBPβ* knockdown (as a control for immunoprecipitation) and quantified by RT-qPCR analysis (Figure 3.11. B).

Results of control experiment show a less amount of C/EBPβ at the *C/EBPβ* promoter upon *C/EBPβ* knockdown. A 3.3-fold enrichment of C/EBPβ (± SEM of 1.210) at the *C/EBPβ* promoter was perceived, when *C/EBPβ-AS* RNA was suppressed.

3.2.5. Evaluation of *C/EBPβ* Role on *C/EBPβ-AS* Expression

According to ChIP-seq data from Human GRCh37/hg19 – UCSC Genome Browser, an enrichment of the transcription factor C/EBPβ at the predicted *C/EBPβ-AS* promoter (estimated as an extension of circa 1000 bp upstream of *C/EBPβ-AS* annotated transcriptional start site) was also identified (Figure 3.11. A). Given that, we set out to investigate if C/EBPβ takes part of *C/EBPβ-AS* regulation.

Firstly, A375 and A375 PR1 were transfected with an siRNA targeting *C/EBPβ* (Figure 3.12.), leading to an average decrease in 74% and 58% (± SEM of 0.021 and 0.080, respectively) of *C/EBPβ* control mRNA levels, respectively. Upon *C/EBPβ* knockdown, *C/EBPβ-AS* transcript levels were downregulated to an average of 69% and 72% (± SEM of 0.040 and 0.024, respectively) of control levels, suggestive of a regulatory role of C/EBPβ in *C/EBPβ-AS* expression.

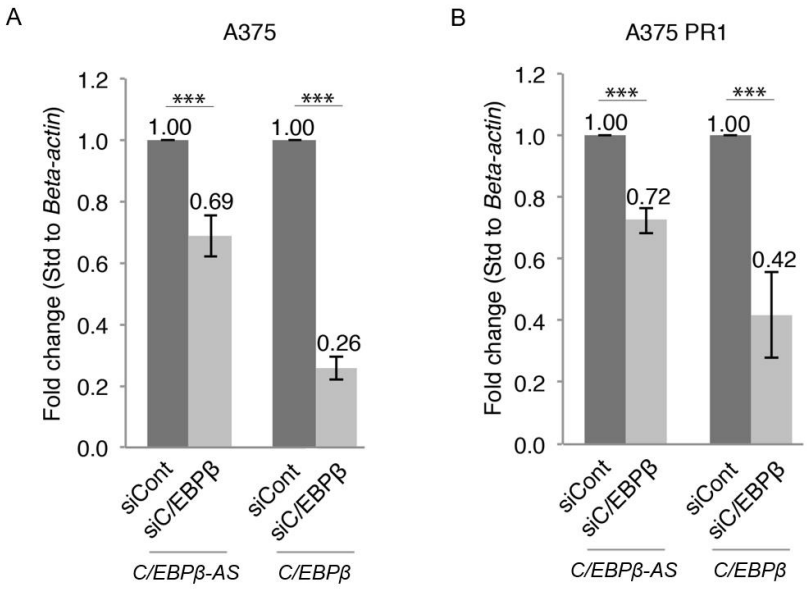

Figure 3.12. *C/EBPβ* knockdown impacts *C/EBPβ-AS* RNA levels.
qRTPCR analysis of *C/EBPβ-AS* RNA levels after 48h siRNA-induced *C/EBPβ* knockdown was performed in **(A)** A375 and **(B)** A375 PR1 cells. Obtained values were standardized to *Beta-Actin*. Results represent the mean of three independent experiments (n=3). The (*) indicates the significance p<0.05, (**) p<0.01, (***) p<0.005, whereas (NS) indicates non-significant, using a Student's T-test. Error bars represent the standard errors of the mean. Data show a reduction in *C/EBPβ-AS* RNA levels upon *C/EBPβ* suppression.

C/EBPβ interaction with the *C/EBPβ-AS* promoter was also evaluated. For this, chromatin immunoprecipitation (ChIP) of C/EBPβ was performed in A375 PR1 cells, upon *C/EBPβ-AS* knockdown

or *C/EBPβ* knockdown (as a control for immunoprecipitation) and quantification of C/EBPβ enrichment at the *C/EBPβ-AS* promoter was assessed by RT-qPCR analysis (Figure 3.13.).

Results of control experiment show a less amount of C/EBPβ at the *C/EBPβ-AS* promoter upon *C/EBPβ* knockdown. A 1.6-fold enrichment of C/EBPβ (± SEM of 0.171) at the *C/EBPβ* promoter was perceived, when *C/EBPβ-AS* RNA was suppressed.

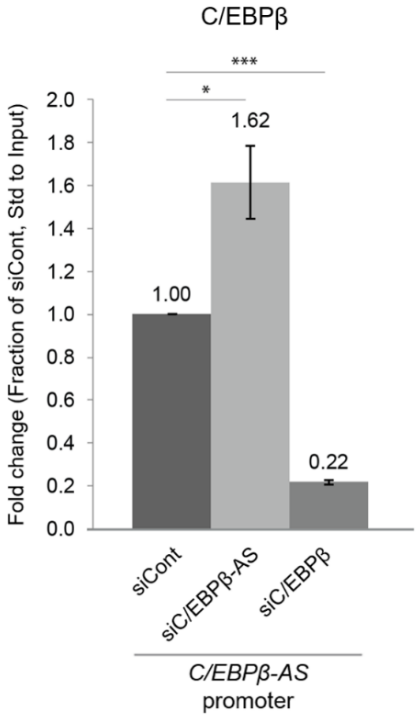

Figure 3.13. *C/EBPβ-AS* knockdown impacts enrichment of C/EBPβ at the *C/EBPβ-AS* promoter.
qRTPCR analysis of C/EBPβ enrichment assessed by ChIP at the *C/EBPβ-AS* promoter, after 48h siRNA-induced *C/EBPβ*-AS *or C/EBPβ* knockdown (pulldown control), in A375 PR1 cells. Obtained values were standardized to input. Results represent the mean of three independent experiments (n=3). The (*) indicates the significance $p<0.05$, (**) $p<0.01$, (***) $p<0.005$, whereas (NS) indicates non-significant, using a Student's T-test. Error bars represent the standard errors of the mean. Data shows an enrichment of C/EBPβ at the *C/EBPβ-AS* promoter upon *C/EBPβ-AS* suppression. Less amount of C/EBPβ is detected at the *C/EBPβ-AS* promoter upon *C/EBPβ* suppression.

3.3. Evaluation of *C/EBPβ-AS* Role on Vemurafenib Sensitivity

A previous study demonstrates a role of C/EBPβ in the regulation of *PTENpg1 asRNA α* (unpublished data produced by Dan Grandér's group), which in turn plays a part in the regulation of *PTEN* expression (Johnsson *et al*., 2013). Given the intensively studied relevance of *PTEN* expression levels in melanoma development and sensitivity to vemurafenib treatment, we set out to investigate if the modulation of C/EBPβ through knockdown of *C/EBPβ-AS* could impact sensitivity of A375 PR1 cells to vemurafenib.

Assessment of cell viability was performed by FACS following *C/EBPβ-AS* transient knockdown (Figure 3.14.). Results showed a minor 3% decrease in cell viability when *C/EBPβ-AS* was suppressed, compared to mock transfection, in A375 cells, and a 6% decrease in A375 PR1 viability. Assessment of cell viability after combination of *C/EBPβ-AS* knockdown with vemurafenib treatment was also performed by FACS, resulting in a small change of A375 viability compared to vemurafenib mono-

treatment, since A375 is classified as a cell line that is originally vemurafenib sensitive. However, results suggest a resensitization of A375 PR1 when vemurafenib treatment is combined with *C/EBPβ-AS* knockdown, leading to over 15% increased sensitivity to 1 μM of vemurafenib, and over 25% increased sensitivity to 10 μM of vemurafenib.

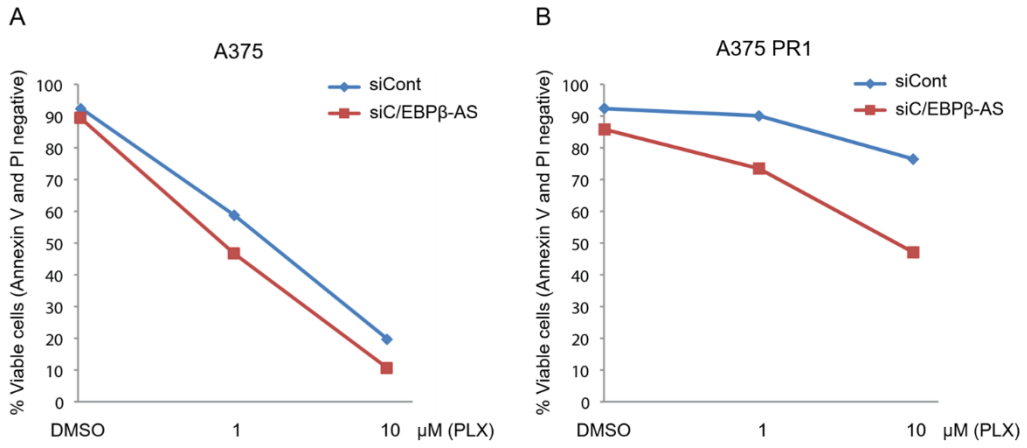

Figure 3.14. *C/EBPβ-AS* knockdown impacts cutaneous melanoma cell sensitivity to vemurafenib. Assessment of cell viability by FACS of **(A)** A375 and **(B)** A375 PR1 cells, after 72h siRNA-induced *C/EBPβ*-AS and 48h treatment with vemurafenib (PLX). Cells were included in a FSC vs SSC gate, aiming to exclude cell debris. The percentage of annexin V and PI unstained cells in each gated cell population corresponds to the proportion of viable cells in each sample. Data suggest that suppression of *C/EBPβ-AS* expression resensitizes the vemurafenib-resistant cutaneous melanoma cell line A375 PR1 to vemurafenib.

3.4. Evaluation of the Impact of *C/EBPβ-AS* Knockdown on MAPK/ERK1/2 and PI3K/AKT Pathways

The established correlation between the dysregulation of MAPK/ERK and PI3K/AKT pathways and CMM development prompted us to evaluate *C/EBPβ-AS* knockdown impact in A375 and A375 PR1 cell lines, regarding different components of both pathways, by western blot analysis (Figure 3.15.). Assessed proteins include the following components of the MAPK/ERK pathway: total MEK1/2, phosphorylated MEK1/2 (S221), total ERK1/2 and phosphorylated ERK1/2 (T202/Y204). MEK1/2 designates the two related proteins MEK1 and MEK2, while ERK1/2 designates the two related proteins ERK1 and ERK2. S221 refers to the activator phosphorylation of the serine residue at position 221 of MEK1/2. T202 refers to the activator phosphorylation of the threonine residue at position 202 or 185 of ERK1 or ERK2, respectively, while Y204 refers to the activator phosphorylation of the tyrosine residue at position 204 or 187 of ERK1 or ERK2, respectively. Components of the PI3K/AKT pathway were also assessed: total AKT and phosphorylated AKT (T308 or S473). T308 and S473 refer to the activator phosphorylation modifications of the threonine residue at position 308 or of the serine residue at position 473 of AKT protein, respectively.

Results show no perceptible change in the levels of total and phosphorylated MEK1/2, upon suppression of the lncRNA *C/EBPβ-AS.*

Remarkably, evident changes are perceived in ERK1/2 levels (downstream of MEK in the MAPK/ERK pathway), with both total and phosphorylated ERK1/2 being downregulated in A375 cell line transfected with siRNA siC/EBPβ-AS, compared to mock transfected A375. An elevation of total and

phosphorylated ERK1/2 levels is perceived in A375 PR1 cell line transfected with siRNA siC/EBPβ-AS, compared to mock transfected A375 PR1.

Regarding the AKT protein, results show no perceptible change in the levels of total AKT upon *C/EBPβ-AS* knockdown. On the other hand, phosphorylated AKT levels appear to be modestly downregulated in A375 cell line transfected with siRNA siC/EBPβ-AS, and notably upregulated in A375 PR1 cell line transfected with the same siRNA, when compared to mock transfected cells.

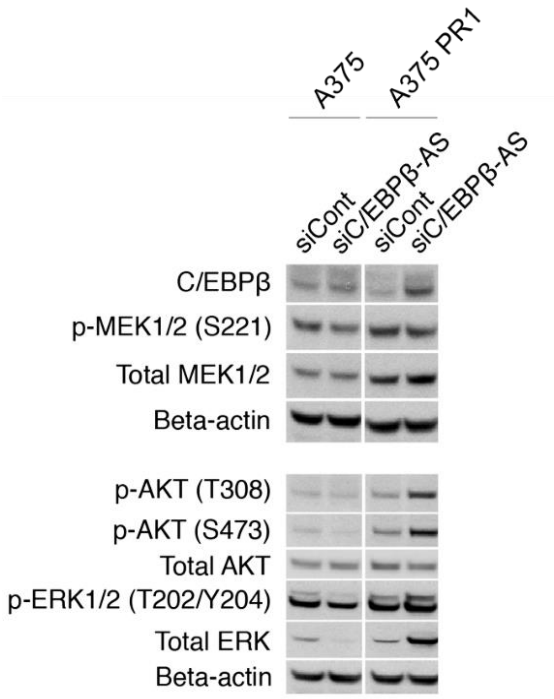

Figure 3.15. *C/EBPβ-AS* knockdown impacts MAPK/ERK and PI3K/AKT signalling pathways.
Western blot analysis of C/EBPβ, total and phosphorylated MEK1/2, total and phosphorylated ERK1/2, and total and phosphorylated AKT protein levels, after 48h siRNA-induced *C/EBPβ-AS* knockdown, in A375 and A375 PR1 cells. The protein input was standardized to Beta-actin. Data suggest that manipulation of *C/EBPβ-AS* expression impacts components of MAPK/ERK and PI3K/AKT signalling pathways.

4. Discussion

While originally considered intermediates between genes and encoded proteins, it now stands apparent that RNA is a multifunctional molecule involved in a wide diversity of molecular processes. Recent advances in sequencing techniques have revealed underappreciated biological roles of ncRNAs and led to the identification of large amounts of such molecules. However, functional investigations focusing on ncRNAs remain limited, requiring further efforts in order to understand and characterize this class of RNA molecules.

In this thesis, we proposed to study the antisense lncRNA *C/EBPβ-AS*, focusing on three main aspects: characterize biologically relevant features of *C/EBPβ-AS* transcript (such as subcellular localization, stability and polyadenylation status), characterize the functional role of *C/EBPβ-AS* considering previously elucidated functional mechanisms of antisense lncRNAs and finally, investigate *C/EBPβ-AS* role in a defined biologic context, specifically concerning cutaneous melanoma.

Firstly, efforts were dedicated to the characterization of *C/EBPβ-AS* transcript.

Subcellular localization of *C/EBPβ-AS* transcript was assessed by a low-resolution technique – subcellular fractionation –, and a high-resolution quantification method – smFISH. Subcellular fractionation and smFISH results indicate a uniform distribution of *C/EBPβ-AS* in the nuclear and the cytoplasmic compartments, despite studies showing that asRNAs, as well as lncRNAs in general, preferentially accumulate in the nucleus (Djebali *et al*., 2012; Derrien *et al*., 2012; Cabili *et al.*, 2015).

While mRNAs tend to accumulate in the cytoplasm (fundamentally acting as intermediators between DNA and proteins), lncRNAs must localize to their particular final site of action, whether in the nucleus or the cytoplasm. Therefore, identification of subcellular localization patterns of lncRNAs provides fundamental insights into understanding their subcellular context and hypothesizing putative molecular roles (Cabili *et al.*, 2015). As such, obtained results propose a diverse biological role of *C/EBPβ-AS,* suggesting that this RNA could be involved in transcriptional regulation (a role associated with transcripts present in the nuclear compartment, as for example the lncRNA Colon Cancer Associated Transcript 1 (*CCAT1-L*) (Xiang *et al*., 2014)) as well as in modulation of translation/post-translational modifications (a role associated with transcripts present in the cytoplasmic compartment, with the lncRNA Non-Coding RNA Activated By DNA Damage (*NORAD*) as an example of such (Lee *et al*., 2016)).

Additionally, widespread cellular distribution of *C/EBPβ-AS* may also be related to the existence of different non-annotated isoforms of *C/EBPβ-AS* transcript. These isoforms may carry different cellular functions in different cellular compartments. This is the case of *PTENpg1 asRNA* isoforms: *α* and *β*. While the isoform *α* localizes to the nuclear compartment and epigenetically modulates *PTEN* transcription, the *β* isoform is found in the cytoplasm and appears to act as a miRNA sponge, ultimately affecting post-transcriptional regulation of PTEN (Johnsson *et al*., 2013). Assessment of transcription of multiple *C/EBPβ-AS* isoforms and their characterization is therefore a relevant follow-up study to be carried, allowing profound understanding of *C/EBPβ-AS* functional biology.

Next, the stability of *C/EBPβ-AS* transcript was evaluated, by blocking transcription with actinomycin D. Results demonstrate a considerably superior stability of *C/EBPβ-AS* transcript as compared to *C/EBPβ* mRNA. Transcriptome analysis of the stability of lncRNAs demonstrates that the half-lives of

non-coding transcripts vary over a wide range, but are generally shorter than those of mRNAs. In such analysis, combining stability data with comprehensive genome annotations led to the identification of many unstable lncRNAs (half-life <2 h) – including intergenic, antisense, and intronic lncRNAs –, as well as lncRNAs showing higher stability (half-life >16 h) (Clark *et al*., 2012). Given that, our data is suggestive of an elevated stability of *C/EBPβ-AS*, inconsistent with previous reported observations of an overall predicted low stability of antisense lncRNAs. As the study of lncRNA decay is considered of importance in the evaluation of the biological function of lncRNAs, our results may ultimately point towards a complex and widespread functionality of *C/EBPβ-AS*.

Next, poly(A) status of *C/EBPβ-AS* was investigated, with results pointing towards *C/EBPβ-AS* identification as a poly(A) positive transcript. Poly(A)-tailed transcripts have previously been associated with translocation of RNA from the nucleus to the cytoplasm (Brodsky and Silver, 2000; Fuke and Ohno, 2008) as well as with improved RNA stability (Bernstein *et al*., 1989). As such, obtained results are consistent with the identification of *C/EBPβ-AS* presence in both nuclear and cytoplasmic compartments, as well as with the perceived elevated stability of the transcript.

Lastly, *C/EBPβ-AS* and *C/EBPβ* 5' end overlap was assessed through a primer walk. Results show that *C/EBPβ* 5' untranslated region (UTR) (comprising *C/EBPβ* transcription start site) does not overlap with the annotated *C/EBPβ-AS* exon 2. This experimental analysis not only contributed to the validation of the annotated transcripts, but was also a fundamental step in the design of siRNAs, namely the siRNA targeting C/EBPβ-AS, and primers, allowing specific targeting and amplification of transcripts. Further investigation would be required in order to validate the annotated transcription start sites of *C/EBPβ-AS* and *C/EBPβ*, as knowledge of the exact position of transcriptional start sites would be crucial for the identification of the regulatory regions that immediately flank *C/EBPβ-AS* and *C/EBPβ*. This could be enabled by performing a 5' Rapid Amplification of cDNA Ends (5' RACE), followed by sequencing of the obtained PCR product. Furthermore, design of new primers sets for a primer walk, along with 5' RACE analysis could allow the identification other putative non-annotated *C/EBPβ* and *C/EBPβ-AS* transcripts' isoforms.

Secondly, our investigation turned to understanding and characterizing the functional role of *C/EBPβ-AS*.

Analysis of complex biologic processes, such as the intricate functions carried out by lncRNAs, can be facilitated by RNA interference (RNAi), enabling loss-of-function studies in mammalian systems (Faghihi *et al.*, 2010). The genomic arrangement of sense:asRNA transcription suggests a plausible regulatory role in a cis-acting manner. As previous studies have shown that lncRNAs regulate transcription is this manner, we chose to utilize siRNA to investigate whether *C/EBPβ-AS* regulates *C/EBPβ* expression.

siRNA-mediated gene silencing can result in highly specific and efficient suppression of gene expression (Fire *et al.*, 1998). Nevertheless, many factors ranging from disparate features of cell trafficking pathways of different cell lines (Capel *et al.*, 2016) to passage number may affect levels of siRNA internalization in a cell type-dependent fashion. These rely among the possible causes that stand behind the detected variability in transfection efficiency between biological replicates as well as between different transfected melanoma cell lines presented in this thesis.

Our results show *C/EBPβ* upregulation upon *C/EBPβ-AS* knockdown in multiple melanoma cell lines suggestive of a negative regulatory mechanism of *C/EBPβ*, by *C/EBPβ-AS*. This role is putatively exerted at the transcriptional level, given that *C/EBPβ* upregulation is perceived at the mRNA level, and it can possibly be achieved by the sole event of transcription of the lncRNA, or by *C/EBPβ-AS* transcript itself. The plausibility of either hypothesis can be supported by considering described mechanisms of gene transcriptional silencing induced by antisense lncRNAs. The lncRNA Antisense Of IGF2R Non-Protein Coding RNA (*AIRN*) is an example of the first supposition – where transcriptional regulation happens as a consequence of simultaneous transcription of the lncRNA and the sense RNA. *AIRN* is transcribed from the opposite strand of the protein-coding gene *IGF2R*, overlapping its 5' region. While *IGF2R* transcriptional silencing is not achieved by the *AIRN* transcript as such, transcription through the *IGF2R* promoter prevents the recruitment of RNA Pol II, ultimately leading to *IGF2R* silencing (Latos *et al.*, 2012). As for the hypothesis regarding the regulatory role played by the lncRNA transcript, this mechanism can be exemplified by CDKN2B Antisense RNA 1 (*ANRIL*). In short, *ANRIL* recruits a Polycomb Repressive Complex 1 (PRC1) component, leading to repression of the neighbouring *INK4b/ARF/INK4a* genes (*Yap et al*., 2010).

As our results indicate that *C/EBPβ-AS* also localizes to the cytoplasm, *C/EBPβ* regulation may not occur at the transcriptional level, but through mRNA destabilization. For example, according to a previously proposed regulatory model, lncRNAs can transactivate Staufen 1 (STAU1)-mediated messenger RNA decay, influencing mRNA processing by post-transcriptional regulation (Gong and Maquat, 2011).

In order to elucidate how the lncRNA *C/EBPβ-AS* modulates *C/EBPβ* expression, assessment of RNA Pol II at the *C/EBPβ* promoter was performed by ChIP. This was carried out considering that RNA Pol II is required for gene transcription of most eukaryotic protein-coding genes. Results suggested an enrichment of RNA Pol II at the *C/EBPβ* promoter, when *C/EBPβ-AS* was suppressed, further supporting a model where *C/EBPβ-AS* acts as a negative regulator of *C/EBPβ*, specifically at the transcriptional level.

Moreover, an increase in C/EBPβ protein levels upon *C/EBPβ-AS* knockdown was observed, in A375 and A375 PR1 cell lines, which further supports the proposed role of *C/EBPβ-AS* in the regulation of global expression of *C/EBPβ*. Further evaluation of results obtained from protein analysis suggests that the transcriptional activator C/EBPβ LAP isoform is the predominant protein isoform in assessed cell lines. This observation will reveal to be of relevance, when evaluating the cellular impact of *C/EBPβ-AS* modulation.

Next, we set out to elucidate the molecular mechanism behind *C/EBPβ-AS*-mediated regulation of *C/EBPβ*.

As lncRNAs have been shown to interact directly with proteins such as epigenetic modulators, affecting gene transcription, we hypothesized that *C/EBPβ-AS* regulates *C/EBPβ* expression in this manner. In order to identify the mechanism by which *C/EBPβ-AS* negatively affects *C/EBPβ* transcription, we started by performing siRNA-mediated knockdown of different players that had previously been implicated in RNA-mediated epigenetic transcriptional regulation – *EZH2*, *G9a* and

DNMT3A. Results showed that knockdown of the histone methyltransferases *EZH2* and *G9a* caused an increase in *C/EBPβ* mRNA levels, while knockdown of *DNMT3A* had no significant effect.

According to a previously described model of asRNA-mediated transcriptional regulation, an asRNA may associate with a complex of epigenetic regulatory proteins including EZH2 and G9a. This complex then localizes to a targeted promoter by the non-coding RNA, inducing chromatin condensation and subsequent silencing of transcription (Morris, 2009). This model was demonstrated by investigating the lncRNA antisense to Oct4 Pseudogene 5, which associates with a complex of epigenetic regulatory proteins including EZH2 and G9a, silencing Octamer-Binding Transcription Factor 4 (*Oct4*) and Oct4 pseudogenes 4 and 5 (Hawkins and Morris, 2010).

Given the effect of EZH2 knockdown on *C/EBPβ* mRNA levels, we assessed the impact of *C/EBPβ-AS* knockdown on chromatin structure at the *C/EBPβ* promoter by ChIP analysis, regarding EZH2 and the H3K27me3 chromatin mark – catalysed and maintained by PRC2. Interestingly, results indicate an enrichment of EZH2 and H3K27me3 at the *C/EBPβ* promoter, after *C/EBPβ-AS* suppression, contrary to expected.

Additionally, assessment of DNA methylation at the *C/EBPβ* promoter upon *C/EBPβ-AS* suppression, with the methylation-dependent endonuclease MrcBC, points towards increased DNA methylation at such promoter. Nonetheless, and considering the lack of statistical significance of such assay, further experiments should be conducted aiming to further elucidate the methylation status of the *C/EBPβ* promoter. Since promoter methylation is often associated with transcriptional silencing, these results do not appear to be in line with observed *C/EBPβ-AS* knockdown effect on *C/EBPβ* upregulation.

Altogether, ChIP and DNA methylation results oppose to the proposed *C/EBPβ-AS*-mediated transcriptional regulatory mechanism based on recruitment of epigenetic remodelers to the *C/EBPβ* promoter.

On the other hand, a C/EBPβ enrichment was observed upon *C/EBPβ-AS* suppression. Given previous identification of C/EBPβ LAP isoform (characterized as a transcription positive modulator) as the predominant isoform present in assessed cell lines, such enrichment stands in accordance with *C/EBPβ-AS* knockdown effect on *C/EBPβ* upregulation.

Overall, results may indicate a different and not previously described regulatory mechanism, where *C/EBPβ-AS* impairs the epigenetic remodeler EZH2 from binding to the *C/EBPβ* promoter. This would lead to the observed enrichment of EZH2 and H3K27me3 at this promoter upon *C/EBPβ-AS* knockdown. Previous studies have shown that EZH2, a Polycomb group protein, is mechanistically linked to DNA methylation systems, serving as a recruitment platform for DNA methyltransferases (Viré *et al*., 2006). Bearing that in mind, EZH2 sequestration by *C/EBPβ-AS*, would also impair methylation of the *C/EBPβ* promoter – hence the detected increased DNA methylation at such promoter upon *C/EBPβ-AS* knockdown. Despite the H3K27me3 chromatin mark and DNA methylation of the cytosine in CpG dinucleotides being typically associated with gene silencing, genomic analyses have identified promoter sequences that are both methylated and transcriptionally active. Particularly, CpG methylation of half-cAMP response element (CRE) sequences create DNA binding sites for C/EBP transcription factors, resulting in gene activation (Rishi *et al*., 2010; Mann *et al*., 2013). According to UCSC Genome Browser annotations, half-CRE sequences are found at the *C/EBPβ* promoter. As such, *C/EBPβ-AS* suppression

would allow EZH2 binding and subsequent DNA methylation at this promoter, enabling binding of C/EBPβ. This would result in transcriptional activation of *C/EBPβ*, leading to the observed C/EBPβ enrichment at the *C/EBPβ* promoter upon *C/EBPβ-AS* knockdown.

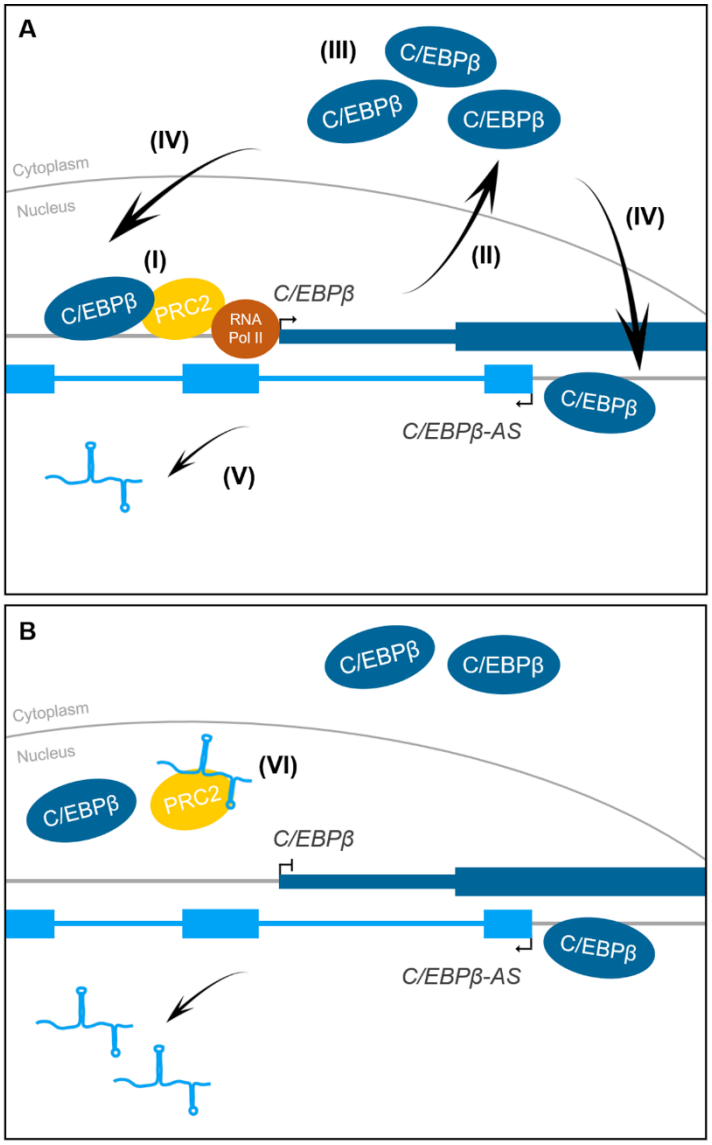

Figure 4.1. Schematic of the proposed mechanism of *C/EBPβ-AS*-mediated regulation of *C/EBPβ*. *C/EBPβ-AS* (light blue gene) and *C/EBPβ* (dark blue gene) locus is depicted. **(A)** Upon low cellular concentration of the lncRNA *C/EBPβ-AS* (light blue), (**I**) Polycomb Repressive Complex 2 (PRC2) (yellow) binds to the *C/EBPβ* promoter, serving as a recruitment platform for DNA methyltransferases (not depicted). This results in methylation of the cytosine in CpG dinucleotides, allowing binding of the transcription factor C/EBPβ (dark blue), ultimately leading to *C/EBPβ* transcription by RNA Polymerase II (RNA Pol II) (orange). (**II**) *C/EBPβ* is then translocated to the cytoplasm, where (**III**) translation and pos-translational modifications occur. (**IV**) The final C/EBPβ protein then translocates to the nucleus, where it binds to the *C/EBPβ* and *C/EBPβ-AS* promoters, leading to *C/EBPβ* and *C/EBPβ-AS* transcription. **(B)** Upon elevated cellular concentration of *C/EBPβ-AS* lncRNA, (**VI**) *C/EBPβ-AS* decoys PRC2 from the *C/EBPβ* promoter. This leads to reduced methylation at the promoter and subsequently impairs C/EBPβ binding to the such promoter. Therefore, *C/EBPβ* translation is suppressed, and C/EBPβ cellular levels decrease. *Student authorship image.*

According to this hypothesis, EZH2 binding to the *C/EBPβ* promoter would drive transcription initiation, however such would not be apparent on *C/EBPβ* observed upregulation upon EZH2 knockdown. On the other hand, EZH2 and G9a, as histone methyltransferases, are playing a genome-wide regulatory role. Therefore, the perceived *EZH2* and *G9a* knockdown effect on *C/EBPβ* may stand as an indirect outcome of EZH2 and G9a function exerted at a broader scale. This might justify the obtained data within the scope of the described hypothesis. In parallel, presented ChIP and DNA methylation data reflect events occurring at the locus level.

Overall, further experiments need to be conducted in order to understand the enrichment of the H3K27me3 chromatin mark (typically associated with repression of transcription) concomitant with increased gene expression. Elucidation of the hypothesized regulatory mechanism of *C/EBPβ* by *C/EBPβ-AS* would contribute to the knowledge of a novel and unconventional mechanism of regulation played by a lncRNA. Within such experiments, RNA immunoprecipitation and RNA pulldown may serve as important and crucial techniques, aiming to further assess RNA-protein interactions involved in such regulatory pathway.

Moreover, regarding Human GRCh37/hg19 – UCSC Genome Browser data, an enrichment of the transcription factor C/EBPβ at the predicted *C/EBPβ-AS* promoter was identified. Given this observation, we set out to investigate if C/EBPβ takes part of *C/EBPβ-AS* regulation. Results showed downregulation of *C/EBPβ-AS* upon *C/EBPβ* knockdown, indicating that the transcription factor C/EBPβ is required for *C/EBPβ-AS* expression.

Additionally, C/EBPβ interaction with the *C/EBPβ-AS* promoter was experimentally detected by ChIP.

Taken together, results suggest a positive feedback loop regulatory system, where C/EBPβ, as a transcription factor, regulates its own promoter. Also, results suggest a negative feedback loop where C/EBPβ binds to the promoter of *C/EBPβ-AS* and leads to its transcription, resulting in increased *C/EBPβ-AS* expression, ultimately leading to the repression of C/EBPβ transcription (Figure 4.1. depicts the overall proposed regulatory mechanism). This hypothesis could also explain the positive correlation previously established between *C/EBPβ* and *C/EBPβ-AS* expression, in TCGA Skin Cutaneous Melanoma cohort.

Given that the majority of the functional studies performed within the presented work was based on siRNA-induced knockdown of the lncRNA *C/EBPβ-AS*, RNA quantification at the level of copy-number performed before and after RNA suppression could provide a fresh perspective in the study of the functional role performed by the lncRNA.

Finally, we set out to investigate *C/EBPβ-AS* role in cutaneous malignant melanoma.

With that aim, the melanoma cell line A375 and the vemurafenib-resistant melanoma cell line A375 PR1 were used. The latter was previously generated and made resistant to vemurafenib by culturing the parental A375 cell line in increasing doses of vemurafenib. Published studies of A375 and A375 PR1 sensitivity to vemurafenib determined that the half maximal inhibitory concentration (IC50) of vemurafenib in A375 cells is < 1μM while the IC50 of vemurafenib in A375 PR1 cells is > 10μM (Azimi *et al*., 2012). As such, we suppressed *C/EBPβ-AS* expression using the siRNA siC/EBPβ-AS and cells were subsequently treated with vemurafenib. Cell viability was then evaluated through FACS analysis.

While *C/EBPβ-AS* knockdown alone showed a small impact on cell viability, results showed that combination of *C/EBPβ-AS* knockdown with 10 μM of vemurafenib induced over a 25% resensitization of A375 PR1 to vemurafenib.

A previous study, conducted with A375 and A375 PR1 cells, demonstrates the role of the transcription factor C/EBPβ in the positive regulation of *PTENpg1 asRNA α* (unpublished data produced by Dan Grandér's group), which in turn plays a part in the repression of *PTEN* expression (Johnsson *et al*., 2013). Additionally, loss of PTEN is an intensively studied molecular event directly associated with reactivation of the PI3K/AKT signalling pathway (Simpson and Parsons, 2001), ultimately contributing to melanoma development and progression, as well as to resistance to targeted-therapy (Aguissa-Touré and Li, 2012). In short, *C/EBPβ* upregulation following *C/EBPβ-AS* suppression would theoretically be reflected on increased *PTENpg1 asRNA α* expression. This would induce subsequent silencing of *PTEN*, triggering activation of the PI3K/AKT pathway, ultimately prompting cell survival. Therefore, *C/EBPβ-AS* knockdown would be expected to enhance the resistance mechanism to BRAF inhibitors observed in CMM patients, where reactivation of the PI3K/AKT pathway occurs after inhibition of mutated $BRAF^{V600E}$ and repression of MAPK/ERK signalling. As a resensitization of A375 PR1 cells to vemurafenib was instead perceived upon *C/EBPβ-AS* suppression, a dose-dependent effect of C/EBPβ expression in sensitivity to vemurafenib can be proposed, with low and elevated cellular levels of C/EBPβ contributing to destabilization of the molecular mechanisms behind resistance to targeted-therapy. This would involve an effect on additional signalling pathways, other than the PI3K/AKT pathway (counteracted by PTEN). Such hypothesis can be correlated with the apparently paradoxical previous observations of involvement of C/EBPβ in both cellular senescence and oncogenic transformation (Sebastian and Johnson, 2006).

The investigation of ncRNAs, namely lncRNAs, has become increasingly attractive as a starting point for identification of new therapeutic targets and development of new pharmacological compounds, with interesting outcomes in the management of the progression of many diseases (Wahlestedt, 2006; Matsui and Corey, 2017). Further focus and effort should be dedicated in characterizing *C/EBPβ-AS* molecular role in melanoma resistance to vemurafenib, ultimately contributing to a novel therapeutic approach. Retrospective studies regarding response of CMM patients to targeted-therapy and *C/EBPβ* and *C/EBPβ-AS* expression levels might reveal a statistical correlation with clinical value.

A large proportion of cutaneous melanomas exhibits mutations in many genes encoding for proteins that are part of the MAPK/ERK signalling pathway – appearing early in benign melanocytic proliferation and preserved through all stages of invasive and metastatic melanoma (Omholt *et al*., 2003). Another possible driver of melanoma is the activation of the PI3K/AKT pathway – promoting survival and cell cycle entry in melanoma cells when loss of the pathway negative regulator PTEN is found (Aguissa-Touré and Li, 2012). Involvement of MAPK/ERK and PI3K/AKT signalling pathways is found not only in melanoma development and progression, but also in underlying molecular mechanisms implicated in acquired resistance to targeted-therapies, namely, to the $BRAF^{V600E}$ inhibitor vemurafenib. In order to elucidate the role of *C/EBPβ-AS* in vemurafenib resistance in melanoma, a preliminary assessment of some protein components of either pathway was performed by protein analysis, upon suppression of the lncRNA *C/EBPβ-AS*. Assessed proteins include components of the MAPK/ERK pathway – total and

phosphorylated MEK1/2, and total and phosphorylated ERK1/2 –, as well as a component of the PI3K/AKT pathway – total and phosphorylated AKT.

Firstly, by establishing a comparison between the vemurafenib-sensitive cell line A375 with the vemurafenib-resistant cell line A375 PR1 (considering control cell lysates), all assessed components appear to be relatively upregulated in A375 PR1 cells, including total and phosphorylated forms of all analysed proteins. Such observation falls in accordance with previously described mechanisms of resistance to targeted-therapy, however detailed characterization of the molecular events prompting cell resistance to vemurafenib in A375 PR1 cells would be of great value in the interpretation of obtained results. Nonetheless, obtained data may serve as a starting point in the formulation of additional and more detailed questions to be addressed in a near future.

A peculiar observation that stands out is the variation of total and phosphorylated ERK1/2 levels, upon *C/EBPβ-AS* knockdown, which seems to occur in a MEK1/2-independent manner – as evident changes in total and phosphorylated MEK1/2 levels (upstream of ERK1/2 in the MAPK/ERK1/2 pathway) are not perceived. This observation gives rise to two main thoughts: first, the idea that phosphorylated MEK1/2 levels are not appropriately being assessed, since MEK1/2 proteins comprehend other phosphorylatable sites, aside from the Ser221 residue, that should likewise be analysed – the residue Ser217; secondly, upon eventual validation of unchanged phosphorylated MEK1/2 levels, a MEK1/2-bypass mechanism that results in a perceptible change of ERK1/2 levels should be considered and investigated.

In parallel, another interesting result is the discordant variation of ERK1/2 and AKT levels between A375 and A375 PR1 cell lines. While a decreased amount of total and phosphorylated ERK1/2 and phosphorylated AKT are detected in the sensitive cell line, elevated levels of the same components can be detected in the resistant cell line. According to aforementioned indirect C/EBPβ effect on PTEN expression, an induction of the PI3K/AKT pathway through increased AKT activation by phosphorylation was expected upon *C/EBPβ-AS* knockdown. ERK1/2 observed levels could be explained by a crosstalk mechanism between PI3K/AKT and MAPK/ERK1/2 pathways – considering the concordant variation of phosphorylated AKT and total and phosphorylated ERK1/2 in both cell lines. However, further experimental analysis would be required for validation of this hypothesis.

Nevertheless, observed induction of components of either analysed pathway in the A375 PR1 cell line upon *C/EBPβ-AS* suppression would, theoretically, contribute to maintenance of vemurafenib resistance, which appears to clash with observed vemurafenib resensitization resulting from *C/EBPβ-AS* knockdown. Additionally, *C/EBPβ-AS* knockdown effect on upregulated C/EBPβ expression may have a genome-wide effect on the regulation of expression of many proteins, considering that C/EBPβ is a transcription factor with many downstream targets and is implicated in many different cellular processes. Therefore, the characterization of direct and/or indirect effects on the analysed pathways may stand as a challenging quest.

Overall, obtained results from protein analysis reinforce the fact that further efforts should be dedicated to understanding such intricate and complex molecular mechanisms, ultimately contributing to research of lncRNAs and melanoma.

Altogether, results point towards a significant indirect role played by the lncRNA *C/EBPβ-AS* in processes in which the transcription factor C/EBPβ is known to take part of, regarding cellular proliferation/senescence.

Along with knockdown-based studies of *C/EBPβ-AS* functional role, forced expression of the lncRNA could provide further crucial clues that would support the construction of a robust model elucidatory of *C/EBPβ-AS* cellular purpose.

5. Conclusion

In the present work, the lncRNA *C/EBPβ-AS* was characterized, regarding biologically relevant features. The transcript was found to have a widespread subcellular distribution, detected in two of the major cellular compartments: the nucleus and the cytoplasm. Additionally, *C/EBPβ-AS* was classified as a highly stable RNA, with a half-life of over 10 hours – an unexpected attribute for a lncRNA according to previous studies of other antisense long non-coding transcripts. *C/EBPβ-AS* identification as a polyadenylated transcript fell in accordance with its detected subcellular localization, as well as its elevated stability. These data point towards a functional role played by *C/EBPβ-AS* in the assessed biological context, i.e. in cutaneous malignant melanoma cell lines.

Furthermore, a regulatory role of *C/EBPβ-AS* was identified in multiple melanoma cell lines, promoting silencing of *C/EBPβ* expression. Regarding obtained results, a mechanism of *C/EBPβ-AS*-mediated regulation of *C/EBPβ* was proposed to occur at the pre-transcriptional level. Such mechanism was hypothesized to depend on impairment of PRC2 binding to *C/EBPβ* promoter by *C/EBPβ-AS*. This would constraint DNA methylation at such promoter, reducing *C/EBPβ* positive regulation by the activator C/EBPβ LAP isoform. Given C/EBPβ implication on several central cellular events, study of its regulation in different biologic contexts reveals to be of great relevance. Further experiments are required to elucidate this regulatory molecular event, clarifying the apparently inconsistent obtained results. *C/EBPβ-AS* regulation by C/EBPβ was also hypothesized, suggesting of a negative feedback regulatory event taking place at the *C/EBPβ-AS* and *C/EBPβ* locus.

Moreover, we provide evidence indicating that modulation of *C/EBPβ-AS* expression impacts the sensitivity of A375 PR1 vemurafenib-resistant melanoma cells to vemurafenib. Furthermore, we show that such modulation affects components of MAPK/ERK and PI3K/AKT pathways (commonly found to be dysregulated in CMM). However, further evaluation is crucial for elucidation of the intricate mechanisms taking place.

In our knowledge, this was the first work characterizing the long non-coding RNA antisense to *C/EBPβ* and exploring *C/EBPβ-AS* functional role in gene regulation.

Along with a myriad of functional roles that have been attributed to lncRNAs, associated with many fundamental cellular processes in physiological as well as pathological settings, our research provides new insights on a novel lncRNA-mediated regulatory mechanism with implications on CMM targeted-therapy resistance.

Future studies may unravel a lncRNA-based therapeutic strategy for CMM patients, delaying or overcoming the onset of targeted-therapy resistance.

5. References

Aguissa-Touré, A.H. and Li, G. 2012. Genetic alterations of PTEN in human melanoma. Cellular and Molecular Life Sciences 69:1475-91.

Amaral, P.P. and Mattick, J.S. 2008. Noncoding RNA in development. Mammalian genome: official journal of the International Mammalian Genome Society 19:454-92.

Askarian-Amiri, M.E., Crawford, J., French, J.D., Smart, C.E., Smith, M.A., Clark, M.B., … Mattick, J.S. 2011. SNORD-host RNA Zfas1 is a regulator of mammary development and a potential marker for breast cancer. RNA 17:878-91.

Azimi, A., Johansson, C.H., Pernemalm, M., Touminen, R., Lehti, J., Hansson, J. and Egyhazi, S. 2012. Unraveling BRAF Inhibitor (PLX4032) Resistance Mechanisms. European Journal of Cancer 48:43.

Balch, C.M., Gershenwald, J.E, Soong, S.J., Thompson, J.F., Atkins, M.B., … Sondak, V.K. 2009. Final version of 2009 AJCC melanoma staging and classification. Journal of clinical oncology 27: 6199-206.

Banfai, B., Jia, H., Khatun, J., Wood, E., Risk, B., Gundling, W.E. Jr., … Lipovich, L. 2012. Long noncoding RNAs are rarely translated in two human cell lines. Genome Research 22: 1646-57.

Bernstein, P., Peltz, S.W. and Ross, J. 1989. The poly(A)-poly(A)-binding protein complex is a major determinant of mRNA stability in vitro. Molecular and cellular biology 9:659-70.

Bhatia, S., Tykodi, S.S. and Thompson, J.A. 2009. Treatment of metastatic melanoma: an overview. Oncology 23:488-96.

Broadbent, H.M., Peden, J.F., Lorkowski, S., Goel, A., Ongen, H., Green, F., … Warkins, H. 2008. Susceptibility to coronary artery disease and diabetes is encoded by distinct, tightly linked SNPs in the ANRIL locus on chromosome 9p. Human molecular genetics 17:806-14.

Brodsky, A.S. and Silver, P.A. 2000. Pre-mRNA processing factors are required for nuclear export. RNA 6: 1737–1749.

Bucheit, A.B., Chen, G., Siroy, A., Tetzlaff, M., Broaddus, R., Milton, D., … Davies, M.A. 2014. Complete loss of PTEN protein expression correlates with shorter time to brain metastasis and survival in stage IIIB/C melanoma patients with BRAFV600 mutations. Clinical Cancer Research 20:5527–36.

Cabili, M.N., Dunagin, M.C., McClanahan, P.D., Biaesch, A., Padovan-Merhar, O., Regev, A., Rinn, J.L. and Rah, A. 2015. Localization and abundance analysis of human lncRNAs at single-cell and single-molecule resolution. Genome biology 16:20.

Calin, G.A., Liu, C.G., Ferracin, M., Hyslop, T., Spizzo, R., Sevignani, C., … Croce, C.M. 2007. Ultraconserved regions encoding ncRNAs are altered in human leukemias and carcinomas. Cancer Cell 12:215-29.

Capel, V., Vllasaliu, D., Watts, P. and Stolnik, S. 2016. Insight into the relationship between the cell culture model, cell trafficking and siRNA silencing efficiency. Biochemical and biophysical research communications 477:260-5.

Carlino, M.S., Long, G.V., Kefford, R.F. amd Rizos, H. 2015. Targeting oncogenic BRAF and aberrant MAPK activation in the treatment of cutaneous melanoma. Critical reviews in oncology/hematology 96:385-98.

Carninci, P., Kasukawa, T., Katayama, S., Gough, J., Frith, M.C., Maeda, N., Hayashizaki, Y. (Genome Network Project Core Group). 2005. The transcriptional landscape of the mammalian genome. Science 309:1559-63.

Chang, F., Lee, J.T., Navolanic, P.M., Steelman, L.S., Shelton, J.G., Blalock, W.L., Franklin, R.A. and McCubrey, J.A. 2003. Involvement of PI3K/Akt pathway in cell cycle progression, apoptosis, and neoplastic transformation: a target for cancer chemotherapy. Leukemia 17:590-603.

Chapman, P.B., Hauschild, A., Robert, C., Haanen, J.B., Ascierto, P., Larkin, J., … McArthur, G.A. 2011. Improved survival with vemurafenib in melanoma with BRAF V600E mutation. New England journal of medicine 364:2507-16.

Chen, L., Yang, H., Xiao, Y., Tang, X., Li, Y., Han, Q., … Zhu, Y. 2016. Lentiviral-mediated overexpression of long non-coding RNA GAS5 reduces invasion by mediating MMP2 expression and activity in human melanoma cells. International journal of oncology 48:1509-18.

Clark, M.B., Johnston, R.L., Inostroza-Ponta, M., Fox, A.H., Fortini, E., Moscato, P., Dinger, M.E. and Mattick, J.S. 2012. Genome-wide analysis of long noncoding RNA stability. Genome research 22:885-98.

Clark, M.B., Mercer, T.R., Bussotti, G., Leonardi, T., Haynes, K.R., Crawford, J., … Dinger, M.E. 2015. Quantitative gene profiling of long noncoding RNAs with targeted RNA sequencing. Nature Methods 12:339-42.

Clark, W.H. Jr., Elder, D.E., Guerry, D. V, Epstein, M.N., Greene, M.H. and Van Horn, M. 1984. A study of tumor progression: the precur- 1. 2. sor lesions of superficial spreading and nodular melanoma. Human pathology 15:1147-65.

Derrien, T., Johnson, R., Bussotti, G., Tanzer, A., Djebali, S., Tilgner, H., … Guigó, R. 2012. The GENCODE v7 catalog of human long noncoding RNAs: analysis of their gene structure, evolution, and expression. Genome Research 22: 1775-89.

Descombes, P. and Schibler, U. 1991. A liver-enriched transcriptional activator protein, LAP, and a transcriptional inhibitory protein, LIP, are translated from the same mRNA. Cell 67:569-79.

Djebali, S., Davis, C.A., Merkel, A., Dobin, A., Lassmann, T., Mortazavi, A., … Gingeras, T.R. 2012. Landscape of transcription in human cells. Nature 489:101-8.

Dumaz, N., Hayward, R., Martin, J., Ogilvie, L., Hedley, D., Curtin, J.A., … Marais, R. 2006. In melanoma, RAS mutations are accompanied by switching signaling from BRAF to CRAF and disrupted cyclic AMP signaling. Cancer research 66:9483-91.

Elbashir, S.M., Harborth, J., Lendeckel, W., Yalcin, A., Weber, K. and Tuschl, T. 2001. Duplexes of 21-nucleotide RNAs mediate RNA interference in cultured mammalian cells. Nature 411:494-8.

ENCODE Project Consortium; Birney, E., Stamatoyannmopoulos, J.A., Dutta, A., Guigó, R., Gingeras, T.R., Marqulies, E.H., … de Jong, P.J. 2007. Identification and analysis of functional elements in 1% of the human genome by the ENCODE pilot project. Nature 447:799-816.

Erdmann, F., Lortet-Tieulent, J., Schüz, J., Zeeb, H., Greinert, R., Breitbart, E.W. and Bray. F. 2013. International trends in the incidence of malignant melanoma 1953–2008—are recent generations at higher or lower risk? International journal of cancer 132:385-400.

Faghihi, M.A. and Wahlestedt, C. 2009. Regulatory roles of natural antisense transcripts. Nature Reviews. Molecular cell biology 10:637-43.

Faghihi, M.A., Kocerha, J., Modarresi, F., Engström, P.G., Chalk, A.M., Brothers, S.P., … Wahlestedt, C. 2010. RNAi Screen Indicates Widespread Biological Function for Human Natural Antisense Transcripts. PLoS One 5: e13177.

Ferlay, J., Soerjomataram, I., Dikshit, R., Eser, S., Mathers, C., Rebelo, M., … Bray, F. 2015. Cancer incidence and mortality worldwide: sources, methods and major patterns in GLOBOCAN 2012. International journal of cancer 136:e359-86.

Fire, A., Xu, S., Montgomery, M.K., Kostas, S.A., Driver, S.E. and Mello, C.C. 1998. Potent and specific genetic interference by double-stranded RNA in Caenorhabditis elegans. Nature 391:806-11.

Flaherty, K.T., Puzanov, I., Kim, K.B., Ribas, A., McArthur, G.A., Sosman, J.A., … Chapman, P.B. 2010. Inhibition of Mutated, Activated BRAF in Metastatic Melanoma. New England journal of medicine 363:809-19

Flockhart, R.J., Webster, D.E., Qu, K., Mascarenhas, N., Kovalski, J., Kretz, M. and Khavari, P.A. 2012. BRAFV600E remodels the melanocyte transcriptome and induces BANCR to regulate melanoma cell migration. Genome research 22:1006-14.

Fuke, H. and Ohno, M. 2008. Role of poly(A) tail as an identity element for mRNA nuclear export. Nucleic acids research 36: 1037–1049.

Garbe, C., Eigentler, T.K., Keilhiolz, U., Hauschild, A. and Kirkwood, J.M. 2011. Systematic review of medical treatment in melanoma: current status and future prospects. Oncologist 16:5-24.

Gong, C. and Maquat, L.E. 2011. lncRNAs transactivate STAU1 -mediated mRNA decay by duplexing with 3′ UTRs via Alu elements. Nature 470:284–8.

Goodstadt, L. and Ponting, C.P. 2006. Phylogenetic reconstruction of orthology, paralogy, and conserved synteny for dog and human. PLOS Computational Biology 2: 1134-50.

Grossman, D. and Altieri, D.C. 2001. Drug resistance in melanoma: mechanisms, apoptosis, and new potential therapeutic targets. Canver metastasis reviews 20:3-11.

Gupta, R.A., Shah, N., Wang, K.C., Kim, J., Horlings, H.M., Wong, D.J., … Chang, H.Y. 2010. Long non-coding RNA HOTAIR reprograms chromatin state to promote cancer metastasis. Nature 464: 1071-6.

Hauschild, A., Grob, J.J., Demidov, L.V., Jouary T., Gutzmer, R., Millward, M., … Chapman P.B. 2012. Dabrafenib in BRAF-mutated metastatic melanoma: a multicentre, open-label, phase 3 randomised controlled trial. Lancet 380:358-65.

Hawkins, P.G. and Morris, K.V. 2010. Transcriptional regulation of Oct4 by a long non-coding RNA antisense to Oct4-pseudogene 5. Transcription 1: 165–175.

Heidorn, S.J., Milagre, C., Whittaker, S., Nourry, A., Niculescu-Duvas, I., Dhomen, N., … Marais, R. 2010. Kinase-dead BRAF and oncogenic RAS cooperate to drive tumor progression through CRAF. Cell 140:209-21.

Helmbach, H., Sinha, P. and Schadendorf, D. 2003. Human melanoma: drug resistance. Recent results in cancer research 161:93-110.

Hoagland, M.B., Stephenson, M.L., Scott, J.F., Hecht, L.I. and Zamecnik, P.C. 1958. A soluble ribonucleic acid intermediate in protein synthesis. Journal of biological chemistry 231:241-57.

Hodi, F.S., O'Day, S.J., McDermott, D.F., Weber, R.W., Sosman, J.A., Haanen, J.B., … Urba, W.J. 2010. Improved survival with ipilimumab in patients with metastatic melanoma. New England journal of medicine 363:711-23.

Hu, W., Yaun, B., Flygare, J. and Lodish, H.F. 2011. Long noncoding RNA-mediated anti-apoptotic activity in murine erythroid terminal differentiation. Genes & development 25:2573-8.

Huarte, M. 2015. The emerging role of lncRNAs in cancer. Nature medicine 21:1253-61.

Johnsson, P., Ackley, A., Vidarsdóttir, L., Weng-Onn, L., Corcoran, M., Grandér, D. and Morris, K.V. 2013. A pseudogene long-noncoding RNA network regulates PTEN transcription and translation in human cells. Nature structural & molecular biology 20: 440–446.

Johnsson, P., Lipovich, L., Grandér, D. and Morris, K.V. 2014. Evolutionary conservation of longnon-coding RNA; sequence, structure, function. Biochimica et biophysica acta 1840:1063-71.

Katayama, S., Tomaru, Y., Kasukawa, T., Waki, K., Nakanishi, M., Nakamura, M., … Wahlestedt, C. (RIKEN Genome Exploration Research Group; Genome Science Group (Genome Network Project Core Group); FANTOM Consortium). 2005. Antisense transcription in the mammalian transcriptome. Science 309:1564-6.

Katz, M., Amit, I. and Yarden, Y. 2007. Regulation of MAPKs by growth factors and receptor tyrosine kinases. Biochimica et biophysica acta 1773:1161-76.

Khorkova, O., Hsia, J. and Wahlestedt, C. 2015. Basic biology and therapeutic implications of lncRNA. Advanced drug delivery reviews 87: 15-24.

Kim, T. and Reitmair, A. 2013. Non-Coding RNAs: Functional Aspects and Diagnostic Utility in Oncology. International journal of molecular sciences 14:4934-68.

Kolch, W. 2000. Meaningful relationships: the regulation of the Ras/Raf/MEK/ERK pathway by protein interactions. Biochemical journal 351 pt2:289-305.

Kretz, M., Siprashvili, Z., Chu, C., Webster, D.E., Zehnder, A., Qu, K., … Khavari, P.A. 2013. Control of somatic tissue differentiation by the long non-coding RNA TINCR. Nature 493:231-5.

Lander, E.S., Linton, L.M., Birren, B., Nusbaum, C., Zody, M.C., Baldwin, J., … Szustakowki, J. (International Human Genome Sequencing Consortium). 2001. Initial sequencing and analysis of the human genome. Nature 409:860-921.

Larkin J., Yan Y., McArthur G., Ascierto P., Liszkay G., Maio M., … Ribas, A. 2015. Update of progression-free survival (PFS) and correlative biomarker analysis from coBRIM: phase III study of cobimetinib (cobi) plus vemurafenib (vem) in advanced BRAF-mutated melanoma. Journal of Clinical Oncology 33:9006.

Latos, P.A., Pauler, F.M., Koerner, M.V., Senergin, H.B., Hudson, Q.J., Stocsits, R.R, … Barlow, D.P. 2012. Airn transcriptional overlap, but not its lncRNA products, induces imprinted Igf2r silencing. Science 338:1469-72.

Lawrence, M.S., Stojanov, P., Polak, P., Kryukov, G.V., Cibulskis, K., Sivachenko, A., … Getz, G. 2013. Mutational heterogeneity in cancer and the search for new cancer-associated genes. Nature 499:214-8.

Lee, S., Kopp, F., Chang, T.C., Sataluri, A., Chen, B., Sivakumar, S., … Mendell, J.T. 2016. Noncoding RNA NORAD Regulates Genomic Stability by Sequestering PUMILIO Proteins. Cell 164:69-80.

Leucci, E., Vendramin, R., Spinazzi, M., Laurette, P., Fiers, M., Wouters, J., … Marine, J.C. 2016. Melanoma addiction to the long non-coding RNA SAMMSON. Nature 531: 518-22.

Li, K. and Ramchandran, R. 2010. Natural Antisense Transcript: A Concomitant Engagement with Protein-Coding Transcript. Oncotarget 1:447-52.

Li, R., Zhang, L., Jia, L., Duan, Y., Li, Y., Bao, L. and Sha, N. 2014. Long non-coding RNA BANCR promotes proliferation in malignant melanoma by regulating MAPK pathway activation. PLoS One 9: e100893.

Lo, J.A and Fisher, D.E. 2014. The melanoma revolution: From UV carcinogenesis to a new era in therapeutics. Science 346:945-9.

Long, G.V. Stroyakovskiy, D., Gogas, H., Levchenko, E., de Braud, F., Larkin, J., … Flaherty, K. 2014. Combined BRAF and MEK Inhibition versus BRAF Inhibition Alone in Melanoma. New England journal of medicine 371:1877-88.

Long, G.V., Fung, C., Menzies, A.M., Pupo, G.M., Carlino, M.S., Hyman, J., … Rizos, H. 2014. Increased MAPK reactivation in early resistance to dabrafenib/trametinib combination therapy of BRAF-mutant metastatic melanoma. Nature communications 5:5694.

Macherey-Nagel 2015. RNA isolation User manual NucleoSpin RNA

Magistri, M., Faghihi, M.A., St.Laurent, G. 3rd and Wahlestedt, C. 2012. Regulation of chromatin structure by long noncoding RNAs: Focus on natural antisense transcripts. Trends in genetics: TIG 28:389-96.

Mann, I.K., Chatterjee, R., Zhao, J., He, X., Weirauch, M.T., Hughes, T.R. and Vinson, C. 2013. CG methylated microarrays identify a novel methylated sequence bound by the CEBPB|ATF4 heterodimer that is active in vivo. Genome research 23:988-97.

Matsui, M. and Corey, D.R. 2017. Non-coding RNAs as drug targets. Nature Reviews Drug Discovery 16:167–79.

Mercer, T.R. and Mattick, J.S. 2013. Structure and function of long noncoding RNAs in epigenetic regulation. Nature structural & molecular biology 20:300-7.

Mercer, T.R., Dinger, M.E., Sunkin, S.M., Mehler, M.F. and Mattick, J.S. 2008. Specific expression of long noncoding RNAs in the mouse brain. Proceedings of the National Academy of Sciences of the United States of America 105:716-21.

Meyskens, F.L. Jr., Farmer, P.J. and Anton-Culver, H. 2004. Etiologic pathogenesis of melanoma: a unifying hypothesis for the missing attributable risk. Clinical cancer research: an official journal of the American Association for Cancer Research 10:2581-3.

Miller, A.J. and Mehm, M.C. Jr. 2006. Melanoma. New England journal of medicine 355:51-65.

Morris, K.V. 2009. Long antisense non-coding RNAs function to direct epigenetic complexes that regulate transcription in human cells. Epigenetics 4: 296–301.

Morris, K.V. and Mattick, J.S. 2014. The rise of regulatory RNA. Nature Reviews. Genetics 15:423-37.

Nazarian, R., Shi, H., Wang, Q., Kong, X., Koya, R.C., Lee, H., … Lo, R.S. 2010. Melanomas acquire resistance to B-RAF(V600E) inhibition by RTK or N-RAS upregulation. Nature 468:973-7.

Nikolaev, S.I., Rimoldi, D., Iseli, C., Valsesia, A., Robyr, D., Gehrig, C., … Antonarakis, S.E. 2011. Exome sequencing identifies recurrent somatic MAP2K1 and MAP2K2 mutations in melanoma. Nature genetics 44:133-9.

Nishizawa, M., Okumura, T., Ikeya, Y. and Kimura, T. 2012. Regulation of inducible gene expression by natural antisense transcripts. Frontiers in Bioscience (Landmark edition) 17:938-58.

Numata K. and Kiyosawa H. 2012 Genome-wide impact of endogenous antisense transcripts in eukaryotes. Frontiers in Bioscience (Landmark edition) 17:300–15.

Omholt, K., Karsberg, S., Platz, A., Kanter, L., Ringborg, U. and Hansson, J. 2002. Screening of N-***ras*** Codon 61 Mutations in Paired Primary and Metastatic Cutaneous Melanomas. Clinical Cancer Research 8:3468-74.

Omholt, K., Platz, A., Kanter, L., Ringborg, U. and Hansson, J. 2003. NRAS and BRAF mutations arise early during melanoma pathogenesis and are preserved throughout tumor progression. Clinical cancer research: an official journal of the American Association for Cancer Research 9:6483-8.

Osada, S., Yamamoto, H., Nishihara, T. and Imagawa, M. 1996. DNA binding specificity of the CCAAT/enhancer-binding protein transcription factor family. Journal of biological chemistry 271:3891-6.

Osato, N., Suzuki, Y., Ikeo, K. and Gojobori, T. 2007. Transcriptional interferences in cis natural antisense transcripts of humans and mice. Genetics 176:1299-306.

Palade, G.E. 1955. A small particulate component of the cytoplasm. Journal of biophysical and biochemical cytology 1:59-68.

Pang, K.C., Frith, M.C. and Mattick, J.S. 2006. Rapid evolution of noncoding RNAs: lack of conservation does not mean lack of function. Trends in genetics: TIG 22:1-5.

Paraiso, K.H., Xiang, Y., Rebecca, V.W., Abel, E.V., Chen, Y.A., Munko, A.C., … Smalley, K.S. 2011. PTEN loss confers BRAF inhibitor resistance to melanoma cells through the suppression of BIM expression. Cancer research 71: 2750-60.

Pleasance, E.D., Cheetham, R.K., Stephens, P.J., McBride, D.J., Humphray , S.J., Greeman, C.D., … Stratton, M.R. 2010. A comprehensive catalogue of somatic mutations from a human cancer genome. Nature 463:191-6.

Poulikakos, P.I., Zhang, C., Bollag, G., Shokat, K.M. and Rosen, N. 2010. RAF inhibitors transactivate RAF dimers and ERK signalling in cells with wild-type BRAF. Nature 464:427-30.

Poulikakos, P.I., Persaud, Y., Janakiraman, M., Kong, X., Ng, C., Moriceau, G., … Solit, D.B. 2011. RAF inhibitor resistance is mediated by dimerization of aberrantly spliced BRAF(V600E). Nature 480:387-90.

Ramji, D.P. and Foka, P. 2002. CCAAT/enhancer-binding proteins: structure, function and regulation. Biochemical Journal 365:561–75.

Ravasi, T., Suzuki, H., Pang, K.C., Katayama, S., Furuno, M., Okunishi, R., … Mattick, J.S. 2006. Experimental validation of the regulated expression of large numbers of noncoding RNAs from the mouse genome. Genome Research 16:11-9.

Richtig, G., Ehall, B., Richtig, E., Aigelsreiter, A., Gutschner, T. and Pichler, M. 2017. Function and Clinical Implications of Long Non-Coding RNAs in Melanoma. International journal of molecular sciences 18:715.

Rinn, J.L., Kertesz, M., Wang, J.K., Squazzo, S.L., Xu, X., Brugmann, S.A., … Chang, H.Y. 2007. Functional demarcation of active and silent chromatin domains in human HOX loci by noncoding RNAs. Cell 129:1311-23.

Rishi, V., Bhattacharya, P., Chatterjee, R., Rozenberg, J., Zhao, J., Glass, K., Fitzgerald, P. and Vinson, C. CpG methylation of half-CRE sequences creates C/EBPalpha binding sites that activate some tissue-specific genes. Proceedings of the National Academy of Sciences of the United States of America 107:20311-6.

Robert, C., Ribas, A., Wolchok, J.D., Hodi, F.S., Hamid, O., Kefford, R., … Daud, A. 2014. Anti-programmed-death-receptor-1 treatment with pembrolizumab in ipilimumab-refractory advanced melanoma: a randomised dose-comparison cohort of a phase 1 trial. Lancet 384:1109-17.

Sarasin, A. 1999. The molecular pathways of ultraviolet-induced carcinogenesis. Mutation research 428:5-10.

Schwarz, T. 2005. Mechanisms of UV-induced immunosuppression. Keio journal of medicine 54: 165-71.

Sebastian, T., Malik, R., Thomas, S., Sage, J. and Johnson, P.F. 2005. C/EBPβ cooperates with RB:E2F to implement Ras^{V12}-induced cellular senescence. EMBO journal 24:3301-12.

Sebastian, T. and Johnson, P.F. 2006. Stop and go: anti-proliferative and mitogenic functions of the transcription factor C/EBPbeta. Cell cycle 5:953-7.

Sharpe, A.H. 2009. Mechanisms of Costimulation. Immunological reviews 229:5-11.

Shi, H., Moriceau, G., Kong, X., Lee, M.K., Lee, H., Koya, R.C., … Lo, R.S. 2012. BRAF amplification Melanoma whole-exome sequencing identifies (V600E) B-RAF amplification-mediated acquired B-RAF inhibitor resistance. Nature Communications 3:724.

Simpson, L. and Parsons, R. 2001. PTEN: life as a tumour suppressor. Experimental Cell research 264:29–41.

Silanes, I.L., d'Alcontres, M.S. and Blasco, M.A. 2010. TERRA transcripts are bound by a complex array of RNA-binding proteins. Nature communications 1:33.

Smalley, K.S. 2003. A pivotal role for ERK in the oncogenic behaviour of malignant melanoma? International journal of cancer 104:527-32.

Solus, J.F. and Kraft, S. 2013. Ras, Raf, and MAP Kinase in Melanoma. Advances in anatomic pathology 20:217-26.

Straussman, R., Morikawa, T., Shee, K., Barzily-Rokni, M., Qian, Z.R., Du, J., … Golub, T.R. 2012. Tumour micro-environment elicits innate resistance to RAF inhibitors through HGF secretion. Nature 487:500-4.

Sun, B.K., Deaton, A.M. and Lee, J.T. 2006. A transient heterochromatic state in Xist preempts X inactivation choice without RNA stabilization. Molecular cell 21:617-28.

Taft, R.J., Pheasant, M. and Mattick, J.S. 2007. The relationship between non-protein-coding DNA and eukaryotic complexity. BioEssays 29: 288–99.

Tay, S.K., Blythe, J. and Lipovich, L. 2009. Global discovery of primate-specific genes in the human genome. Proceedings of the National Academy of Sciences of the United States of America 106:12019-24.

Thompson J.F., Scolyer R.A., Kefford R.F. 2005. Cutaneous melanoma. Lancet 365:687-701

Trask, D.K. and Muller, M.T. 1988. Stabilization of type I topoisomerase-DNA covalent complexes by actinomycin D. Proceedings of the National Academy of Sciences of the United States of America 85: 1417–1421.

Tripathi, V. Ellis, J.D., Shen, Z., Song, D.Y., Pan, Q., Watt, A.T., … Prasanth, S.G. 2010. The nuclear-retained noncoding RNA MALAT1 regulates alternative splicing by modulating SR splicing factor phosphorylation. Molecular cell 39:925-38.

Venter, J.C., Adams, M.D., Myers, E.W., Li, P.W., Mural, R.J., Sutton, G.G., …Zhu, X. 2001. The sequence of the human genome. Science 291:1304-51.

Villanueva, J., Vultur, A., Lee, J.T., Somasundaram, R., Fukunaga-Kalabis, M., Cipolla, A.K., … Herlyn, M. 2010. Acquired resistance to BRAF inhibitors mediated by a RAF kinase switch in melanoma can be overcome by cotargeting MEK and IGF-1R/PI3K. Cancer cell 18:683-95.

Villegas, V.E. and Zaphiropoulos, P.G. 2015. Neighboring Gene Regulation by Antisense Long Non-Coding RNAs. International journal of molecular sciences 16:3251-66.

Vinson, C.R., Sigler, P.B. and McKnight, S.L. 1989. Scissors-grip model for DNA recognition by a family of leucine zipper proteins. Science 246:911-6.

Viré, E., Brenner, C., Deplus, R., Blanchon, L., Fraga, M., Didelot, C., … Fuks, F. 2006. The Polycomb group protein EZH2 directly controls DNA methylation. Nature 439:871-4.

Wagle, N., Emery, C., Berger, M.F., Davis, M.J., Sawyer A., Pochanard, P., … Garaway, L.A. 2011. Dissecting therapeutic resistance to RAF inhibition in melanoma by tumor genomic profiling. Journal of clinical oncology: official journal of the American Society of Clinical Oncology 29:3085-96.

Wahlestedt, C. 2006. Natural antisense and noncoding RNA transcripts as potential drug targets. Drug discovery today 11:503-8.

Weber, J.S., D'Angelo, S.P., Minor, D., Hodi, F.S., Gutzmer, R., Neys ,B., … Larkin, J. 2015. Nivolumab versus chemotherapy in patients with advanced melanoma who progressed after anti-CTLA-4 treatment (CheckMate 037): a randomised, controlled, open-label, phase 3 trial. Lancet. Oncology 16:375-84.

Welm, A.L., Timchenko, A.N. and Darlington, G.J. 1999. C/EBPα Regulates Generation of C/EBPβ Isoforms through Activation of Specific Proteolytic Cleavage. Molecular and cellular biology 19:1695-704.

Whiteman, D.C., Whiteman, C.A. and Green, A.C. 2001. Childhood sun exposure as a risk factor for melanoma: a systematic review of epidemiologic studies. Cancer causes & control: CCC 12:69-82.

Xiang, J.F., Yin, Q.F., Chen, T., Zhang, Y., Zhang, X.O., Wu, Z., … Chen, L.L. 2014. Human colorectal cancer-specific CCAT1-L lncRNA regulates long-range chromatin interactions at the MYC locus. Cell research 24:513-31.

Xiong, W., Hsieh, C.C., Kurts, A.J., Rabek, J.P. and Papaconstantinou, J. 2001. Regulation of CCAAT/enhancer-binding protein-beta isoform synthesis by alternative translational initiation at multiple AUG start sites. Nucleic acids research 29:3087-98.

Yan, X., Hu, Z., Feng, Y., Hu, X., Yuan, J., Zhao, S.D. and Zhang, L. 2015. Comprehensive Genomic Characterization of Long Non-coding RNAs across Human Cancers. Cancer Cell 28:529-40.

Yap, K.L., Li, S., Muñoz-Cabello, A.M., Raguz, S., Zeng, L., Mujtaba, S., Walsh, M.J., and Zhou, M.M. 2010. Molecular interplay of the noncoding RNA ANRIL and methylated histone H3 lysine 27 by polycomb CBX7 in transcriptional silencing of INK4a. Molecular cell 38:662-74.

Young, T.L., Matsuda, T. and Cepko, C.L. 2005. The noncoding RNA taurine upregulated gene 1 is required for differentiation of the murine retina. Current biology: CB 15:501-12.

Supplementary

Supplementary Table S.1. siRNAs used in cationic lipid-mediated transfection of cells.

Designation of used siRNAs, respective RNA targets, target sequences and suppliers (extended version of Table 2.1).

siRNA designation	Target	Target sequence	Supplier
siC/EBPβ-AS	*C/EBPβ-AS*	CCCGGCTTTAGAAAGAAGACTTGACGC	IDT
siC/EBPβ	*C/EBPβ*	GAAGTTGATGCAATCGGTTTAAACATG	IDT
siEZH2	*EZH2*	TTGATAGTTGTAAACATGGTT	Eurofins
siDNMT3a (a pool of two siRNAs was used)	*DNMT3A*	AATTCAATCATGGGCTTGTTCTG	Eurofins
		CTCAGTGGTGTGTGTTGAGAA	Qiagen
siG9a	*G9a*	ATCGAGGTGATCCGCATGCTA	Qiagen
siCont	(non-targeting negative control)		IDT

Supplementary Table S.2. Primer sets used in RT-qPCR or semi-quantitative PCR reactions.

Targets of primer sets used in RT-qPCR or semi-quantitative PCR reactions, respective primer sequences and designation of respective experiments in which primers were used.

Target of primer set	Primer sequence	Respective method(s)
C/EBPβ-AS	F: ACTGAGGCGATTTGCCAAG	Assessment of expression levels (RT-qPCR); Cellular localization (semi-quantitative PCR)
	R: CTGGCTGATTTCTAAGCCCTTT	
C/EBPβ	F: GGAGCCCGTCGGTAATTT	Assessment of expression levels (RT-qPCR); Cellular localization (semi-quantitative PCR)
	R: TCTGCATGTGCGGTTGG	
Beta-actin	F: AGGTCATCACCATTGGCAATGAG	Assessment of expression levels - control (RT-qPCR); Poly(A) depletion control (semi-quantitative PCR)
	R: CTTTGCGGATGTCCACGTCA	
7SK	F: AATGAGGACCAGCTGAGTAGA	Cellular localization control (semi-quantitative PCR)
	R: GGAGGGATGAGAATGCATGAG	
U48	F: AGTGATGATGACCCCAGGTA	Poly(A) depletion control (semi-quantitative PCR)
	R: GGTCAGAGCGCTGCGGTGAT	
C/EBPβ; *C/EBPβ* upstream sequence	R0: GCTGCTCCACCTTCTTCTG	*C/EBPβ* primer walk
	F0: CGCGACAAGGCCAAGAT	
	F1: CTTTAGCGAGTCAGAGC	
	F2: CTTCTCCTGGAGCTAGA	
	F3: CAAGTCTTCTTTCTAAAGCC	
EZH2	F: CAGTTTGTTGGCGGAAGCGTGTAA	Assessment of expression levels (RT-qPCR)
	R: AGGATGTGCACAGGCTGTATCCTT	
DNMT3A	F: TTTGAGTTCTACCGCCTCCTGCAT	Assessment of expression levels (RT-qPCR)
	R: GTGCAGCTGACACTTCTTTGGCAT	
G9a	F: TGCAGAAGGTGATCCTGATGC	Assessment of expression levels (RT-qPCR)
	R: CGCTGCTGTTTGTCCACTGCA	
C/EBPβ-AS promoter	F: TAAACTCTCTGCTTCTCCCTCT	Protein enrichment at *C/EBPβ-AS* promoter (ChIP)
	R: CGATTGCATCAACTTCGAAACC	
C/EBPβ promoter	F: CGTAAGCCTTAGGTTTGGGA	Protein enrichment at *C/EBPβ* promoter (ChIP); DNA methylation at *C/EBPβ* promoter
	R: TGCAATCCATGAAGGGTGT	

Supplementary Table S.3. Target sequences of oligonucleotides used for *C/EBPβ-AS* smFISH.

Oligonucleotide target	Oligonucleotide sequence
C/EBPβ-AS transcript	AGTAGTTCAGACGCCGTTAAGCAAGAACTGCAAG AAGCCGAGTAGTTCAGACGCCGTTAA
	AGTAGTTCAGACGCCGTTAATAAGAGGGGAGTCG TCACAGAGTAGTTCAGACGCCGTTAA
	AGTAGTTCAGACGCCGTTAAAGCGCGGGGCAAG AGAAGACAGTAGTTCAGACGCCGTTAA
	AGTAGTTCAGACGCCGTTAACAAGTGGTCAGAAG GCCTTGAGTAGTTCAGACGCCGTTAA
	AGTAGTTCAGACGCCGTTAATCAAAGCAGCCACG TGGATCAGTAGTTCAGACGCCGTTAA
	AGTAGTTCAGACGCCGTTAATAAGCCCTTTTGCA GAACACAGTAGTTCAGACGCCGTTAA
	AGTAGTTCAGACGCCGTTAAGGATCTTCACGCAT GTGAATAGTAGTTCAGACGCCGTTAA
	AGTAGTTCAGACGCCGTTAATTTCCTGATCCCAG AGCAAGAGTAGTTCAGACGCCGTTAA
	AGTAGTTCAGACGCCGTTAACTGTGTGCATCTAT CACATCAGTAGTTCAGACGCCGTTAA
	AGTAGTTCAGACGCCGTTAATTCGTTGGACACTC TGGTTCAGTAGTTCAGACGCCGTTAA
	AGTAGTTCAGACGCCGTTAAGAAGGTTGAGCACT GTTTTCAGTAGTTCAGACGCCGTTAA